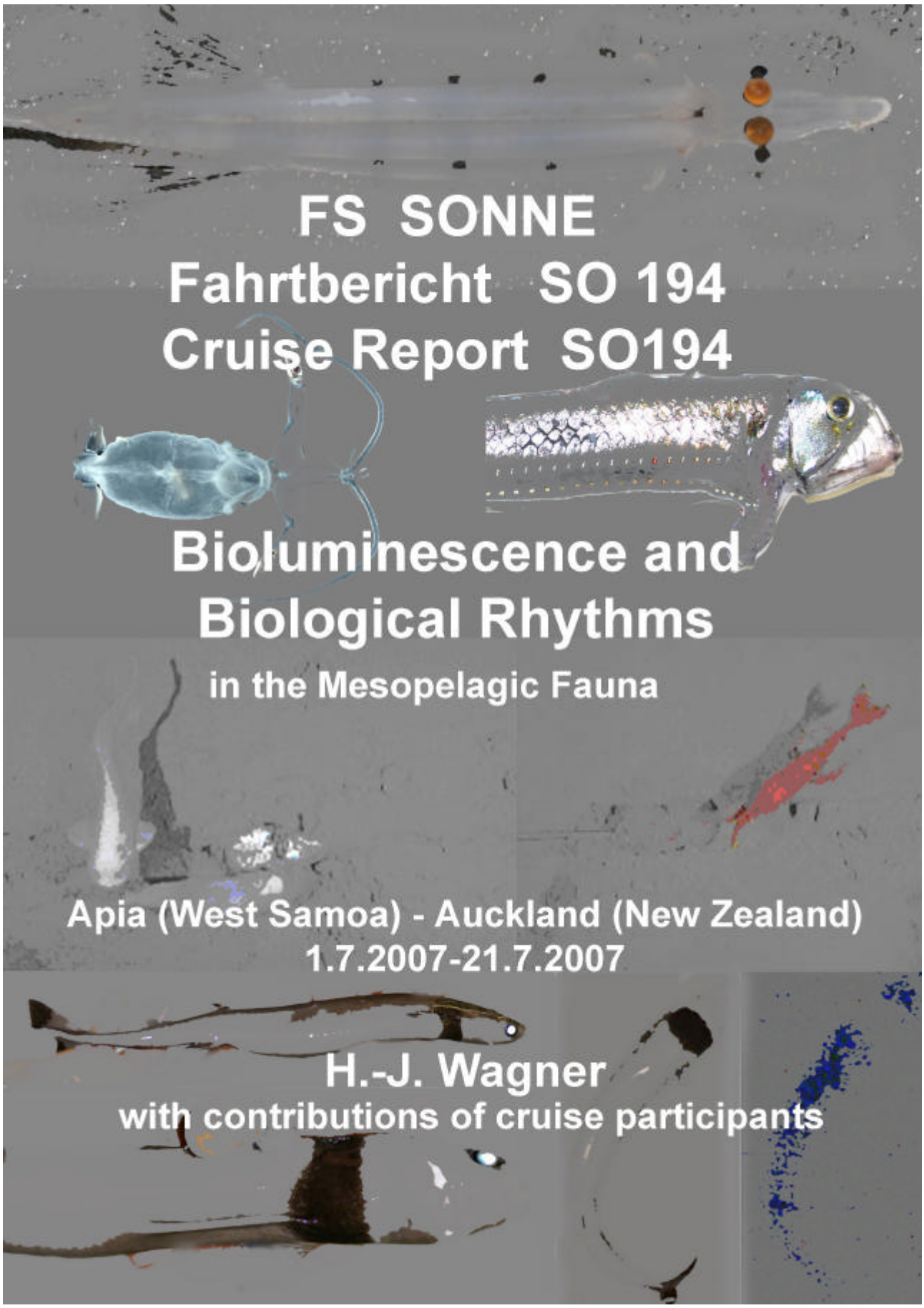

FS SONNE
Fahrtbericht SO 194
Cruise Report SO194

Bioluminescence and Biological Rhythms

in the Mesopelagic Fauna

Apia (West Samoa) - Auckland (New Zealand)
1.7.2007-21.7.2007

H.-J. Wagner
with contributions of cruise participants

Table of contents

Abstract

The main purpose of the cruise was to study the perception mechanisms of bioluminescence in the mesopelagic fauna. Furthermore, the presence of endogenous diel oscillators were investigated as a possible control mechanism for the daily vertical migrations of midwater animals. We conducted 20 trawls between 200 and 700 m depth and collected eyes and brains of mesopelagic fish for immediate experimentation on board or fixation and subsequent investigation in the home laboratories.

In addition to these projects, the samples were also used to assess the effect of high pressure on the physiology of muscle fibres, and the toxicity of iatrogenic pollutants (PCBs, DDTs) on the liver metbolism.

Another major project involved the study of hadal faunal communities. Five deployments of University of Aberdeen Oceanlab autonomous landers were carried out at depths of 6,000m, 7049m, 8170m, 9,000m and 10,015m. The landers were equipped with baited traps and took time-lapse videos over a period of 12h after which they were recovered. The sighting of the fish at 7100m is possibly the first real scientific observations of a hadal fish species in regard to behaviour and in an in situ context. Furthermore, predation in the hadal zone was aslo recorded for the first time. The collection of amphipods serves to perform population genetic studies, taxonomy and define the zonation of scavenging amphipods through the trench depths. Temperature data were also collected and proved that indeed there is a rise in temperature from 5000 to 10,000m. The 10,000m deployment was a technological milestone that will lead to further investigations and general interest/awareness of the hadal and trench environments.

The investigation of the visual pigments in 47 of them myctophids belonging to around 20-25 species will allow for the first time an analysis of the adaptive radiation of deep sea rhodopsins whithout the confounding variables of depth and vertical migration because it is restricted to a single family. An additional and unexspected finding was the occurrence of red shifted visual pigments in *Photostomias sp*. which is therefore the fourth species of dragonfish with this capability. (R. Douglas, J. Partridge)

Morphological investigations of the visual system will focus on three major aspects: We shall investigate the optic tectum of deep sea fish and compare its functional morphology to that of the zebrafish as a current model system. Furthermore, in five speciments of pearleyes the specific role of bundles photoreceptors will be studied because they occur next to randomly arranged rods in the same retina and allow a direct comparison of the cellular basis of signal processing in the inner retina. Finally the visual system of the four-eyed fish *Dolichopteryx sp.* will be studied. (Wagner)

For the study of biological rhythms melatonin samples were collected in several species of mesopelagic fish and cell lines established destined at testing the molecular biology of clock genes. In addition, ERG data in crustations prepared by T. Frank show that only species of the shallower depths show an endogenous component of their sensititvity profile whereas species of the deeper water layers do not.

Finally, 23 ocean bottom seismometers were deployed for long term recording of seismic activity in the subduction zone where the Louisville Ridge undersects and separates the Tonga and Kermadec Trenches. This is part of a new project of seismic investigations (TOTAL) to start officially ìn January 2008. In addition, bathymetric profiling of the trech regions and the Louisville gap was performed (E. Flueh).

Zusammenfassung

Hauptgegenstand dieser Fahrt war die Untersuchung der Wahrnehmungsprinzipien von Biolumineszenz in der Faune der mittleren Wassertiefen zwischen 200 und 700m. Weiterhin sollte das Vorkommen von endogenen circadianen Oszillatoren geprüft werden, die als mögliche Auslöser für die täglichen vertikalen Wanderungen dieser Tiere angesehen werden können. Wir führten 20 Fänge zwischen Tiefen von 200 und 700m durch und entnahmen Augen und Gehirne von mesopelagischen Fischen. Diese wurden zum Teil für akute Experimente an Bord verwendet oder fixiert und zur weiteren Untersuchung in den Heimatlabors konserviert.
Von den gefangenen Fischen wurden andere Gewebe für weitere Untersuchungen verwendet. Dazu gehörten zum einen elektrophysiologische Messungen zur Aufklärung der Wirkung von hohen Drücken auf das Membranpotential von Skelettmuskelzellen, und zum anderen Experimente zur Toxizität von iatrogenen Umweltgiften wie PCBs und DDTs auf den Lebermetabolismus.
Ein weiteres wichtiges Projekt umfasste die Untersuchung von Lebensgemeinschaften der hadalen Fauna. Zu diesem Zweck wurden fünf Tauchgänge mit den Autonomen Vehikeln des Oceanlabs der Universität Aberdeen in Tiefen von 6000m, 7049m, 8170m , 9000m und 10,015m durchgeführt. Diese Geräte tragen Köder und sind mit einer Kamera ausgerüstet, welche in festgelegten Zeitintervallen den Besuch der Köderfallen registriert. Nach 12 h am Boden steigt das Gerät an die Oberfläche und wird an Bord genommen. . Dabei wurde in 7.100m Tiefe Fischen gesichtet (*Notoliparis kermadecensis*) , was eien Premiere daratellt, da dabei auhc Verhaltensmuster in situ aufgezeichnet wurden. Auch Fressverhalten in der Hadalzone konnte erstmals dokumentiert werden. Weiterhin wurden hunderte von Amphipoden mit an Bord gebracht, welche die Basis für genetische Populationsanaylsen darstellen und auch die Zonierung der beutefangenden Amphipoden entlang des Grabenprofils áufzeigen werden. Temperaturdaten, welche ebenfalls gesammelt wurden zeigten einen linearen Anstieg der Temperatur von 5000m bis 10.000m. Die 10.000m Marke stellt auch in technologischer Hinsicht einen wichtigen Meilenstein dar, welcher nunmehr weitere systemische Erforschungen der Lebensgemeinschaften in den Tiefseegräben möglich machen wird.
Bei 47 Exemplaren von Laternenfischen (Myctophiden) aus 20-25 Spezies wurden die Photopigmente untersucht . Durch diesen vresuchsansatz wird es erstmals möglich die adaptiven Veränderungen ohne die Störvariablen wie Tiefe oder vertikale Wanderung innerhalb einer Faimliezu analysieren. Ein weiterer und unerwarteter Befund war die Entdeckung eines Photopigments mit Absorptionsmaximum weit im Langwelligen bei *Photostomias sp*.. Dies ist damit die vierte Art von Drachenfischen mit dieser ungewöhnlichen Spezialisierung. (R. Douglas, J. Partridge).

Die morphologischen Untersuchungen des visuellen Systems konzentrieren sich auf drei wesentliche Komplexe: Das Tectum opticum der Tiefseefische soll im Vergleich zur „Modell-Spezies“ Zebrafisch analysiert werde. Weiterhin bieten die fünf Exemplare von *Scopelarchus* die Gelegenheit, die Funktion von Photorezeptorbündeln zu studieren, da bei dieser Art Stäbchen in Bündeln und ohne Ordnung nebeneinander vorkommen und damit einen direkten Vergleich der zellulären Basis der intraretinalen Informations-verarbeitung ermöglichen. Schließlich soll das visuelle System des „vieräugigen“ Fischs *Dolichopteryx sp* untersucht werden.

Zur Untersuchung der biologischen Rhythmen wurden Melatoninproben bei mehreren mesopelagischen Arten gesammelt und Zell-Linien etabliert, welche die Aufklärung Molekularbiologie von Oszillatorgenen von Tiefseefischen ermöglichen werden. Bei Crustaceen konnte T. Frank in ihren ERG Versuchen zeigen, dass oberflächennahe Arten

eine ausgeprägten endogenen Rhythmus der visuellen Empfindlichkeitbesitzen, tiefer lebende Arten dagegen nicht.

Schließlich wurden noch 23 OzeanBodenSeismometer (OBS) ausgebracht, um die Subduktionszone in dem Bereich zu untersuchen, wo der Louisville-Rücken den Tonga und den Kermadec-Graben durchschneidet und trennt. Diese Arbeiten gehören zu dem TOTAL Projekt, welches im Januar 2008 in vollem Umfang beginnen soll. Während der gesamten Fahrt wurden darüber hinaus bathymetrische Profile erstellt aus den Graben Regionen sowie aus dem Bereich des „Louisville gaps“.

1. Introduction

1.1.Bioluminescence

A number of recent biological cruises in the eastern North Atlantic have included studies of the photobiology of the midwater fauna as a key objective. This research field mainly comprises the linked elements of visual physiology and bioluminescence. It is important that the generalisations and hypotheses that have arisen from this work (for reviews see: Douglas et al., 1998a, Wagner et al., 1998) should be tested on a wider faunal and environmental range. The opportunity to extend these studies to the fauna of the Pacific is therefore a very timely one.

There are two basic aspects in the study of vision in deep sea animals. Firstly, since sunlight plays only a minor role between 500 and 1,000m of depth, and is no longer detectable below 1,000 m, bioluminescence is the major source of light; it is found in numerous species inhabiting this mesopolagic habitat (Herring, 1987, 1996, 2002). Observations in the "wild" from submersibles, and from specimens recovered alive from catches in the laboratory have shown a remarkable diversity of spatial and temporal patterns of bioluminescence. Unfortunately the biological significance of these often highly elaborate displays are largely a matter of speculation. The probable uses range from camouflage by counterillumination of the ventral side (hatchetfish), disturbance of predators by release of luminous clouds; intraspecific signalling or identification of sexual mates; luminous lures (anglerfish); illumination of potential prey by "headlight photophores" (some lanternfishes). In general, the wavelengths emitted by the photophores match closely the colour of the downwelling sunlight at mesopelagic depths, i.e. the light produced is bluish-green (λ_{max} about 480nm). In very few cases (which are also of special interest during this cruise), however, dragonfish carry light organs emitting far red light under their eyes, in addition to the ordinary blue photophores elsewhere on their bodies.

Secondly, the receiver of this bioluminescence needs to be studied, including the special adaptations of the optical media (cornea, lens), and the visual pigments of the photoreceptors. A number of deep-sea fishes have conspicuously yellow lenses, or yellow pigments embedded in their retinae (e.g. some Scopelarchids). Douglas et al. (1998a) could show that this apparently counterproductive adaptation can be used to break the counterillumination camouflage of bioluminescent fishes such as hatchetfishes. Recent studies of the visual pigments in the outer segments of retinal photoreceptors have yielded a number of highly interesting observations. Bleaching of these visual pigments by photons triggers the stimulation cascade which ultimately leads to a visual perception. Visual pigments (rhodopsins) contain a protein moiety, the amino acid composition of which ultimately determines their spectral sensitivity. In a broad comparative analysis of nearly 200 species of deep-sea fishes Douglas et al. (1995, 1998a) and Douglas & Partridge (1997) have shown that in these animals, the spectral sensitivity of the rhodopsins is so tuned as to make them maximally sensitive to both the residual sunlight and the bioluminescent emissions (λ_{max} 460-490nm).

Three genera of deep-sea dragon fish (*Malacosteus, Aristostomias* and *Pachystomias*), whose suborbital photophores have emission maxima beyond 700nm, have visual pigments very different to those of other deep-sea fish (see above). To enable them to see their own far-red bioluminescence, which will be invisible to all other animals in the deep-sea, these animals have been shown, using retinal extracts and microspectrophotometry, to posses two long-wave shifted visual pigments, giving them a private wave-band which they can use for covert illumination of prey or for intraspecific communication immune from detection by potential predators (Partridge & Douglas, 1995). These 2 pigments form a so called ‘pigment pair’; in which both pigments utilise the same opsin which in some

photoreceptors is bound to the chromophore retinal (an aldehyde of vitamin A_1) forming a rhodopsin pigment, while in other receptors the same opsin is bound to the vitamin A_2-derived chromophore 3, 4 dehydroretinal, forming a porphyropsin pigment. Recently, using a retinal wholemount technique, we have demonstrated the existence of an additional longer-wave absorbing, pigment in the retinae of *Aristostomias tittmanni* (Partridge & Douglas, 1995) and *Pachystomias microdon* (Douglas et al., 1988a). This pigment is a rhodopsin, utilising retinal as its chromophore bound to a second, longer-wave absorbing, opsin. Perhaps surprisingly, we have been unable to find a similar third pigment in *Malacosteus niger*. This species instead employs a chlorophyll-derived photosensitizer to enhance its long-wave sensitivity (Douglas et al., 1998b). The demonstration of a chlorophyll-derived photosensitizer in *M. niger* is in many way astonishing. Firstly, it has never before been suggested that chlorophyll, which is central to plant photosynthesis, might have a role to play in animal vision. Secondly, photosensitizers were previously unknown in vertebrate eyes. We hope to collect additional specimens of dragon fishes in order to obtain new material which will enable us to continue these exciting investigations (carried out by Prof. R. Douglas, City University, London and Dr. J. Partridge, University of Bristol).

The morphological organisation of the retina in deep-sea fishes shows a number of striking adaptations which can be interpreted in terms of optimising the catch of the rare photons available in the mesopelagic habitat. Above all, deep-sea fish retinae, as a rule, contain only the more sensitive rods. In addition, the surface of the photoreceptive membrane, i.e. the number of discs in the rod outer segments has been greatly increased based on two alternative mechanisms: Either the rod outer segments are unusually long, far exceeding 100µm, or there are shorter rods, but arranged in multiple tiers, again adding up to a total length of up to 200µm or more. At the same time, the overall thickness of the neural retina and the density of retinal neurons is markedly decreased. Notably, however, every major transmitter system typically found in other vertebrate retinae is also present in the specialised retinae of deep-sea fishes (Wagner et al., 1998).

A further specialisation of some deep-sea retinae is found in the ganglion cell layer (and sometimes also in the photoreceptor layer). It regards regions of particularly high cell densities (areae retinae) or even foveae (similar to primates) suggesting that some sectors of the visual fields are processed at high resolution. In these regions, the high convergence rates from rods to ganglion cells which usually are the hallmark of high sensitivity are markedly reduced (Collin et al., 1997). We have pursued these studies and refined them by using special labelling techniques which allow the unequivocal identification of retinal ganglion cells. In some cases we have also been able to microinject retinal ganglion cells in order to study their differentiation, and compare them to the number of ganglion cell types in other vertebrate retina. Whereas about two dozen different ganglion cell types are found primates, the deep-sea eel Synaphobranchus kaupii retina contains less than half that number, i.e. ten different types (Hirt and Wagner (2005). This indicates that viusal processing in the retina must substantially different in deep sea fish.

Two projects arise from these previous findings which are relevant for the cruise So-194:

In the first experiment we want to study the ganglion cell differentiation in the pearleye Scopelarchus, because its retina contains several regions with distinct differennces, among them areas with grouped and ungrouped photoreceptors (Wagner et al., 1998) . Grouped photoreceptors have also been found in a number of surface-living teleosts, and their biologcal funtion is currently under investigation in several labs during DFG funded project. The pearleye retina offers a unique opportunity to approach this question because it contains the “control”region in the same retina.

Second, since there is an obvious reduction in the complexity of visual processing in the

retina in deep sea fish, the next logical step is to ask whether the optic tectum also reflects this trend. Therefore, we want to use classical silver stainng in addition to immun-staining against several neural and glial markers to characterise the functional morphology of the optic tectum in several species of mesopelagic fish and compare them to the tectum of the zebrafish as a model for a highly developed optic tectum.

1.2. Biological rhythms in the deep sea

Regions of the deep sea below the reach of sunlight i.e. 1,000m were long thought to present a habitat of particularly stable conditions whereas the upper water layers are governed by sunlight-dependent, diurnal rhythms demonstrated e.g. by the massive vertical migrations of the mesopelagic fauna. However, there are other important physical factors such as water currents that penetrate to abyssal depths. Several massive thermohaline currents in the North Atlantic lead to a layering of the deep water column, and the impact of tidal current changes is effective down to the bottom of the deep sea (Gould and McKee, 1973; James, 1982; Lampitt *et al*., 1983; Vangriesheim and Khripounoff, 1990) imposing a temporal structure on this domain. In this way, the solar rhythms of the surface layers could be substituted by tides that are predominantly under lunar control and regulate the biological activity in deep demersal habitats. Unfortunately, long term recordings of current flow velocities and directions are more easily accomplished than observations of the behavioural activity of demersal animals, which require frequent trawls or continuous video monitoring. In a previous investigation we studied a possible correlation between cyclic current changes and biological rhythms in the deep sea eel *Synaphobranchus kaupii* and the grenadier *Coryphaenoides (Nematonurus) armatus* (Wagner et al., 2007).
In case of the mesopelagic fauna a vast population undertakes vertical migrations from daytime depths of about 600m to about 200 m at night, in order to feed in the nutrient-richer upper water layers at lower risk from predation. Their mid-water habitat is clearly reached by residual sunlight, therefore it may be expected that light plays a decisive factor in the control of their diel activity cylce. However, it is unclear whether the migration is controlled by a strategy where the fish choose to remain at a constant level of illumination, or whether an internal clock controls this behaviour; it is also possible that both mechanisms are used in conjunction.

In order to study the presence of an internal diel clock (oscillator) we study the level of melatonin in the pineal organ and the retina. Melatonin is a mediator hormone which transmits central nervous system (CNS) generated biological rhythms to organs of the somatic periphery via the systemic circulation in all vertebrates (Reiter, 1991). It is synthesised and secreted by photoreceptors, and photoreceptor-derived neuroendocrine cells in the pineal gland and the retina of the lateral eyes (Ekström and Meissl, 2003). An additional source of melatonin may be the gastrointestinal system (Huether, 1993). In teleosts, the pineal gland is the essential source of systemic melatonin, whereas retinal melatonin is thought to have a more paracrine role for the control of adaptational processes (Behrens *et al*., 2000). In lower vertebrates the pineal gland is photosensitive and capable of perceiving the duration and intensity of the ambient light phases. Pineal photoreceptors are well suited for this purpose because, contrary to their retinal counterparts, they act as luminance detectors with sustained, intensity related membrane potentials during steady illumination (Kusmic *et al*., 1992). In addition to its role as a photoendocrine transducer, the pineal organ in the shallow-water teleosts studied contains a complete rhythm generating system, located within individual photoreceptors (Falcon *et al*., 2003) and maintaining a circadian pattern of melatonin secretion in the

absence of external light stimuli. This clock can be reset by light stimuli. The function of the circadian clock has been studied in culture systems of isolated pineals or photoreceptors where the amount of melatonin release could be monitored. The biological effect of melatonin rhythms in teleosts has been best characterised with relation to locomotor activity patterns (e.g. catfish *Heteropneustes fossilis*, Garg and Sundararaj, 1986). On the other hand, there is little direct evidence to date for a major role for melatonin in the control of reproduction (review: Ekström and Meissl, 1997).

An alternative approach to the study of biological rhythms is the investigation of the molecular "machinery" reponsible for cyclic changes in the gene expression and physiology of a cell. The following relevant genes have been characterised in zebrafish: *clock*, *bmal1*, *bmal2*, *per1*, *per2*, *per3*, *cry1a*, *cry1b*, *cry2a*, *cry2b* and *cry3.* The presence of these genes in mesopelagic fish needs to be established as a first step by establishing a cDNA library from several tissues and to test for sequences known from zebrafish. This will enable us to synthesise PCR primers and to study the experssion of the oscillator genes in mesopelagic fish. For this purpose, cell culture systems need to be established on board that can be preserved for transfer to the home lab, and recultures there und standard conditions.

1.3. Scavenging fauna of the Kermadec and Tonga Trenches (6000-10,000m)

Oceanlab, University of Aberdeen, UK& Oceanographic Research Institute, Japan
Dr. Alan Jamieson, Dr. Martin Solan, Dr. Toyonobu Fujii (Oceanlab),
Dr. Asako Matsumoto (ORI)

Background

From the sea surface to the hadal zone (6000-11,000m) there is progressive increase in pressure and remoteness from surface-derived food. Food from the surface arrives at the deep sea floor in two main forms, particulate organic matter (POM) and carrion such as fish or cetaceans carcasses. The quantity of POM reaching the sea floor decreases with depth so that at >6000m food supply is extremely sparse but in principle carrion falls should occur independent of depth since beyond 1000m there are no pelagic scavengers or mechanisms to impede descent to the sea floor. This concept is supported by Priede *et al.* (1990) who found higher numbers of scavenging Marcourids attracted to baited cameras at 5900m in the oligotrophic Central North Pacific than at 4100m under the productive California current. This was explained in terms of optimal foraging theory, that fish at 4100m had alternative food supplies to exploit whereas in the Central Pacific they are more dependent of carrion falls. Similarly Hessler *et al.* (1978) suggested that mobile scavengers may play a proportionately more important role in hadal communities. Observations of fish at the transitional depths between the abyssal plains and hadal trenches are extremely sparse. Observations made close to 6000m on the edge of the Philippine trench and the Chile Trench yielded similar results to equivalent depths representative of abyssal plains (Hessler et al., 1978). However, no fish were observed at baits placed into the trenches beyond 6000m (6717 and 7196m in the Chile trench, 9600m in the Philippine trench, and 10,500m in the Mariana trench). These baited camera observations however, were made at the lower depths where the occurrence of fish has been proven and at the maximum depth of the trenches where fish perhaps do not inhabit, but is difficult to confirm due to lack of major sampling effort. The trawling efforts of the Soviets and Danish expeditions have proven fish do inhabit the hadal zone therefore a reasonable conclusion that although fish populations exist in the trenches beyond 6000m, there are low in numbers and density can be drawn.

The combined historical data do not allow a strong determination of depth succession of fish species in the abyssal-hadal transition zone as no quantitative analysis has been seriously attempted. With the limited number of trawls at depths exceeding 8500m (about 35) and number of baited camera**s** deployed in the abyssal-hadal transition zone (<10) it is possible that the apparent decline in numbers and abundances of fish species will prove to be incorrect when more adequate sampling efforts become available.

Objectives;

- To observe the transition between abyssal and hadal scavenging species.
- Observe behavioural/physiological adaptations of fish at extreme depths
- Identify the maximum depth at which fish occur.
- Collect hadal amphipods for taxonomic, population structure and genetic analysis.
- Prove new technology capable of operating at 10,000m+.

1.4. Anthropogenic pollutants in the Deep-Sea (B. Lemaire, J.-F. Rees)

Several studies have shown that deep-sea fishes are severely contaminated by organochlorine compounds, such as PCBs and DDTs. However, none has ever shown the physiological consequences of such a contamination. These substances can possibly exert their toxicity in the liver during the phase 1 of detoxication process (involving cytochrome P450), by the generation of reactive oxygen species. Last year, for the first time in a deep-sea fish, positive correlations were found in liver samples of *Coryphaenoides rupestris* between the levels of activity of antioxidant enzymes (CAT and SOD), those of EROD (CYP450 activity) and the levels of PCBs/DDTs contamination. In vivo studies (using Precision Cut Liver Slices) are now being conducted to determine whether this species is resistant or not to the toxicity of such pollutants due to of the low levels of EROD activity found.

Organochlorine compounds (OCs) are ubiquitous man-made chemicals which consist of carbon skeletons with chlorine atoms covalently bound to it. Among these micropollutants are the long-lived PCBs (209 congeners, 1 to 10 chlorine atoms substituted) and DDTs (DDT/DDD/DDE). PCBs have been of major interest for industries during last century (antifouling paints, transformers, condensers) due to their high resistance to physical, chemical and biological degradations. DDT, on the other hand, was a main insecticide used in agriculture at that time. In the latter, anaerobic/aerobic degradation can occur, but, unfortunately, metabolites (DDD, DDE) seem to exert at least the same toxicity as DDT. OCs are comprised in the group of Persistent Organic Pollutants (POPs), like HAPs, furans and dioxins.

PCBs and DDTs are highly lipophilic and therefore can adsorb onto organic matter (OM). The deep-sea floor acts as a global sink for these compounds, due to the inputs of OM in the deep layers of oceans during marine snow process. Those pollutants, concentrate on the deep-sea floor and are ingested by bottom feeders. The demersal trophic chains, starting from those invertebrates, ends at the level of the benthopelagic carnivorous fishes. It is well established that the level of contamination found in any organism is positively correlated to its trophic level (bioaccumulation process). Considering this, it is not surprising that deep-sea fishes are 10 to 100 times more contaminated than shallow ones.

Once those micropollutants are ingested (through the integument and by prey ingestion) they distribute in the body and “nest” in the fat tissues, before being submitted to the

detoxication process (which is not always efficient for OCs). A particularly important organ for such micropollutants is the liver, the major site of lipid storage and detoxication.

During phase 1 of detoxication, polar groups are added to the xenobiotics (action of cytochrome P450 ; CYP450). This event helps to conjugate them to small biomolecules for the excretion in bile or urine. To achieve its function, CYP450 uses the electrons withdrawn from molecular oxygen. The reductase sub-unit can sometimes work inefficiently and leakage of electrons leads to the formation of Reactive Oxygen Species (ROS). These are highly reactive radicals, i.e. molecules that can easily oxidise lipids, proteins and DNA. Therefore PCBs and DDTs can exert their toxicity notably by oxidative stress, which can be defined as the unbalance between prooxidant and antioxidant forces. Of great concern are the deep-sea fishes, because, while being heavily contaminated, they show low activities of antioxidant enzymes (EAOX).

Last year, we studied the hepatic levels of contamination in a top predator of the Northern Atlantic slope, the benthopelagic rattail *Coryphaenoides rupestris* (samples from RRS Discovery cruises, September 2000 to September 2002). We also investigated the physio-pathological consequences of such a contamination by studying the levels of activity of antioxidant enzymes (CAT, SOD) and of a well known CYP450 activity, EROD (CYP1A1). Importantly, this study was realised with 51 liver samples (very rare in deep-sea fish studies), selected to represent as best as possible the natural populations.

Our study has clearly demonstrated, for the first time ever in a deep-sea fish, signs of a physiological impact, since positive correlations were found between the levels of activities of EAOX, EROD, and the levels of PCBs (23 congeners) and DDTs contaminations. However, while the levels of CAT activities were huge, levels of EROD were found quite low with regard to the levels of contamination.

1..5. Project TOTAL – Seismic Investigations (E. Flueh, IFM-GEOMAR, Kiel)

Subduction zones are the seismically most active Regions of the Earth. Especially thrust events in the seismogenic zone between 10 and 40 km depth pose threat to costal populations. Where the Louisville Ridge intersects and separates the Tonga and Kermadec Trenches a remarkable seismic gap is seen. This can be interpreted as an asperity, that potentially can break in the near future. Project TOTAL (**TO**nga subduction zone **T**hrust earthquake **A**sperity at **L**ouisville ridge) aims at studying this asperity (Figure 1.4.1). The seismic gap is much wider than the characteristic width of the seamounts that comprise Louisville Ridge (Figure 1.4.2). We therefore speculate that other structures than the volcanic edifices in senso strictu are responsible for the seismic coupling. Studying the structure and composition and thermal state of both the incoming and the upper plate will therefore lead to a better understanding of asperities in subductions zones.

Project TOTAL is scheduled to be carried out using RV SONNE in January/February 2008. The planned work comprises seismic, seismological, gravimetric, magnetic, geothermal and hydrographic data collection. Due to the fortunate circumstances that RV SONNE is cruising in the area during SO194, it was decided to deploy a seismological network during this cruise and thereby extend the observation period to more than six month. This network will allow us to determine if smaller events (not detectable at telesesimic distances) do occur in the seismic gap or if coupling is 100 % perfect.

On global maps a retreat of the volcanic front, the trench and the forearc north of Louisville Ridge is quite apparent. This erosion of the upper plate should be documented in the deformational style of the forearc, which can be seen in detailed bathymetric maps. We therefore also used cruise SO194 to collect bathymetric data in an optimized way, rather than random profiles as necessary for the biological work that SO194 is aiming at.

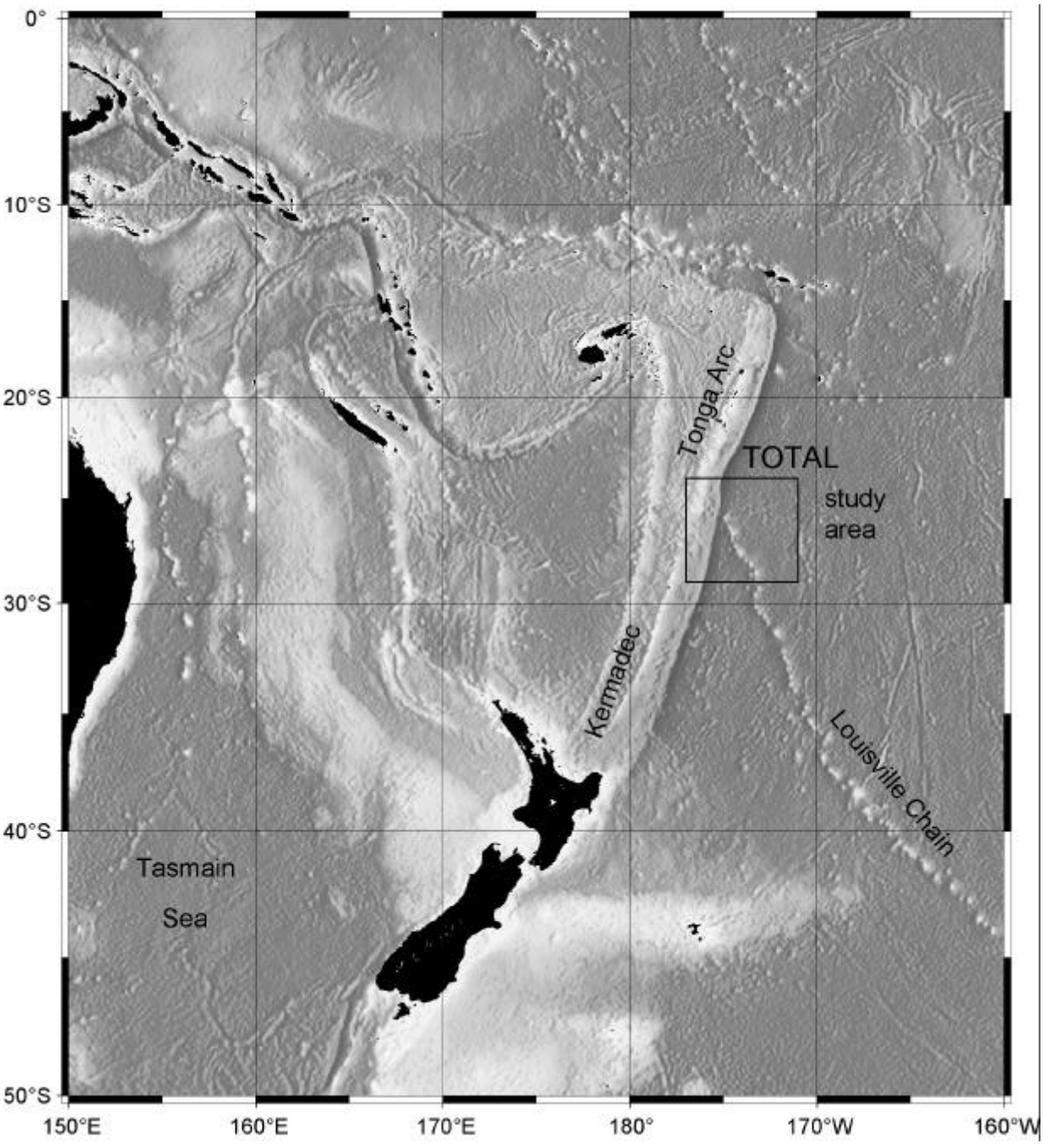

Figure 1.6.1: Study area of TOTAL with main morphological units**.**

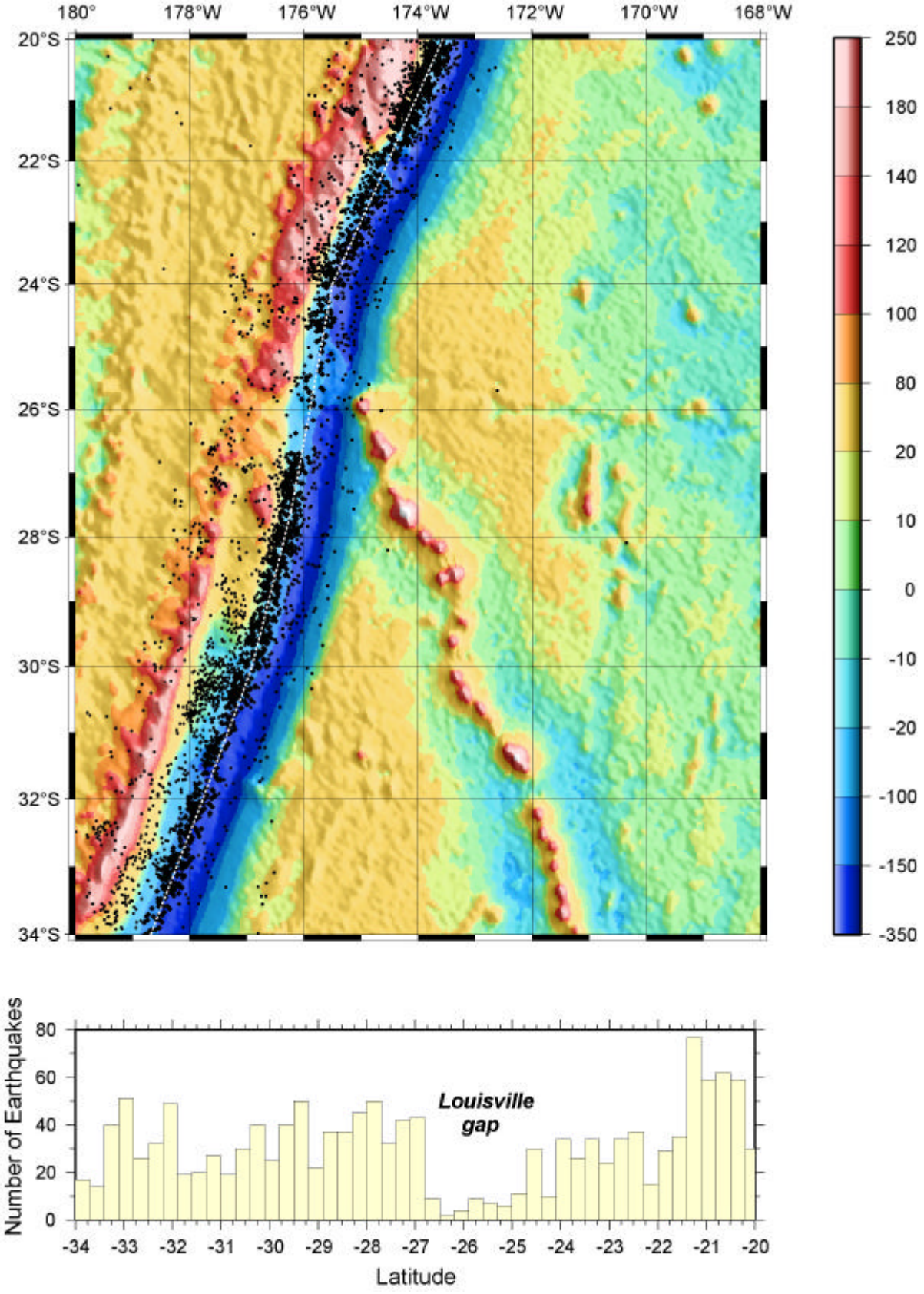

Figure 1.6.2: Top:Gravity Field of the working area and earthquakes after Engdahl and Villasenor, (2002); bottom: number of earthquakes averaged in 1 degree segments.

2. Participants

2.1. Scientific party

Wagner	Hans-Joachim	Uni Tübingen	Chief Scientist
Flüh	Ernst	IFM-GEOMAR	Co Chief Scientist
Mattheus	Ulrich	Uni Tübingen	
Wendlandt	Nils	Uni Tübingen	
Brunn	Wiebke	IFM-GEOMAR	
Rohde	Anne-Dörte	IFM-GEOMAR	
Jamieson	Alan	OCEANLAB	
Solan	Martin	OCEANLAB	
Fujii	Toyonobu	OCEANLAB	
Matsamoto	Asako		
Douglas	Ron	City Univ. London	
Partridge	Julian	Bristol University	
Friedrich	Oliver	Uni Heidelberg	
Haas	Tobias	Uni Heidelberg	
Lemaire	Benjamin	Uni Louvain	
Frank	Tamara	HBOI	

2.2. Crew

MEYER, Oliver	German	Kapitän / Master
ADEN, Nils-Arne	German	I. Offizier / Ch. Mate
BÜCHELE, Heinz-Ulrich	German	Naut. Wachoffizier / NWO
KORTE, Detlev	German	Naut. Wachoffizier / NWO
DR. SCHLENKER, Wilhelm	German	Schiffsarzt / Surgeon
GUZMAN-NAVARRETE, Werner	German	I. Ingenieur / Ch. Engineer
REX, Andreas	German	II. Ingenieur / 2nd Engineer
BUSS, Jörg	German	II. Ingenieur / 2nd Engineer
RIEPER, Uwe	German	Elektriker / Electrician
ANGERMANN, Rudolf	German	Ltd. Elektroniker / Ch. Electron.
-		Elektron. (Zusatzpers.)
GROSSMANN, Matthias	German	System-Manager / Sys.-Man.
-		Sys.-Man. (Zusatzpers.)
BLOHM, Volker	German	Decksschlosser / Fitter
STEGMANN, Tim	German	Motorenwärter / Motorman
NOACK, Robert	German	Motorenwärter / Motorman
-		SM-Azubi / Apprentice
TIEMANN, Frank		Koch / Ch. Cook
ORYSZEWSKI; Krysztof	Polish	Koch / 2nd Cook
GRUEBE, Gerlinde	German	I. Steward / Ch. Steward
POHL, Andreas	German	II. Steward / 2nd Steward
MUCKE, Hans-Peter	German	Bootsmann / Boatswain
DEHNE, Dirk	German	Matrose / A.B.
HÖDL, Werner	German	Matrose / A.B.
KRAFT, Jürgen	German	Matrose / A.B.
BIERSTEDT, Torsten	German	Matrose / A.B.
FRYE, Thorsten	German	Matrose / A.B.
FINCK,Christiian	German	Matrose / A.B.
FINCK, Christian	German	Matrose / A.B. oder SM-Azubi
HEINRICH, Finn-Janning	German	SM-Azubi/Apprentice

2.3. Affiliation and Addresses of Scientific party

Prof. Dr. H.-J. Wagner, U. Mattheus, N. Wendlandt
Anatomisches Institut
Universität Tübingen
Österbergstr. 3
D-72074 Tübingen
Germany
hjwagner@anatu.uni-tuebingen.de

Prof. Ron Douglas
Department of Optometry & Visual Science
City University
Northampton Square
London EC1V 0HB
UK
r.h.douglas@city.ac.uk

Dr Julian C Partridge
Reader in Zoology
School of Biological Sciences
University of Bristol
Woodland Road
Bristol BS8 1UG
UK
T: +44 117 9287591
E: j.c.partridge@bristol.ac.uk

Dr. Alan Jamieson, Dr. M. Solan, T. Fujii
PostDoc Research Fellow
Oceanlab, University of Aberdeen
Department of Zoology
School of Biological Science
Main Street
Newburgh, Aberdeenshire AB41 6AA
a.jamieson@abdn.ac.uk

Dr. Dr. Oliver Friedrich, T. Haas
Institute of Physiology & Pathophysiology
Medical Biophysics Group
University of Heidelberg
Im Neuenheimer Feld 326
69120 Heidelberg
Germany
Tel. +49-6221-54-4143
FAX: +49-6221-54-4123
e-mail: oliver.friedrich@physiologie.uni-heidelberg.de

Benjamin Lemaire (Ph.D.)
BANI Lab
Institut des Sciences de la Vie

Universite Catholique de Louvain-la-Neuve
B-1348 Louvain-la-Neuve (Belgium)
benjamin.lemaire@student.uclouvain.be
lemaire@bani.ucl.ac.be

Prof. Dr. Ernst R. Flüh, W. Brunn, A.D. Rohde
Leibniz-Institut für Meereswissenschaften
IFM-GEOMAR
Wischhofstr. 1-3
D-24148 Kiel
Germany
eflueh@ifm-geomar.de
WEB: http//:www.ifm-geomar.de

Dr. Asako K. Matsumoto
The Nippon Foundation-
Hadal Environmental Science/Education Program(HADEEP)
Ocean Research Institute,
University of Tokyo
1-15-1, Minamidai, Nakano-ku, Tokyo 164-8639
Japan
mail1:amatsu@gorgonian.jp
mail2:amatsu@ori.u-tokyo.ac.jp

3. Agenda of the cruise SO 194

Thursday, June 28 through Saturday, June 30th, and July,2nd:
Search, locate and recover equipment which has not arrived in time:
personal baggage, trawling net, buoyancy gear
First conference with capitain O. Meyer on Friday, June 29th

Sunday, July 1st:, 10th
Scientific party joins the ship; all present except M. Lemaire;
buoyancy gear still missing
General presentation of scientists and students; unpacking begins
Coordination of projects and activities
Diplomatic activity re Tongan observer; presence on board is waived; research activities granted

Monday, July 2nd
J.M. Lemaire arrives on board at 7.15; buoyancy gear arrives for landers
paperwork for Samoan authorities
Sonne leaves Apia at 9.00
Conference with capitain, members of the crew to specify ship's requirement for Tucker trawl net, lander deployment and recovery, and deployment of OBS
19.00:first trawl (200m,2h): good catch: hatchetfish, pearleye, dragonfish

Tuesday, July 3rd
!0.30h second trawl (500m, 2h) medium catch: hatchetfish, dragonfish
18.30 third trawl (150m 2.5h) good catch hatchetfish, dragonfish, lanternfish

Wednesday, July 4th
8.30h: Releaser Test OBS
Whale watching: Pod of 6-8 minkwhales joins the ship for more than 2h
12.45h fourth trawl (650m 2.5h) good catch hatchetfish, dragonfish, lanternfish, loosejaw, viperfish, pearleye
18.30h fifth trawl (200m, 2.5h)¸good catch hatchetfish, dragonfish, lanternfish, pearley, cookie-cutter shark with luminous belly

Thursday, July 5th
8.30h sixth trawl (550m, 2.5h) medium catch: hatchetfish, dragonfish, lanternfish
18.30h seventh trawl (250m, 2.5h) medium catch: hatchetfish, dragonfish, lanternfish, pearleye

Friday, July 6th
OBS deployment;
lander deployment 6000m
No trawl

Saturday, July 7th
Lander release and recovery
15.30 eigth trawl (500m, 2h) poor catch: few hatchetfish & lanternfish
18.00h lander deployment 7,000m
18.30h ninth trawl (50m 1.5h) poor catch:hatchetfish, lanternfish, cockie cutter shark

Sunday, July 8th

9.30h tenth trawl (700m, 3h) poor catch: hatchetfish, lanternfish, heteropods
16.00h lander release and recovery: good results: fish and shrimp at 7,000m
18.30h trawl #11 (200m, 2.5h) medium catch: hatchetfish, loosejaws, lanternfish

Tuesday, July 10th

Lander deployment: 8.000m
8.00 Trawl #12 (600m, 3h) Steel wire breaks on recovery! Repair on board
poor catch: loosejaw, hatchetfish, squid, heteropods
18.30 Trawl #13 (159m 2.5h) poor catch: loosejaw, hatchetfish, lanternfish

Wednesday, July 11th

OBS deployment
11h trawl #14 (550m 2h) poor catch. Loosejaw, hatchetfish
OBS deployment
18.45: trawl #15 (2oom 2.5h) poor catch, Loosejaw, hatchetfish, many heteropods
ocean floor bathymetry

Thursday, July 12th

Stormy wheather (force 6 and gales)
8.30h trawl #16: (700m, 3h) net comes back with severely bent top bar; needs repair; catch contains numerous baby myctophids
Lander recovery at force 5-6
ocean floor bathymetry

Friday, July 13th

Sea still too rough for trawling
10.30 deployment for 10,000m
ocean floor bathymetry

Saturday, July 14th

Lander recovery 10.30
11.00h trawl #17 (700m 3h) Dolichopterus, 4-eyed fish
17.00 lander deployment (9,000m)
18.30h trawl #18 (200m 2.5h) catch: hatchetfish; myctophid

Sunday, July 15th

8.00h trawl #19 (600m, 4h): hatchetfish, myctophids; viperfish
15.00h lander recovery
18.00h trawl #20 (200m 2.5h) good catch: Scopelarchus, Echiostoma, myctophids, Gonostoma; Melamphaeids

Monday, July 16th- Friday, July 20th

Transit to Auckland with intermittant bathymetry

4. Scientific equipment

4.1. Tucker trawl net (T. Frank)

We used a Tucker trawl net with an opening area of 3 m by 4 m, equipped with a timer controlled closing cod end brought by T. Frank from HBOI. The HBOI net (Tucker trawl) consists of 4 bars:

1) The tow bar, which is fitted with brackets to protect the instrumentation attached to it. In this case, a timer and a depth sensor were utilized.
2) The opening bar, which runs through the top sleeve of the net
3) The closing bar, which runs through the bottom sleeve of the net
4) The weight bar, carrying 350 pounds of weight and ensuring that the net remains at depth when open.

The 15 m long primary net consists of 5 mm knotless nylon, and funnels down gradually from a mouth opening of 12 m^2 to a 1 m diameter ring. Attached to this ring is a secondary net, 5 m long, composed of 292 μ nytex, which funnels down to a 15 cm diameter canvas sleeve. The dimensions and construction of the net are designed for a large initial capture area with sufficient flow through the knotless nylon to minimize drag on the net as well as damage to the animals.

The opening and closing bars are attached to bridles which are attached to the programmable net timer via a moving pin. The timer has two programmable cycles – during the first cycle, the pin pulls back to the first stop, releasing the bottom net bar and opening the net. During the second cycle, the pin pulls back to the second stop, releasing the top net bar and closing the net. The release cycles can be set in 10 minute increments from 10 minutes to 9 hours.

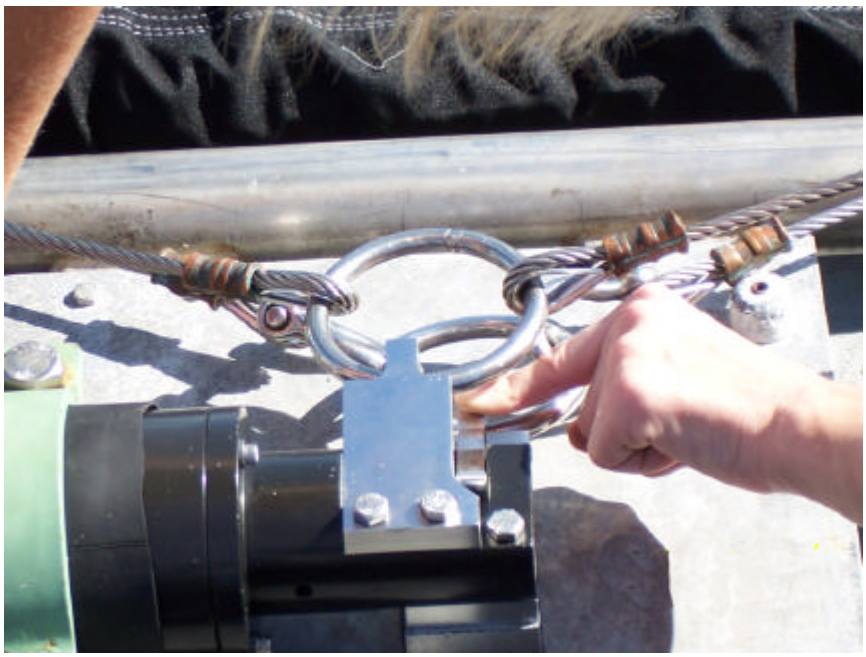

The net is sent down closed, to avoid clogging the net with gelatinous zooplankton (which are often abundant in surface waters) before it reaches fishing depth. During deep daytime trawls, the net was programmed to open after 30 minutes. During shallow nighttime trawls, the timer was programmed to drop the opening bar after 20 minutes.

The canvas sleeve of the secondary net attaches to temperature insulated, light tight

(when closed) cod-end. The cod-end, custom made by the engineering department at Harbor Branch, is constructed of 1.2 cm thick PVC, with ball valves at either end. Inside the cod-end is a canvas bag composed of 1 mm mesh. The ball valves are held open with a trigger pin attached via a line to the top net bar, and is sent down open. The section of the cod-end attached to the net contains a venturi, preventing the formation of a bow valve at the net to cod-end interface, which would reduce the entry of organisms into the cod-end. The trigger pin line is looped over the tow bar, so that when the top bar of the net closes, it pulls the trigger pin out of its holder, releasing the ball valves and closing the cod-end. The canvas sleeve on the secondary net is attached to a PVC end-cap, which fits onto the cod-end and is held in place via three removable speed pins. After the net is brought onboard, the cod-end is removed from the net and carried to a light-tight room (the environmental room), where animals are removed and sorted under dim red light. The use of a closing cod end is an essential prerequisite for most of the physiological and morphological work planned for this cruise. The closing cod end brought animals on board ship which were isolated against the high temperatures in the upper water layers, protected from mechanical damage during hauling, and shielded against the sunlight, i.e. dark adapted.

.A depth sensor from a Sonne CTD was attached to the frame, giving us information that could be downloaded after the trawl, on the depths at which the organisms used in our studies were captured.

4.2. Spectral photometer (R. Douglas & J. Partridge)

Measurements of visual pigment absorbance spectra were made from retinal whole-mounts and from detergent extracts of retinal cells, dissected from the eyes of deep sea fish.

4.2.1. Animals

Animals were caught in a $3m^2$ Tucker trawl fitted with a closing cod end (as described elsewhere in this report). In order to protect photolabile retinal pigments from exposure to light the entire catch was quickly transferred to the cold room, where the catch was sorted under dim red light. Selected animals were placed in light-tight containers in cold sea water before further processing. After removal of tissue, bodies were preserved in 10% formaldehyde solution in sea water and preliminary identifications were made using keys: Whitehead *et al*. (1986a,b, 1989), and, for myctophids, Wisner (1974).

4.2.2. Preparation of visual pigment extracts

For the extraction of visual pigments, eyes were removed under dim red illumination (head-torches fitted with red acetate filters passing wavelengths greater than 670 nm) after which they were subjected to procedures detailed by Douglas *et al.*, (1995). Briefly, eyes were dissected and retinae from a single animal placed in a 1.5ml Eppendorf tube and physically homogenized in 300 microlitres of TRIS buffered saline (pH 7.2, 280 mOsm/kg) with 30 microlitres of the detergent beta-D-maltoside (200mM in TRIS buffered saline). The tubes were wrapped in aluminium foil to exclude all extraneous light and placed on a rotator at room temperature (24-26^{o}C) for 1 hour before being placed in a cooled (4 ^{o}C) centrifuge and spun at 15k rpm (= 23000 g) for 10 mins in a Hettich Universal 30FR cooled centrifuge, the supernatant being retained for measurement..

4.2.3. Spectrometry of visual pigment extracts

150 microlitres of supernatant was removed from the visual pigment extract and placed in a quartz glass cuvette (Helma black-sided low volume: 105.201-QS). Normally 15 microlitres of 1 molar hydroxylamine in TRIS buffered saline would be added to the reaction at this stage and the cuvette placed in a holder in the spectrophotometer and left for 15 minutes to allow time for the hydroxylamine to convert all free retinal to the retinaloxime before absorption spectra were recorded. However, we has specific interest in longwave visual pigments which are often sensitive to hydroxylamine so this step was avoided.

Spectra (300-800 nm) were recorded using a Shimadzu UV-2101PC UV-VIS spectrophotometer before and after bleaching with actinic irradiation from a high intensity quartz halogen(QI) light source. Difference spectra between these measurements allowed the separation of the photo-labile visual pigments from photo-stable pigments such as blood and melanin.

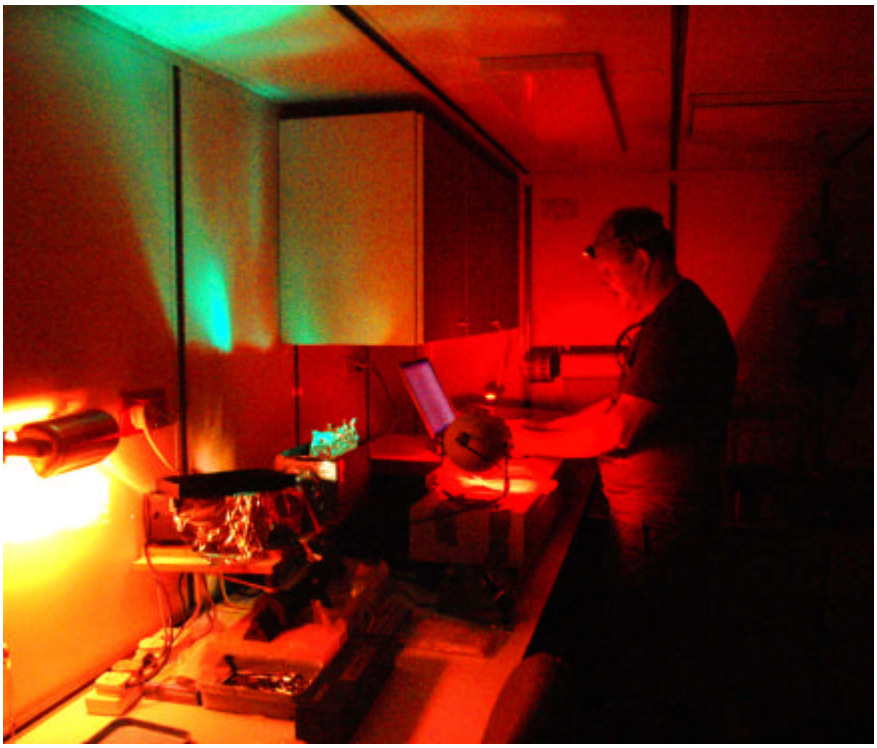

Figure 4.2.3.1: Darkroom with centrifuge, spectrophotometer, and bleaching light source

In order to determine whether extracted visual pigments were homogenous or mixed, partial bleaching methods were used. This procedure involved the controlled bleaching of the extract with longwave light generated by irradiating the sample with light produced by passing the output of the QI light source through Balzer B40 narrow band (25 x 25 mm, 10 nm FWHM bandwidth) interference filters. Absorption spectra were recorded following exposures to progressively shorter wavelengths, with difference spectra between sequential scans being calculated to reveal photolabile pigments (visual pigments in the case of retinal extracts) preferentially bleached by each light exposure, and hence whether such pigment(s) within each sample were single or multiple.

Visual pigment absorbance spectra were analysed first by creating sequential difference spectra and determining the wavelength of peak absorbance ($?_{max}$) with a VisualBASIC macro running in MS Excel. Data from the Shimadzu spectrometer were exported as ASCII text files in 1 nm intervals and a rhodopsin template best-fitted to the longwave limb of the data as described by Douglas *et al.* 1995. If the $?_{max}$ remained stable from bleach to bleach, indicative of a homogenous visual pigment extract, an overall difference spectrum was calculated between first and last measured absorbance spectra and the $?_{max}$ determined from these data. (See Fig of homogenous pigment partial bleach in results section)

Where mixed visual pigments were indicated by a shift in $?_{max}$ of the sequential difference spectra, the first difference spectrum which showed significant bleaching and the last difference spectrum were used to determine the $?_{max}$ values of the two visual pigments. (See Fig. of mixed pigments partial bleach in results section)

4.2.4 Spectrometry of pigments in retinal wholemounts

A modification of the protocol used for visual pigment extracts allowed measurements of pigments within intact retinal cells. In this case the visual pigment extraction stage was replaced by physically holding retinal samples, using specially made tissue holders (see figure) that fitted within the spectrometer cuvettes and which allowed the tissue to be held in the light path of the spectrophotometer. This method is optically challenging due to light scattering but has the advantage that pigments otherwise degraded by detergent extraction can be detected. For example, we have previously shown that the retinas of two genera of deep sea fish, *Pachystomias* and *Aristostomias*, have longwave pigments that cannot be isolated from retinal extracts.

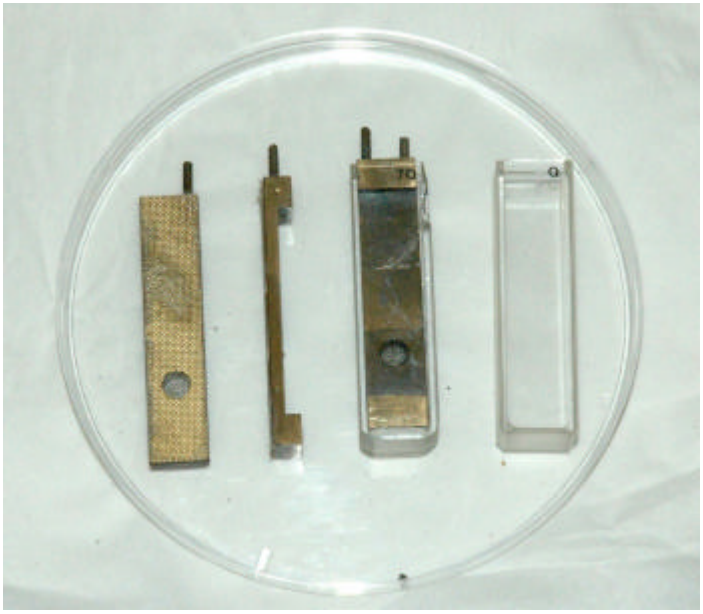

Figure 4.2.4.1: purpose built tissue holders used to hold sheets of retina in the light path of the spectrometer, within a standard 10 x 10 mm cuvette.

Retinal wholemount tissue from target species, especially *Photostomias*, a Malacosteid relative of *Artistostomias*, was held using the tissue holders and bathed in TRIS buffered saline, and was subject to partial bleaching and measurement protocols as described above. No hydroxylamine was added to the reaction conditions to avoid destroying certain pigments, including longwave sensitive visual pigments, which are often hydroxylamine sensitive.

4.3. Electroretinograms (ERGs, T. Frank)

4.3.1. Animals

Animals were removed from the cod-end and sorted into light tight containers under dim red light. They were maintained at 7^{o} C for at least 24 hours (with one exception) before being used in experiments, to ensure complete recovery from light-adaptation resulting from the bioluminescence of the various species in the cod-end.

4.3.2. Experimental set-up

Animals were attached dorsally to a plastic support with cyanoacrylate gel adhesive, and attached to an acrylic rod within a chilled seawater bath. In this preparation, animals remained alive and active during experiments lasting up to 3 d. Differential ERG recordings were made by placing a metal microelectrode (8-10 mO.) sub-corneally, a differential electrode on the animal's body, and an AgCL-coated wire grounding electrode in the seawater bath. The eye was dry in air during electrode placement to ensure a closed circuit, and then the water level was adjusted such that a small portion of the specimen's eye was in air above the water surface while the rest of the eye and the body were submerged in water. The A.C. signal obtained from the eye was amplified by a Haer XCELL 3 microelectrode amplifier, digitized by a National Instrumentents DAQ board, analyzed with a program written in Labview, and stored to disk for later of peak to peak response heights and flicker fusion frequencies.

The monochromatic stimulus light (Spectral Products, Model CM110 monochromator) was directed onto the eye of animals via one branch of a bifurcated, randomized fiber optic light guide (EXFO). In this way, the whole eye was bathed in diffuse light. A Uniblitz shutter (Model VS25) provided a stimulus flash duration of 100 ms, and stimulus irradiance was adjusted using a neutral-density wheel driven by a stepper motor, both of which were under computer control. Irradiance was calibrated with a radiometer (UDT Instruments, Model S370) using a calibrated radiometric probe. A fiber optic illuminator (Dolan-Jenner, DC-950) connected to the other branch of the light guide provided accessory illumination for experiments involving light adaptation. White light from the lamp was filtered with a 486 nm interference filters (Melles Griot, FWHM 10 nm). Irradiance of the adapting light was controlled by neutral-density filters.

The temperature of the water in the animal holding chamber was maintained by running cooling coils circulating an anti-freeze water mixture from a Lauda chilling circulator. The temperature of the Lauda was adjusted such that the temperature at the animal body, measured via an Omega HH11a microprobe thermometer placed 1 mm from the animal's body, was at the required temperature.

The microscope, water bath and microelectrodes were fastened to an aluminum plate to prevent movement during heavy seas. The aluminum plate was placed on air feet to dampen vibrations generated by the ship's engines, which are otherwise picked up by the microelectrodes, and attached to the top of the bench. A Faraday cage

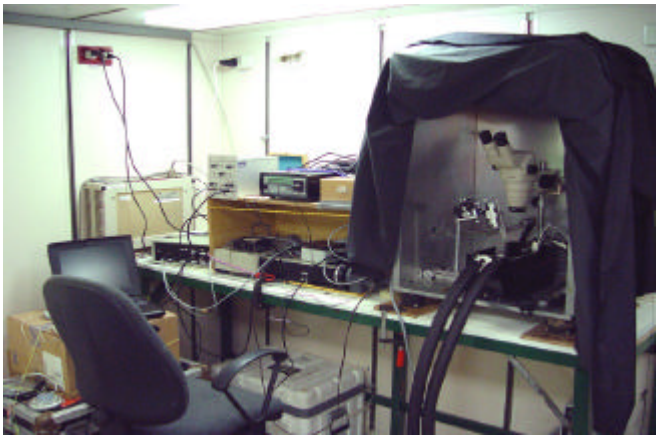

covered with a black cloth prevented introduction of stray light and electrical noise during the course of an experiment.

The gravimeter laboratory was used for electrophysiological recordings

4.3.3. Experimental Protocol

The extracellular response recorded from the eye, the electroretinogram (ERG), is the summed mass response from a large number of receptor cells. The electroretinogram was used to determine the photosensitivity, temporal resolution, and the presence of absence of a circadian rhythm in photosensitivity .

4.3.3a *Photosensitivity:* Peak to peak ERG response heights (*V*) were measured in response to 0.5 log unit increases in irradiance. These data can be used for comparisons of photosensitivity using the Zettler modification of the Naka-Rushton equation to generate VlogI curves. The model slope (m) and the log irradiance evoking 50 % of the maximum response amplitude (log *K*) can be used to provide an estimate of sensitivity The eye's dynamic range, defined as the log irradiance range evoking 5 – 95 % of the maximum response amplitude, can also be utilized as a measure of photoreceptor sensitivity.

4.3.3b Temp*oral Resolution*: Temporal resolution is inversely related to temporal summation, which is essentially extending the period during which photons can be sampled, much like holding the shutter on a camera open longer. With lower temporal resolution, which means longer summation, the object may be blurred, but at least there is sufficient contrast between the object and background that the object is visible. The temporal resolution of the eye were quantified using two methods: (1) response waveform dynamics, and (2) flicker fusion frequency. Waveform dynamics of the ERG in response to individual flashes of light will be analyzed for response latency and time-to-peak, defined as the amount of time elapsed from the onset of the light stimulus until the onset of the photoreceptor response (response latency) or the peak response (time-to-peak). Both parameters are calculated from flashes yielding response amplitudes approximately 50 % of the maximum amplitude, as determined from *V*/log *I* curves. Flicker fusion frequency experiments involved presenting the eye with a flickering stimulus light for 2 s at a given frequency with a 50:50 light:dark ratio, and recording the corresponding ERG . The frequency at which the eye could no longer respond to individual light flashes over a 0.5 s interval was defined as the critical flicker fusion frequency (CFF). As the irradiance of the stimulus light is increased, CFF increases to a maximum and then plateaus. Experiments began by determining CFF for the irradiance evoking an ERG response 20 µV above background noise. CFF was then determined for 0.5 log increases in irradiance until three successive irradiance increases did not result in CFF increases, providing a maximum CFF value.

Response latency, time-to-peak, and CFF were obtained from dark-adapted specimens at 6.5, 8.5, 10.5 and 12.5^{O} C, as increases in temperature have been shown to increase temporal resolution in insect photoreceptors. In addition, as light adaptation is known to improve the temporal resolution of euphausiid crustaceans, which were used in this study, data were also obtained from specimens in the presence of a dim adapting light under the various temperature regimes.

In all experiments conducted on dark-adapted individuals, test flashes of dim light were given after each stimulus or stimulus train to ensure the eye recovered to its initial state of adaptation before the next stimulus train was presented.

4.3.3c Circadian Rhythm in the ERG

Nocturnally active shallow water crustaceans possess a clear rhythm in the amplitude of the ERG in response to a flash of the same wavelength and irradiance over a 24 hour cycle, with sensitivity increasing at sunset and decreasing at sunrise. While deep-sea crustaceans might not appear to obtain any benefits from enhanced sensitivity at night, there are a number of species that undergo substantial vertical migrations, spending the day in deep dark waters between 600 – 800 m, and ascending at sunset to between 100 and 300 m. As their vertical migrations are cued to changes in downwelling irradiance, there might be a benefit to enhanced sensitivity at night. The presence of a circadian rhythm in one species of vertical migratory was tested. A program was written in LabView to present one flash (of predetermined wavelength and irradiance to generate a response slightly above background noise, to ensure that the test flash was not light-adapting the eye) every hour for 48 hours, and store the response amplitude to an excel file. Peak to peak response amplitude graphed vs. time will determine if any rhythmicity in the amplitude exists.
.

4.4. Intracellular Recordings (O. Friedrich)

A combined two-microelectode voltage clamp and Ca^{2+} epifluorescence microscopy setup was brought from the home lab in Heidelberg, Germany, and assembled in the Magnetic Laboratory on the FS Sonne.
The **electrophysiology rig** for intracellular stimulation and recording consisted of:

- GeneClamp 500 amplifier (Axon Instruments)
- AD/DA board Digidata 1200B (Axon Instruments)
- Microelectrode Headstages
- Electrically driven, 3-axis micromanipulators with joystick control
- Microelectrode puller (PiP5 HEKA)
- PC and aquisition software
- Glass pipettes, recording chambers, microelectrode holders, cable connectors, model cell

The **epifluorescence rig** for intracellular Ca^{2+} fluorescence imaging consisted of:

- Olympus CK40 inverted microscope
- Hamamatsu CCD camera
- Hamamatsu residual light intensifier with control unit
- Frame grabber and acquisition PC
- Polychromator illumination unit (Till Photonics) with glass fibre transmission
- Filter sets appropriate for excitation at 488nm (dichroic mirror, Omegafilters) and recording between 510 and 560 nm (bandpass filter, Omegafilters).
- Fluochrome Fluo-4 AM

For **preparation of single cells**, surgical micro-forceps and scissors, digestive proteins, preparation dishes and salts for physiological salines were brought. A binocular from the chief scientists lab was borrowed for preparation.

The setup was assembled and calibrated during the first three days (see Figure 1).

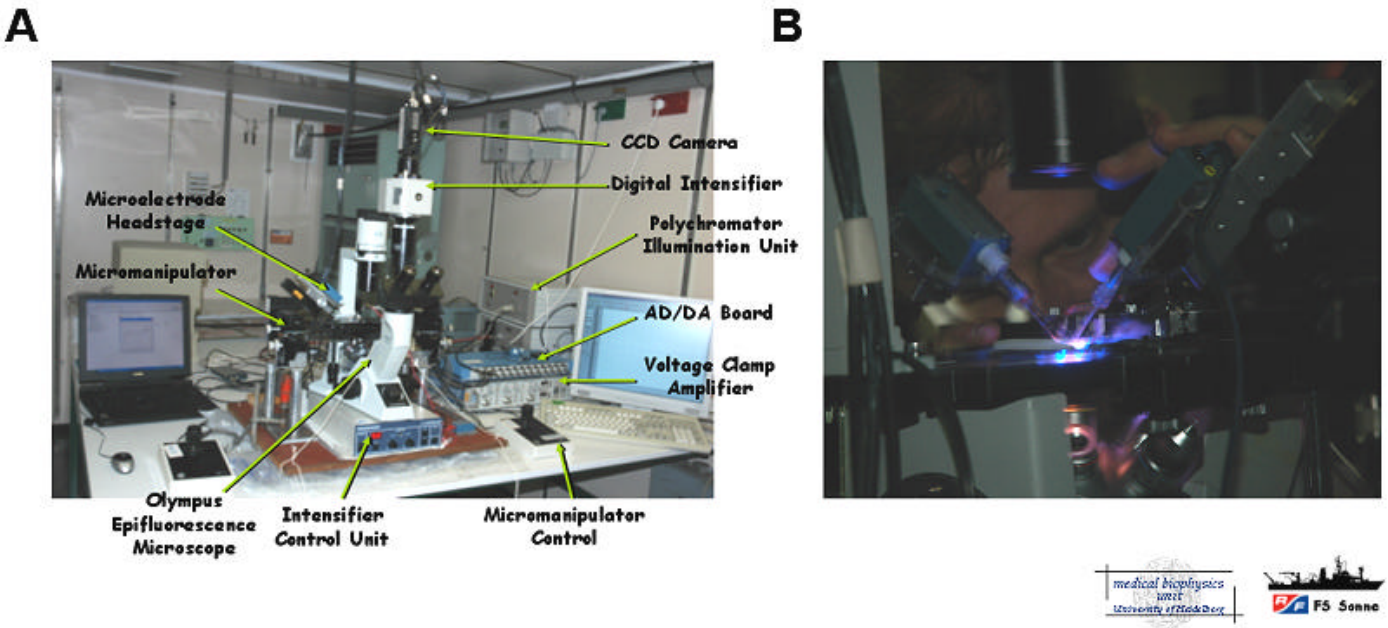

Fig.1: A, combined electrophysiology/epifluorescence microscopy setup for intracellular recordings of membrane potentials and Ca^{2+} flucorescence signals in single muscle fibres. **B,** adjustment of the optical beam pathway**.**

4.5. Scientific equipment in cell biology and biochemistry (Wagner, Wendlandt, Lemaire)

The equipment brought on board Sonne consisted of two stereomicroscopes with epi-illumination. These were put at the disposal of all members of the team requiring difficult identification tasks or delicate dissection procedures. Dissection was particularly difficult for exposing and mapping the brains and pineal organs of fish.

4.5.1 Harvesting cells for cell cultures

In order to obtain fibrocyted and epithelial cells for culturing we removed the skin from the fish's flanks Dissection as well as the following procedure of rinsing, mincing, filtering and preparing for freeze storing were performed under sterile conditions in a laminar flow bench (Holenair, HV2436) modified by adding alumium foil on its working surface (see Fig. 4.5.1). Cells were pelleted with Labofuge GL (Heraeus) kindly made available by Eva Küppers (Tübingen). Care was taken to keep all samples sterile during further handling by rinsing with 70% ethanol before use.

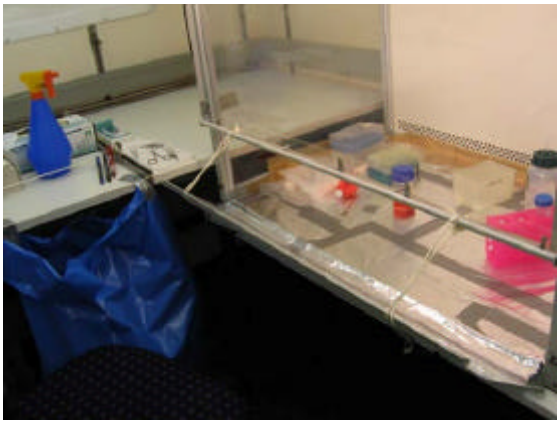

Fig. 4.5.1 ***Modified cleanbench (HV2436) on RF Sonne where sterile procedures took place***

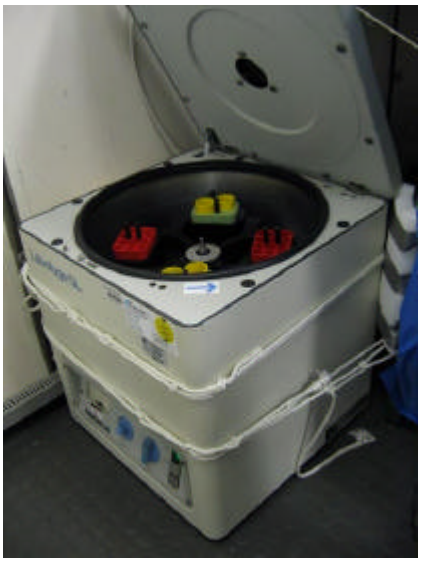

Fig 4.5.2Labofuge GL (Heraeus)

4.5.2 Experimental contaminations and subsequent analysis

The preparation of experimental media and the 24 wells plates was done under sterile conditions using the modified laminar flow bench (Holenair, HV2436).. Gill samples were homogenised with a pestle adapted to Eppendorf vials. Subsequent analysis needed the use of a microfuge Eppendorf 5415D and a Berthold luminometer Lumat LB9501.

Fig. 4.5.3.*Microfuge Eppendorf 5415D*

Fig. 4.5.4. ***Luminometer Berthold Lumat LB9501***

4.6 Lander technology

Two free-fall baited camera landers, rated to 12000m operational depths, designed and constructed by Oceanlab were used to image the seafloor and associated fauna congregating at bait. Landers are free falling instrument packages that comprise a basic delivery system and scientific payload. The delivery system consists of a 100m long mooring line with positively buoyant floatation modules coupled to it (off-line) ten metres apart. The floatation module are 4 –6 twin sets of 17" glass spheres rated to 1200bar operational depth (Nautilus marine Services, Germany). Spacing them 10 metres apart on the mooring prevents chain-reaction implosions in the unlikely event of failure at depth. Tethered under the mooring is an aluminium instrument tripod that protects the scientific payload. Within the frame are two purpose built titanium acoustic releases (IXSEA, France) that can be acoustically triggered from the ship to jettison three clumps of steel ballast weights. When the landers are deployed (with ballast attached), they are negatively buoyant and descend at a rate of ~50 m/min until crash landing on the seafloor. The lander the remains on the seafloor unattached to the ship (the ship is then free to undertake other tasks) for about 12 hours or more until the acoustic command is sent from the ship upon its return. When the ballast weights are jettisoned the lander becomes positively buoyant and ascends to the surface at about 35 m/min. A flag, VHF beacon and flashing strobe light (Novatech, Canada) aid location on the surface. The lander is then recovered over the side via the starboard gantry and winch.

The first lander, known as Hadal-Lander A is equipped with a 3CCD video camera (Hitachi, Japan) positioned one metre above the seafloor looking vertically down at bait (~1kg of Tuna). The camera is illuminated by twin 50W bulbs housed in 120mm diameter glass spheres. The video is recorded autonomously by an on-board PC (NetMc Marine, UK) and powered by a 24v lead-acid battery (DSP&L, USA). The video camera and control/logging system are housing in stainless steel 255 pressure housings rated to 12,000m operational depth, designed by Oceanlab. The video camera also uses a specially designed sapphire viewport, also designed by Oceanlab. The system can record up to 3 hours of footage in MPEG2 format, time-lapsed throughout the bottom time. The lander also has three baited invertebrate funnel traps to collect scavenging amphipods.

The second lander (Hadal-Lander B) has the same basic delivery system as Hadal-Lander A. The Hadal-Lander B scientific payload comprises a 5 megapixel digital stills camera and single flash gun (Kongsberg Maritime, Norway). The camera and flash are powered by a 12v lead acid battery (DSP&L, USA). The camera is capable if taking over 1000 images per deployment in JPEG format. The camera is also positioned vertically downward looking at 1 metre off the seafloor and focussed on ~1kg of tuna.

Temperature and depth are recorded in situ by both landers by SBE-39 loggers (Seabird Electronics, USA).
The lander principle has the advantage of full ocean depth capabilities with small ships and ship that may not have winch wires of sufficient depths. Also the autonomous principle allow long periods of time on the seafloor without requiring any ship time. The deployment of each lander from the FS Sonne took approximately 20 minutes. The recovery takes about 30 minutes per 100 metres to rise waiting time and about 40 minutes to recover it on board.

The scavenging amphipods collected from the funnel traps were sorted to species, and counted. Each species were equally split with half preserved in ethanol and the other in DMSO pending population genetic analysis later.

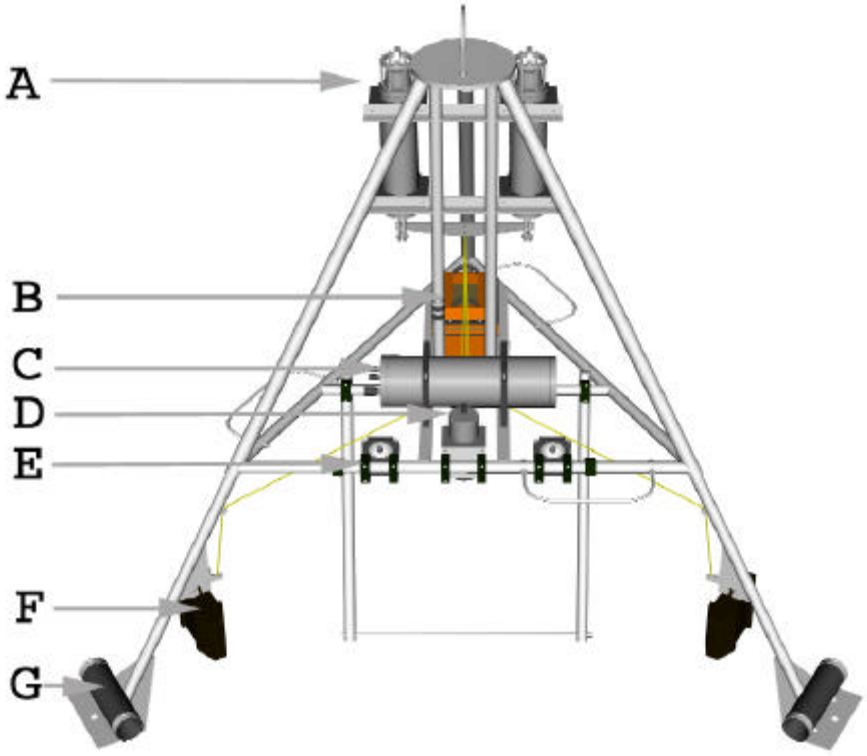

Fig. 4.6.1 CAD model of Hadal-Lander A where; A-Acoustic releases, B-24V battery, C-video control/logger, D- 3CCD video camera, E-two 50W lamps, F-ballast weights, G-invertebrate funnel traps.

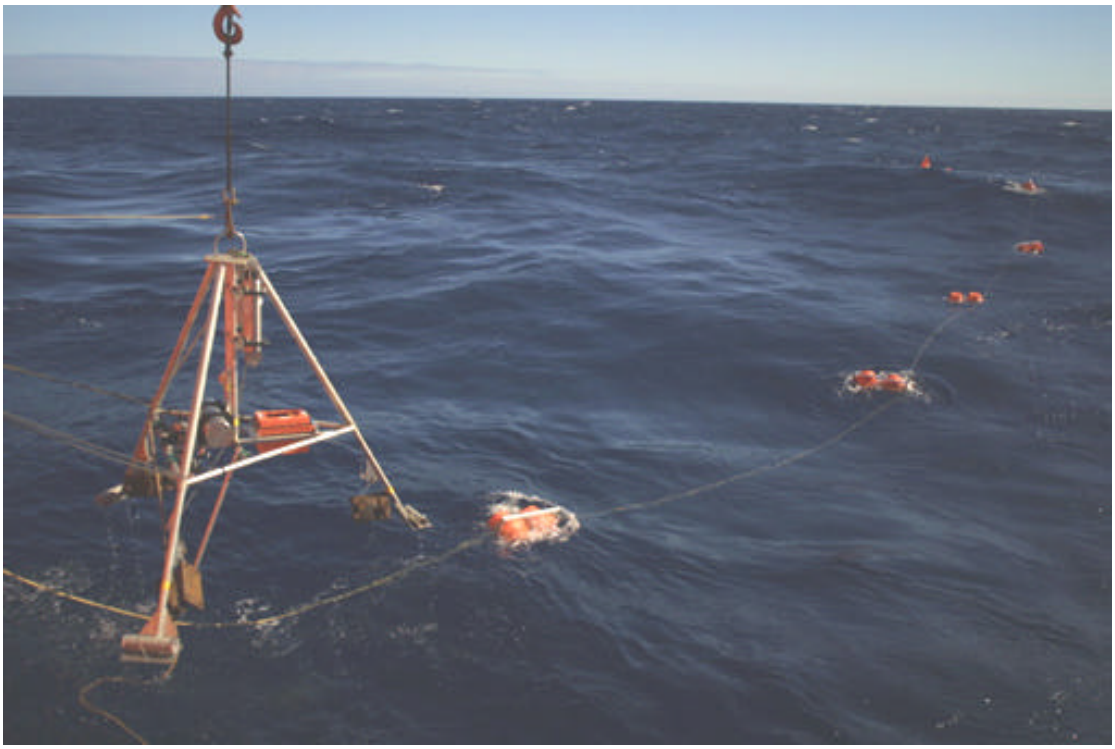

Fig. 4.6.2.The Hadal-Lander A (Video) being deployed from Sonne

4.7 OBH/OBS Seismic Instrumentation (E. Flueh)

The Ocean Bottom Hydrophone (OBH)
The first IFM-GEOMAR Ocean Bottom Hydrophone was built in 1991 and tested at sea in January 1992. This type of instrument has proved to have a high reliability; more than 4000
successful deployments were conducted since 1991. A total of 2 OBH and 21 OBS instruments were available for SO194 and depoyed. The principle design and a photograph showing the instrument upon deployment are shown in Figure 4.7.1. The design is described in detail by Flueh and Bialas (1996).

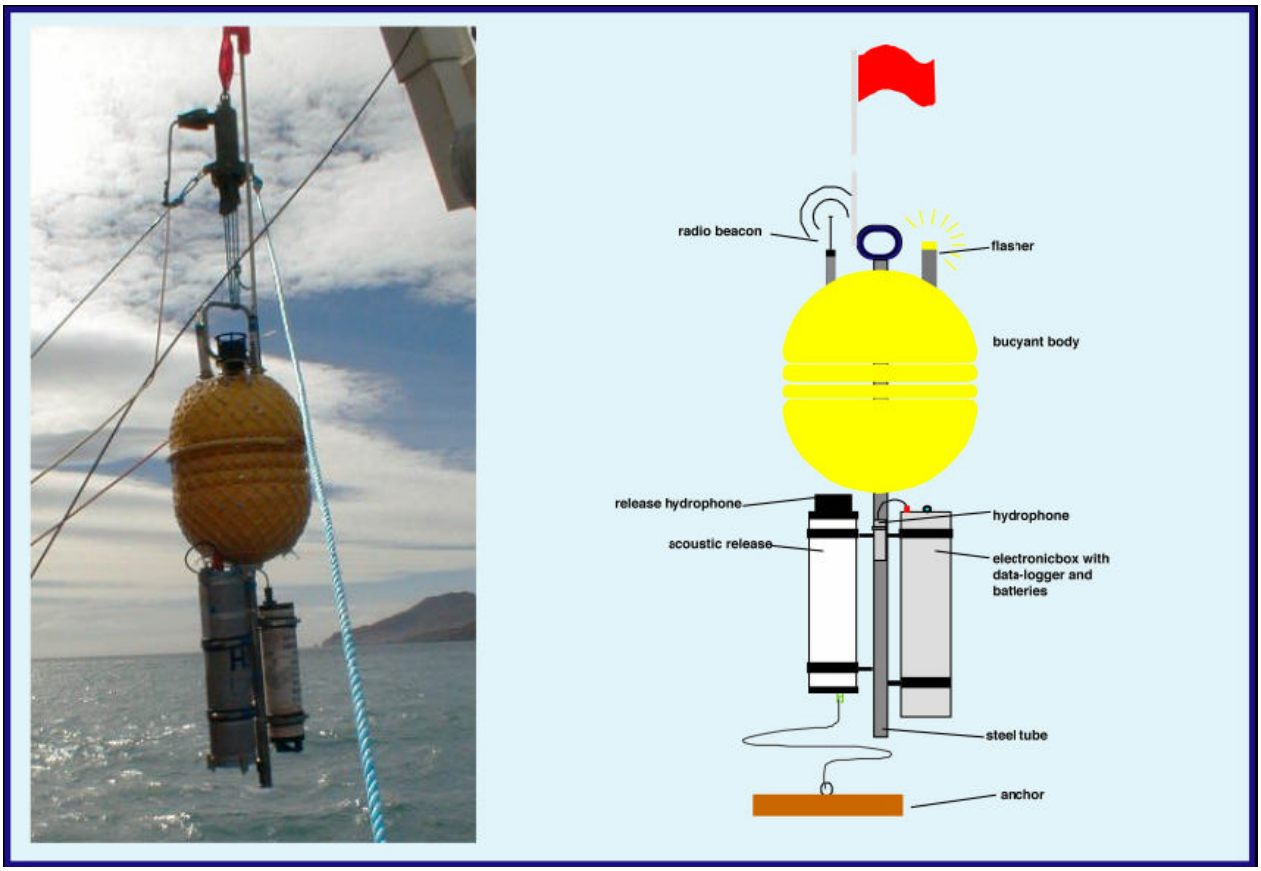

Figure 4.7.1: Principle design of the IFM-GEOMAR OBH (right panel, after Flueh and Bialas, 1996) and the instrument upon deployment (left panel).

The system components are mounted on a steel tube, which holds the buoyancy body on its top. The buoyancy body is made of syntactic foam and is rated, as are all other components of the system, for a water depth of 6000 m. Attached to the buoyant body are a radio beacon, a flash light, a flag and a swimming line for retrieving from aboard the vessel. The hydrophone for the acoustic release is also mounted here. The release transponder is a model *RT661CE* or *RT861* made by *MORS Technology* which recently became *IXSea*, or alternatively a *K/MT562* made by *KUM GmbH*. Communication with the instrument is possible through the ship's transducer system, and even at maximum speed and ranges of 4 to 5 miles release and range commands are successful. For anchors, we use pieces of railway tracks weighing about 40 kg each. The anchors are suspended 2 to 3 m below the instrument. The sensor is an *E-2PD* hydrophone from *OAS Inc.*, the *HTI-01-PCA* hydrophone from *HIGH TECH INC* or the *DPG* hydrophone, and the recording device

is an *MBS, MLS* or *MTS* recorder of *SEND GmbH*, which is contained in its own pressure tube and mounted below the buoyant body opposite the release transponder (see Figure 4.7.1).

The three-leged Ocean Bottom Seismometer (OBS)
The three-leged Ocean Bottom Seismometer (OBS) has identical acoustic release, pressure tubes, and hydrophones like a OBH. Aditionally, there is a seismometer to record threedimensional data. It is fixed to the OBS on a cantilever construction and connected to the pressure tube by a cabel.

The IFM-GEOMAR Ocean Bottom Seismometer 2002
The IFM-GEOMAR Ocean Bottom Seismometer 2002 (OBS- 2002) is a new design based on experiences gained with the IFM-GEOMAR Ocean Bottom Hydrophone (OBH; Flueh and Bialas, 1996) and the IFM-GEOMAR Ocean Bottom Seismometer (OBS, Bialas and Flueh, 1999). For system compatibility the acoustic release, pressure tubes, and the hydrophones are identical to those used for the OBH. Syntactic foam is used as floatation body again but this time in a less expensive cylinder shape. The entire frame can be dismounted for transportation, which allows storage of more than 50 instruments in one 20” container. Upon cruise preparation onboard all parts are screwed together within a very short time. Four main floatation cylinders are fixed within the system frame, while additional disks can be added to the sides without changes. The basic system is designed to carry a hydrophone and a small seismometer for higher frequency active seismic profiling. The sensitive seismometer is deployed between the anchor and the OBS frame, which allows good coupling with the sea floor. While the OBS sits on the seafloor, the only connection from the seismometer to the instrument is a cable and an attached wire, which retracts the seismometer during ascent to the sea surface. The three component seismometer (*KUM*) is housed in a titanium tube, modified from a package built by Tim Owen (Cambridge) earlier. Geophones of 4.5 or 15 Hz natural frequency are available. The signal of the sensors is recorded by use of the *Marine Longtime Recorder (MLS),* and *Marine Tsunameter Seismocorder (MTS)*, which are manufactured by *SEND GmbH* and specially designed for long-time recording of low frequency bands. The hydrophone can be replaced by a differential pressure gauge (DPG) as described by Cox et al (1984). While deployed to the seafloor the entire system rests horizontally on the anchor frame. After releasing its anchor weight the instrument turns 90° into the vertical and ascends to the surface with the floatation on top. This ensures a maximally reduced system height and water current sensibility at the ground (during measurement). On the other hand the sensors are well protected against damage during recovery and the transponder is kept under water, allowing permanent ranging, while the instrument floats at the surface. A few of these instruments are designed for an expanded deployment depth of 8000 m.

The DEPAS Ocean Bottom Seismometer

Similar in mechanical design to the flat structured IFM-GEOMAR OBS 2002 the DEPAS instruments, operated by AWI, Bremerhaven for use by other scientists, were also used during the cruise. They are equipped with a broadband seismic sensor, the Güralp TM40. Alos the datalogger is a new design. Details can be found at http//:www.AWI-Bremerhaven.de. Nine of these instruments as shown in Figure 4.7.2 were used during the cruise.

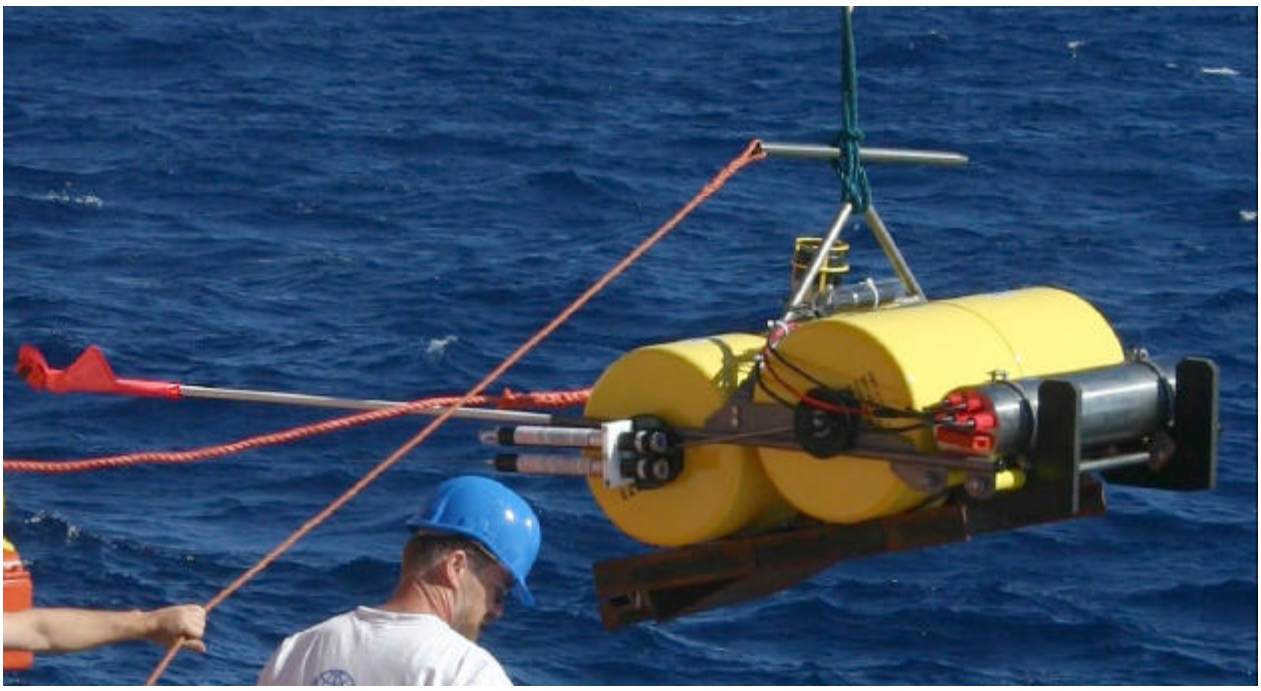

Figure 4.7.2: The DEPAS OBS upon deployment.

The Marine Longtime Seismograph (MLS)
For the purpose of low-frequency recordings such as seismological observations of earthquakes during long-term deployments of about one year time a new data logger, the Marine Longtime Seismograph (MLS) was developed by *SEND GmbH* with support by IFM-GEOMAR. The MLS is again a four channel data logger whose input channels have been optimised for 3-component seismometers and one hydrophone channel. Due to the modular design of the analogue front end it can be adapted to different seismometers and hydrophones or pressure sensors. Currently front ends for the Spahr Webb, PMD and Güralp seismometers as well as for a differential pressure gauge (DPG), a pressure sensor of high sensitivity and the OAS/HTI hydrophone are available. With these sensors we are able to record events between 50 Hz and 120 s. The very low power consumption of 250 mW during recording together with a high precision internal clock (0.05 ppm drift) allows data acquisition for one year. Data storage is done on up to 12 PCMCIA type II flashcards or microdrives, now available with a capacity of up to 2 GB. The instrument can be parameterised and programmed via a RS232 interface. After low pass filtering the signals of the input channels are digitised using Sigma-Delta A/D converters. A final decimating sharp digital low-pass filter is realised in software by a Digital Signal Processor. The effective signal resolution depends on the sample rate and varies between 18.5 bit at 20 ms and 22 bits at 1 s. Playback of the data is done under the same scheme as described for the MBS above. After playback and decompression the data is provided in PASSCAL format from where it can be easily transformed into standard seismological data formats.

The Marine Tsunameter Seismocorder (MTS)
This data logger is based on the experiences with the MBS and MLS devices. The GEOLON-MTS has been developed by *SEND GmbH* and is a high precision instrument for acquisition, processing, storage of seismic signals and additionally pressure data. Like the MLS it is optimised for long time (more than 1 year) standalone operation on the ocean bottom, data storage capacity is also up to 12 PCMCIA cards. The four channel data

logger is prepared for connection with a hydrophone (also different types like e.g. HTI, OAS, or the Differential Pressure Gauge, DPG) and different types of three component seismometers as described above for the MLS. Additionally a digital absolute pressure gauge can be connected to the auxiliary connector, which were not used during SO190-2. Playback of the data is done according to the scheme described for the MBS and MLS above. After playback and decompression the data is provided in PASSCAL format.

Figure 4.7.3: The Marine Tsunameter Seismocorder (MTS).

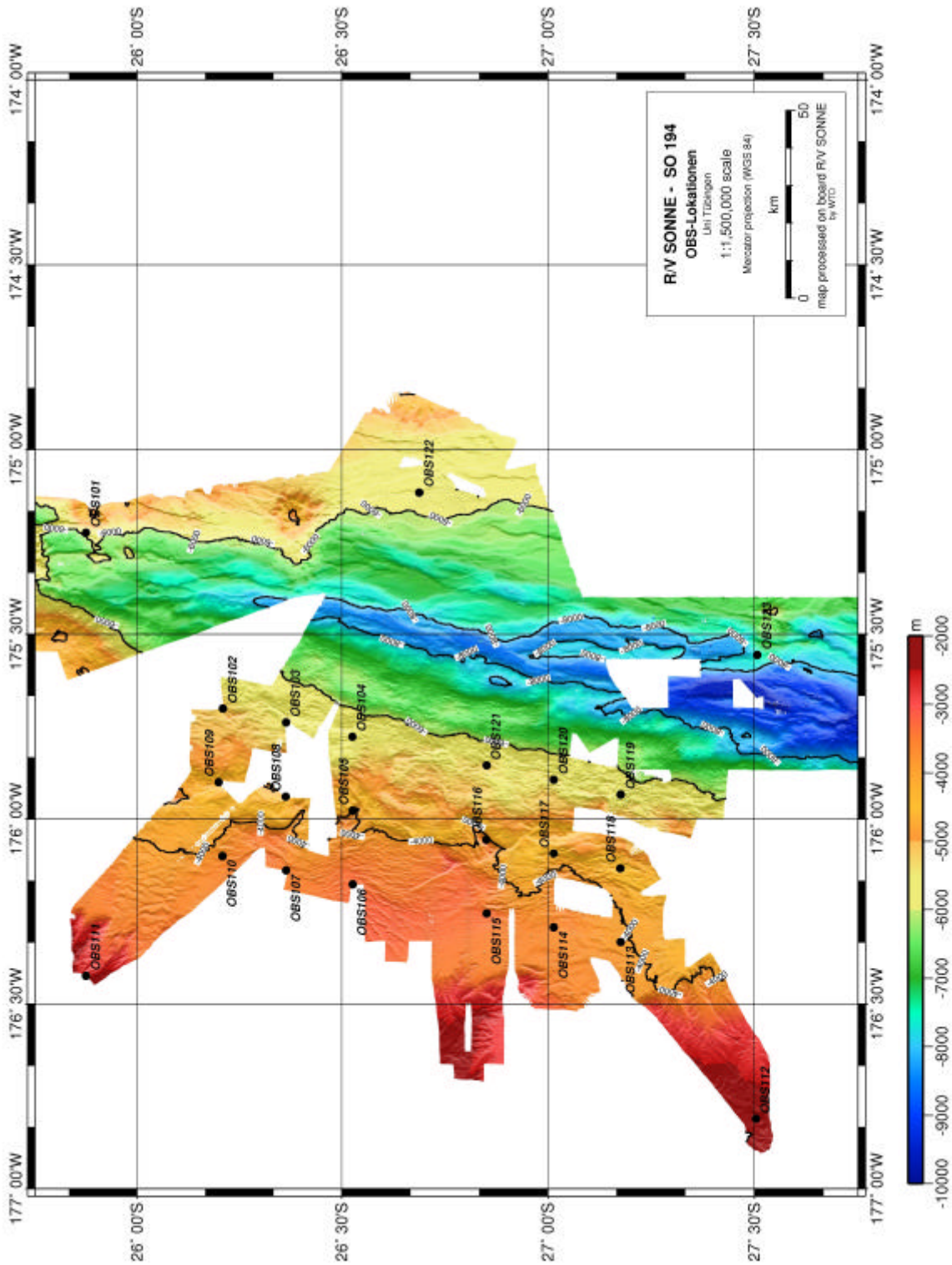

Figure 4.7.4: Location of the OBS deployment of SO-194-cruise

5. Result of trawls

Twenty trawls were conducting during the cruise. Due to the paucity of animals, trawls were conducted at a variety of depths, in hopes of finding the optimum depth of occurrence for the species of interest.

FS Sonne Samoa to New Zealand July 2007

Trawl #	Date	Longitude (S)	Latitude (W)	Bearing	Net Launched	UTC Time	Depth (m)	Time Open (hrs)
			UTC time 12 hour ahead					
1	2-Jul-07	15° 12.401	171° 40.46	60°	19:20	7:20	250 - 325	2
2	3-Jul-07	17° 47.200	172° 35.00	350°	10:35	22:35	720 - 850	2.5
3	3-Jul-07	18° 21.952	172° 45.888	335°	18:50	6:50	225 - 280	2
4	4-Jul-07	20° 19.691	173° 23.900	223°	12:50	0:50	500 - 625	2.5
5	4-Jul-07	20° 47.380	173° 32.600	186°	18:30	6:30	175 - 250	2.5
6	5-Jul-07	22° 45.881	174° 35.801	95°	8:35	20:35	800 - 925	3
7	5-Jul-07	23° 42.226	174° 35.801	95°	18:35	6:35	200 - 250	2.5
			Crossed dateline - UTC time 12 hours behind					
8	7-Jul-07	26° 45.006	175° 16.028	249°	14:40	2:40	450 - 500	2.5
9	7-Jul-07	26° 48.800	175° 18.280	260°	20:10	8:10	110- 160	1.2
10	8-Jul-07	26° 46.472	175° 15.395	225°	9:00	21:00	500 - 600	3.2
11	8-Jul-07	26° 45.783	175° 54.779	36°	18:30	6:30	200 - 300	2
12	10-Jul-07	26° 54.840	175° 30.469	51°	8:15	20:15	500 - 600	3
13	10-Jul-07	27° 53.912	175° 28.735	46°	18:30	6:30	200 - 250	2
14	11-Jul-07	27° 13.113	176° 13.336	268°	11:25	23:25	490 - 550	3
15	11-Jul-07	27° 30.115	176° 48.295	280°	18:50	6:50	275 - 375	2
16	12-Jul-07	25° 55.963	175° 30.24	300°	8:35	20:35	700 - 900	3
17	14-Jul-07	24° 14.997	175° 08.739	336°	11:05	23:05	600 - 800	3
18	14-Jul-07	24° 0.378	175° 16.091	195°	18:20	6:20	250 - 400	2
19	15-Jul-07	24° 6.475	175° 9.540	203°	8:05	20:05	600 - 800	4
20	15-Jul-07	24° 38.139	175° 17.211	180°	18:35	6:35	225 - 300	2.5

Short characterisation of the Pacific fauna sampled during this cruise

The most abundant fishes taken during the cruise were species of *Cyclothone*, with larger gonostomatids, especially *Gonostoma gracile*, also numerous.. Sternoptychids (*Argyropelecus and Sternoptyx*) were also regularly sampled. Among the Stomiatoid fishes we caught several specimens of *Photostomias* . Other groups of fishes were very well represented, particularly the myctophids (*Diaphus, Lampanyctus,* and others). The tubular eyed *Scopelarchus* occurred sporadically. Melamphaeids were also found rarly, and

anglerfish were completely missing from the catch. Two particular specimens need to mentioned, because they were particularly rare:
On July14th, we caught an individual of the opisthoproctidae family, possibly *Dolichopteryx sp.*, which has 4 eyes. Photography by Dr Tammy Frank indicated that only the upward pointing tubular eyes produced eyeshine when viewed from above. Neither eye produced such a tapetal reflex when seen from the side, while the smaller eye displayed eyeshine when seen from below. This clearly indicates the 2 eyes have different fields of view. The optic tectum was labelled with fluorescent dextranes and the head fixed subsequently for a study of the functional morphology of its visual system.

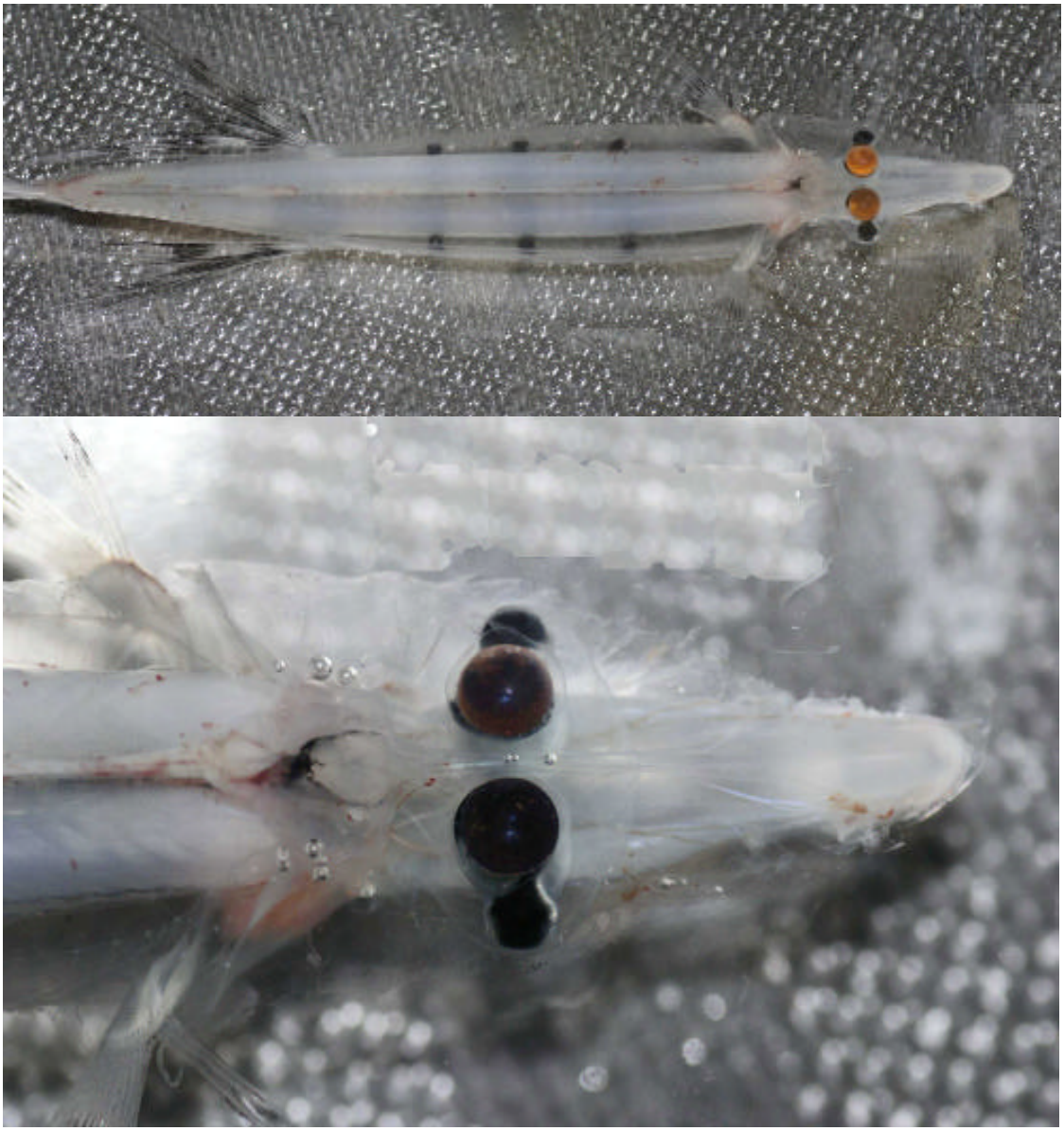

Fig. 5.1.: The "four-eyed "fish Dolichopteryx sp.

We also unexpectedly caught a small cookie cutter shark (*Carcharhinus dussumieri*) . These animals have circular jaws that bite into fish like tuna and then rotate them with a flick of their tail, removing a cookie shaped piece of flesh. It has been suggested that in dim light their ventral surface bioluminesces pale blue (while the dorsal surface is dark). This, like in many mesopelagic teleosts, is a form of camouflage, because if they had a dark belly and were seen from below in the upper 1000m (where there is some sunlight), their dark bodies would cast a silhouette. Lighting up their ventral surface to match the dim downwelling sunlight makes them disappear when seen from below. Interestingly a dark coloured collar separates the head from the body in this species. So, when seen from below, with the glowing belly hiding the animal, all that can be seen is a small dark patch just by the animal's jaws. It has been suggested that tuna might mistake these small dark patches for small fish and that they approach the invisible shark to eat what they think are fish. When they get there they are surprised to find a much larger shark that bites into their side and removes a cookie sized piece of flesh! This hypothesis provides an explanation for how a relatively slow swimming animal like the cookie cutter can catch one of the fastest fish in the ocean.

Fig. 5.2. The cookie cutter shark (Isistius sp.) Note the bioluminescent ventral side for counterillumination camouflage (right) including a dark "collar"

In general, we were surprised about the paucity of the fiah fauna present in our catches. Whereas as a rule numerous small/young and larval specimens were found, we had frequently not more than half a dozen adult fish in the net.

Squid were relatively infrequent but of considerable variety. *Pyroteuthis* and *Histioteuthis* were commonest in the shallower samples, while the deeper ones included the cranchiids *Sandalops, Helicocranchia* and *Taonius*, as well as *Octopoteuthis, Discoteuthis, Mastigoteuthis, Bathyteuthis* and *Abraliopsis*. A few small *Ctenopteryx* were also recorded.

In addition, one unknown species of squid with an odd iridescent tunic was collected, and this specimens will be sent a squid expert, as we suspect that it is a rare specimen. No ommastrephids were taken in the trawls, though frequently seen at the surface during the night. These squid are too active to be effectively sampled by a slow-moving trawl.

Fig. 5.3 Unknown squid species

Decapod shrimp comprised the third major nektonic category captured. Of the Oplophoridae the mesopelagic *Acanthephyra purpurea* and *Systellaspis debilis* were regularly found in both daytime and night trawls. Of the penaeids, species of *Gennadas Sergia* and *Sergestes* were most often encountered. Planktonic euphausiids were also frequently encountered, with very small *Euphausia* sp most frequently encountered, as well as several of the large bilobed *Nematobranchion boopis* species.

The gelatinous fauna was most frequently represented by *Pyrosoma*, salps and numerous small medusae. Occasional siphonophores were also taken, but were never numerous. In addition, in many of the night trawls, several large (5-8 cm long) heteropods were always present.

Many specimens could not be identified on board to species. It is possible that some are new and certainly some of the known species were larger than had previously been recorded. The individual specimens will be preserved for later detailed taxonomic study.

6. Experiments conducted, completed, first results

6.1 Bioluminescence

6.1.1 The visual pigments of mesopelagic teleosts (R.H. Douglas & J.C. Partridge)

6.1.1.1. Myctophidae

In previous studies, by us and others, a large variety of visual pigments have been isolated from over 200 species of deep-sea fish. Although most have a single visual pigment absorbing maximally ($?_{max}$) around 480-490nm, several have more than one visual pigment &/or pigments with $?_{max}$ outside the normal range (Figure 1). It is difficult to relate visual pigment absorption spectra to any particular parameter, such as depth or vertical migration, as any trends are confounded by phylogenetic variables. We are therefore performing an in depth study of the visual pigments of a single family; the myctophidae. These are one of the most important and diverse components of the mesopelagic fauna.

During this cruise we have collected 70 animals, 47 of them myctophids belonging to around 20-25 species (definitive identification of some species will have to be performed on return to the UK). The visual pigment content of most of these animals has yet to be determined. Their eyes or retinae have been frozen in either buffer or as retinal extracts, for later analysis in the UK. Once the visual pigments of these animals have been characterised these data will be put together with data collected on 2 previous Sonne cruises (in 1999 and 2003), hopefully allowing an interpretation of the significance of diverse retinal pigments.

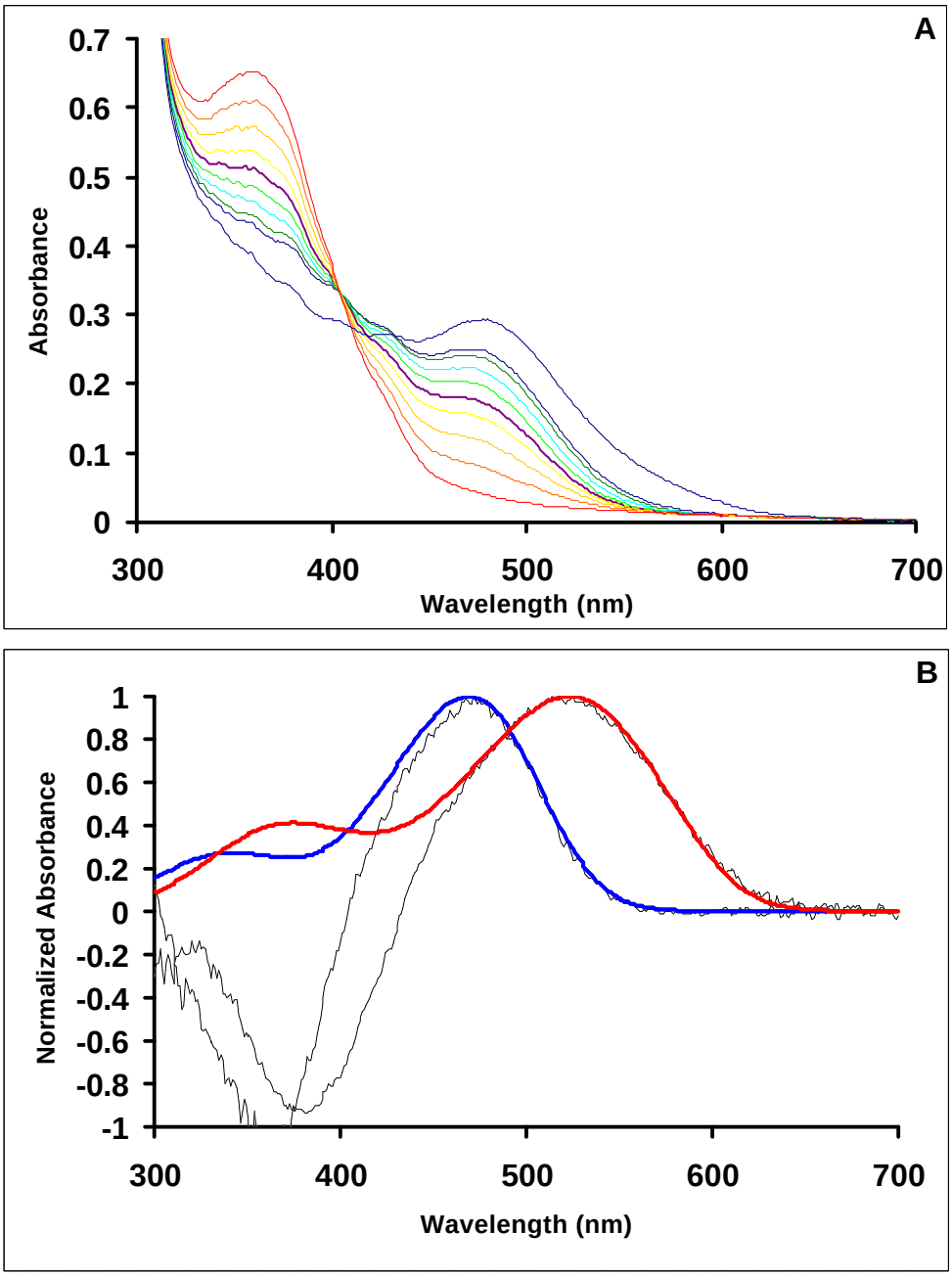

Figure 6.1.1.1.1. **(A)** Absorbance spectra of a retinal extract of *M. nitidulum* following various durations of exposure to monochromatic light. In order of decreasing absorbance at 500 nm the absorbance spectra are: (a) initial measurement of the unexposed extract 10 min after the addition of 50 µl 1M hydroxylamine to 500 µl of extract; (b) after 10 min exposure to monochromatic light of 634 nm; (c) another 5 min 634 nm; (d) 3 min 609 nm; (e) 2 mins 586 nm; (f) 2 mins 576 nm; (g) 1 min 565 nm; (h) another 2 min 565 nm; (i) 1 min 552 nm; (j) 2 min 501 nm.

(B) Normalized difference spectra (dashed lines) constructed using the curves shown in Fig. 2a; (k) a-b, (l) i-j. These were best fit to templates (solid lines) revealing a porphyropsin with λ_{max} 523.3 nm, and a rhodopsin with λ_{max} 469.0 nm.

6.1.1.2. Photostomias sp.

We have also caught 9 individual *Photostomias sp.*. These are of interest as they are closely related to 3 species of dragon fish (*Aristostomias, Pachystomias* & *Malacosteus*) that, unusually, produce red bioluminescence. We have previously shown that these red light producing species have longwave shifted visual pigments compared to other deep-sea fish, which conventionally produce blue bioluminescence.

During the last week, we have shown for the first time, by extract spectrophotometry, that *Photostomias* also has red shifted visual pigments, its retinae containing both a rhodopsin absorbing maximally ($?_{max}$) at 525nm and a porphyropsin with $?_{max}$ at 554nm (Figure 2). Whole mount spectroscopy indicates it also has a photolabile substance (possibly a visual pigment) absorbing maximally around 600nm. These findings are novel and completely unexpected.

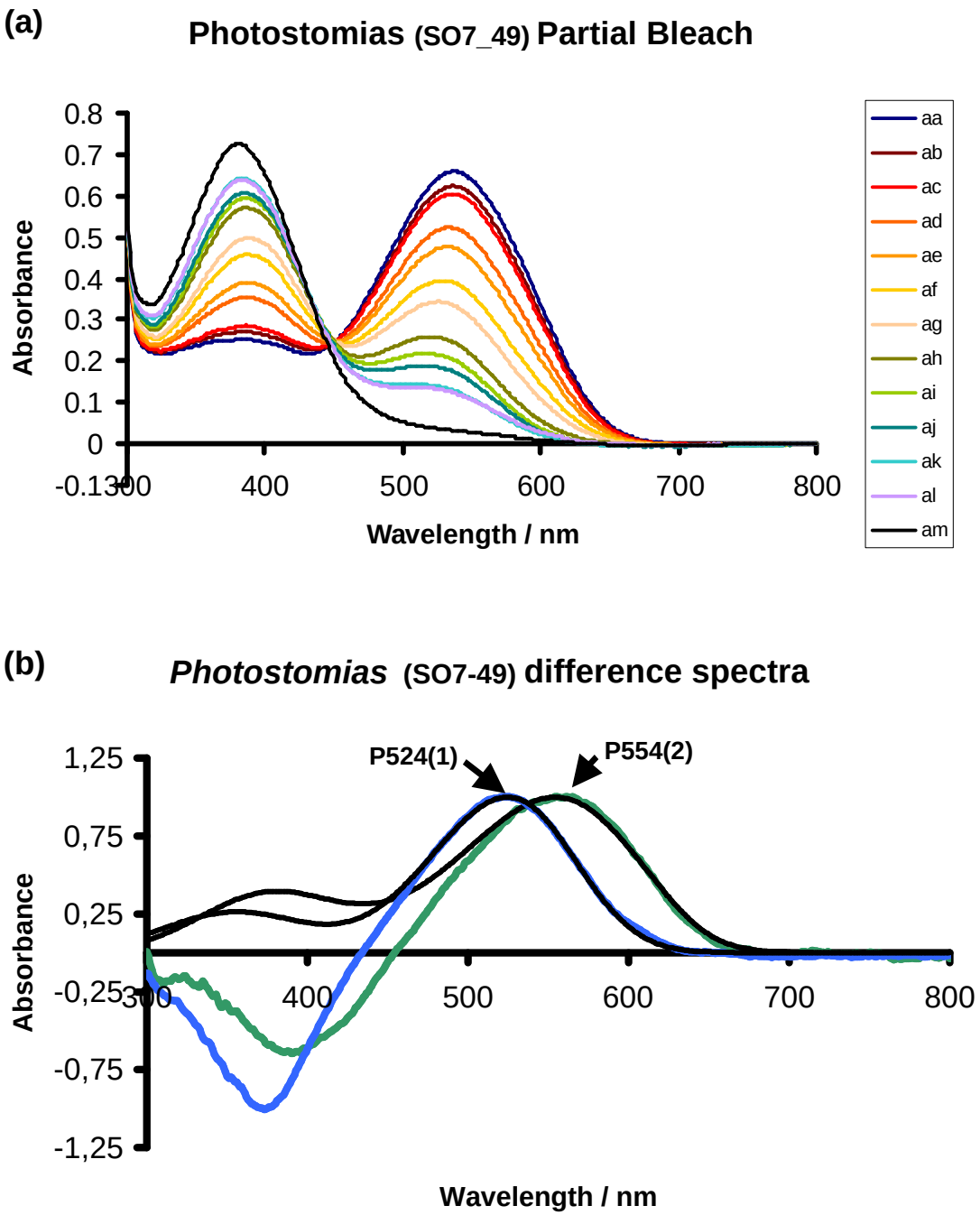

Figure 6.1.1.2.

(a) Absorbance spectra recorded during partial bleaching of visual pigments extracted from *Photostomias* sp. Line aa is the initial unbleached scan. Subsequent scans after sequential bleaches at the following wavelengths: ab, ac 609 nm; ad, ae 666 nm; af, ag 650 nm; ah, ai 634 nm; aj, ak 609 nm; al 586 nm; am 501 nm. Bleach times varied.

(b) Difference spectra calculated by subtracting spectra from data in (a). Green line aa-ac; Blue line al-am; Black lines are best-fitting visual pigment templates corresponding to a porphyropsin with a $?_{max}$ of 554 nm ($P554_2$) and a rhodopsin with a $?_{max}$ of 524 nm ($P542_1$). Photoproducts at 390 and 375 nm are characteristic of A1 and A2 pigments.

6.1.2 Retinal adaptation (H.-J. Wagner)

We collected 60 eyes and retinaeof 10 different species for light and electron microscopic examination. Many of these will serve as controls for three particular species which will be studied in greater detail. Among these controls are well known species such as *Gonostoma*, *Argyropelecus*, and *Chauliodus*. By contrast, the retinae of *Scopelarchus analis, Photostomias guernei*, and *Dolichopteryx sp.* have various specialised features that need further clarification.

The eyes of *Scopelarchus analis* have previously studied and up to seven different retinal specialisations demonstrated within a single eye (Collin et al., 1988). Of particular interest

The eye of *Scopelarchus michaelsarsi* (Pearleye)

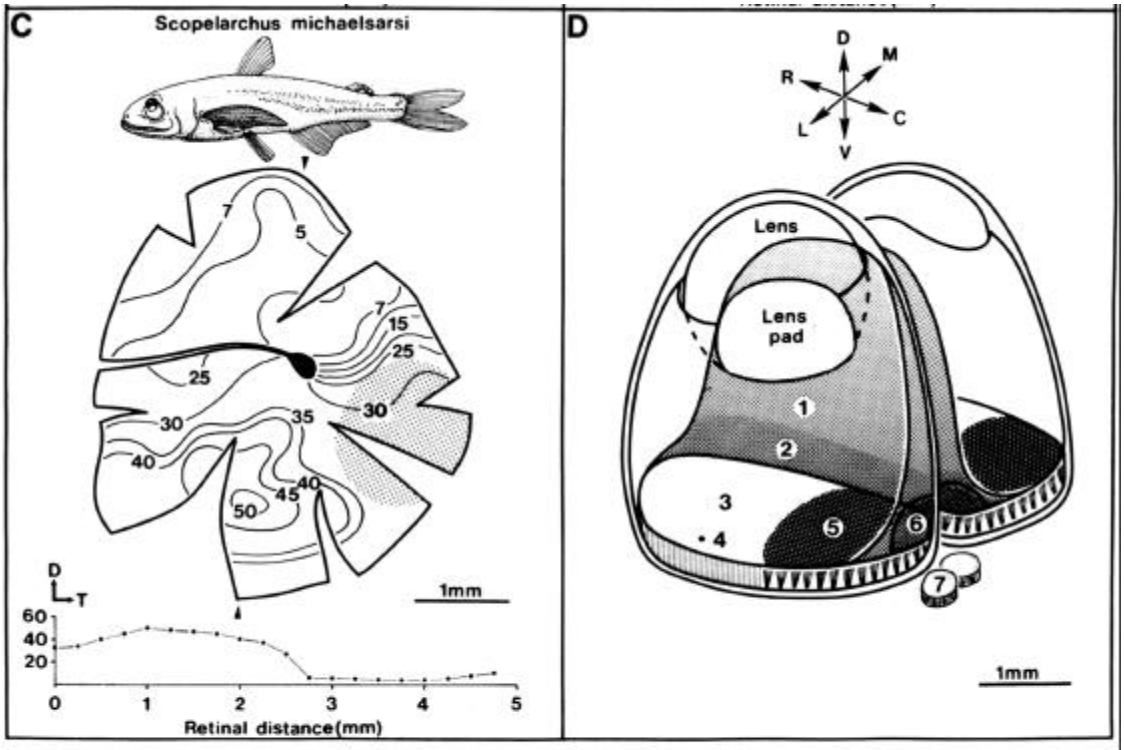

Fig. 6.1.2.1 C. *Scopelarchus michaelsarsi* showing the pronounced AR in the main retina and the extent of the area giganto cellularis (shaded area in temporal retina). D. Three dimensional diagram of the seven specialisations in the eye of *Scopelarchus michaelsarsi*. 1, grouped rods in the accessory retina; 2, grouped rods and cones in the ventral region of the accessory retina; 3, ungrouped rods in the main retina; 4, Area retinae in the centro-lateral region of the main retina; 5, grouped rods in the main retina; 6, temporal area giganto cellularis in the main retina; 7, retinal diverticula located medial to the temporal insertion of the optic nerves. C, caudal; D, dorsal; L, lateral; M, medial; R, rostral; V, ventral

Collin et al., 1998

is the coexistence of a region of randomly arranged photoreceptors (3 in the above figure) and a region of “grouped” photoreceptors (5, 6). The difference in photoreceptor arrangement has profound consequences for retinal signal processing, since the overall thickness of the inner retinal layers is reduces by half unerneath the grouped rods.
The direct comparison of these two regions provides an ideal opportunity to investigate the special function of the grouped photoreceptor arragement. This is found a number of other deep sea fish, but also several freshwater species, among them the weakly electric fish like mormyrids. Together with three other German laboratories in Leipzig, Bonn, and Erlangen we are currently investigating this particular specialisation in the elephantnose fish (*Gnathonemus petersii)* with the help of DFG funding. We have for a long time looked

for a control species against which to compare the specific properties of the elephantnose fish retina. The retina pearleye is the perfcect object for this task.

We have caught five specimens during this cruise, two of which were still alive and suitable for tracing experiments. These have been microinjected with fluorescent dextranes into the optic tectum and cultured for 2 days in order to label isolated ganglion cells in the retina. The hypothesis to test is that not only are there quantitative differences in cell densities but also qualitative differences in the number of ganglion cell types. Retinal wholemounts will be prepared and labelled ganglion cell dendrites visualised in 3D with a confocal microscope. Ideally these same preprarations can also be immunostained with and anitserum to PKC in order to reveal the density of a particular type of On-center bipolar cell, allowing to calculate convergence rates in the two regions of the retina. If this double label does not work the remaining retinae will be used for immunocytochemistry.

The retina of *Photostomias guernei* is of perticular interest because it contains a photolabile substance (possibly a visual pigment) absorbing maximally around 600nm see above, Fig. 6.1.1.2). This is somewhat similar to the situation in another species of red senstive dragonfish, namely *Malacosteus*.in which it has been shown that the photosensitiser is bacteriochlorophyll We have recently reexamined the retina of *Malacosteus* in the electron microscope and found indications that bacteria-like particles are present in great abundance in the pigment epitheial cells ensheathing the photosensitive outer segments of the rod cells. We had hoped to find *Malacosteus* in the catch of the present cruise in oder to do further work to identify the putative bacteria; since we got none, we need to obtain this species elsewhere. The eyes and retinae of *Photostomias* have not been studied in detail before. They will therefore be investigated for the presence of particles similar to those in *Malacosteus* and, should we find them, subject to the same extended tests, including in situ hybridisation and immunocytochemistry in order to characterise these structures as the potential sites of the bacteriochlorophyll.

Finding the “four-eyed” fish *Dolichopterus* in our catch was a fortuitous event. As noted above, the main eye is tubular and its visual field points upwards (dorsal) while the smaller accessory eyes have a downward orientation of their visual fields. This arrangement is similar but not identical to *Bathylichnops exilis*, where, however, the “accessory” eye is markedly smaller and apparently less well developed. The single specimen received microinjections into the optic tectum in order to determine the central representation of both eyes via the ganglion cell projection. In order to investigate the topographic relationship, optical properties and functional relationship of the two eyes, the entire head will be documented after fixation. Subsequently serial sections will be prepared. An attempt will be made to isolate the retinae of one side wihtout disturbing the position of the outer ocular layers, in order to study cell densities in a wholemount preparation similar to the abve figure of *Scopelarchus.* The reconstruction of the serial sections will enable us to assess the optical axes of the individual eyes including their dioptric aaparatus, and the study of the retinal structure will tell us the receptoral and neural constraints of perception.

6.1.3. Electrophysiology of crustacean photoreceptors (T. Frank)

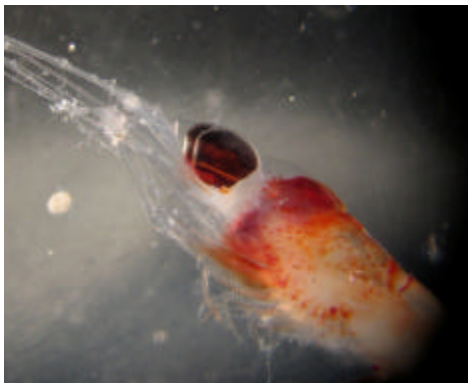

***Temporal resolution*:** Experiments were completed on 6 specimens of the large (relatively speaking) euphausiid *Nematobranchion boopis*. This species has a bilobed eye, with the upper lobe optically designed for lower sensitivity, higher resolution, while the lower lobe is better adapted for higher sensitivity, lower resolution. All the experiments on this species were conducted on the upper lobe. Temporal resolution and response latencies were measured in dark adapted individuals at 6.5^{o}C (n = 5), 8.5^{o}C (n = 4), 10.5^{o}C (n = 4) and 12.5^{o}C (n=5). Preliminary analysis of the data indicate that temperature has a significant effect on temporal resolution, increasing the maximum CFF from 28 Hz (± 1.5) at 6.5^{o}C to 42 Hz (± 1.7) at 12.5^{o}C.

An example of the temperature effects on response latency is shown for one specimen. The voltage vs. log irradiance data at the two temperature extremes tested in this animal – 6.5 and 12.5 ^{O}C were generated by normalizing the data to the peak response at each temperature, and plotting the data on semilogarithimic coordinates. These curves were fit with the Zettler modification of the Naka Rushton equation, which describes the intensity response function of photoreceptors. From these graphs, one can obtain the irradiance at which the response amplitude is 50% of the maximum response amplitude (50% V_{max}) to ensure that the same parameters are being compared under each temperature, even if the peak response amplitude changes. For these normalized data, the shape of the two curves should be identical if the condition of the photoreceptor has not degraded during the experiment, an important consideration for experiments that last up to 48 hours under multiple temperature and lighting regimes. In this individual, the response latency at 50% V_{max} was 10 ms at 12.5°C vs. 24 ms at 6.5°C.

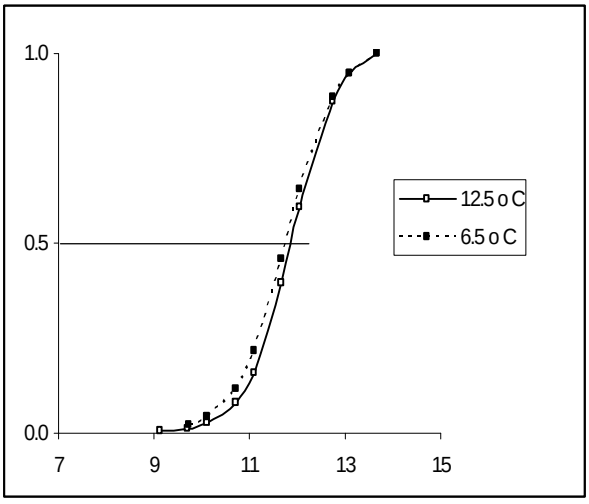

In addition, light adaptation increases temporal resolution even further. For example, at 12.5^{o}C, the temperature at which the temporal resolution in the dark-adapted eye is highest, light adaptation increased the CFF from a mean of 42 Hz (± 1.7) in the dark-adapted eye to a mean of 51.5 Hz (± 1.7), which is close to the CFF of a light-adapted human eye. While it was previously known that light-adaptation significantly enhances the resolution of bilobed euphausiid eyes, the data here suggest that even at night, when this species migrates into warmer surface water to feed, they will experience an increase in temporal resolution (and hence the ability to track their prey) due to the warmer temperatures in surface waters alone. As this species preys primarily on a species of bioluminescent copepod, they can afford to sacrifice sensitivity (contrast detection) for greater temporal resolution (tracking ability), due to the substantially greater contrast between a flashing or glowing prey item against a dim background vs. that of a dark prey item.

Interestingly, one individual of a euphausiid species with the standard round crustacean eye was also tested at different temperatures, with dramatically different results. *Thysanopoda cristata* is a deep-living species that is not known to undergo vertical migrations. Preliminary analysis of the CFF indicates that temperature apparently has no effect on temporal resolution, with temporal resolution remaining at 14 Hz at 6.5^{O}C, 8.5^{O}C and 12.5^{O}C

6.2. Biological Rhythms

6.2.1 Melatonin Experiments

Blood melatonin levels are a classical indicator of the physiological diel cycle. Unfortunately, the amount of blood that can be recovered from most mesopelagic fish is not sufficient for biochemical analysis. As an alternative we used the pineal gland i.e. the organ of origin for systemic melatonin and determined the its melatonin content by ELISA. In previous cruises (including Sonne) cruises we have already sampled a number of mesopelagic species; preliminary results indicate that, as expected, melatonin levels are low during the day and high at night (Fig. 6.2.1.). During the current cruise we have

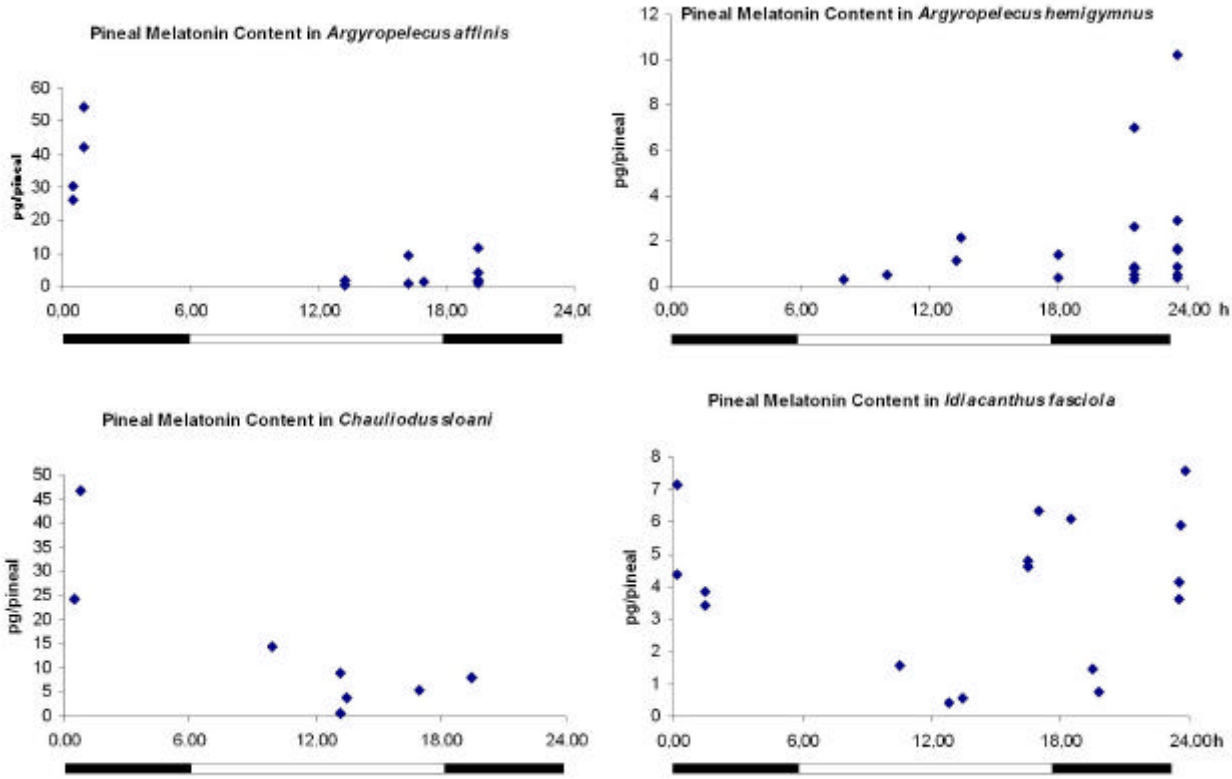

Fig. 6.2.1. Cyclic variations in pineal melatonin content in four species of mesopelagic fish

continued to collect pineals for ELISA. During the night trawls we were able to sample 25 pineals form 6 different species, and during the day trawls, we isolated 11 pineals of 5 species. These samples will provide sufficient new data to conclude this type of analysis.

What this study is able to show is whether the daily melatonin levels change in accordance (or response) to the changes in external stimuli, i. e. the solar cycle. It does, however, not answer the question whether the changes may also be the expression of an endogenous circadian oscillator. We had planed to keep isolated pineals in organ culture and to monitor their release pattern of melatonin under constant temperature and darkness conditions. The necessary prerequisites such as the closing cod end and a uninterrupted dark conditions were realised. Preliminary experiments had shown that a minimum of five pineals need to be pooled in order to obtain amounts that are above the detection limit of our system. Unfortunately, none of our trawls yielded the sufficient number of adult specimens of a single species. Therefore, this experiment could not be carried out.

6.2.2 Molecular biology of clock genes in mesopelagic fish

To establish cell cultures of mesopelagic fishes the main goal was to collect samples of selected tissue, in this case epithelial and connective tissue. These tissues were prepared as primary culture in order to allow freezing for the transfer to Tübingen. Additionally, samples of biopsies from skin and muscle tissue were taken and conserved in RNA later (Ambion) in order to measure the gene activity of the core clock genes.

Fish of the catch were shared with the other participants and used sequentlally. Only fish caught repeatedly and big enough to collect a sufficient amount of skin were used. We chose G*onostoma gracile*, *Echiostoma spec.* and *Chauliodus sloani*. We prepared a large number of samples because we were facing unknown growing conditions and possibly higher microbiotic contermination, as mentioned in the few reports on deep see fish cell cultures.

To minimize microbiotic contermination decapitated fish were rinsed in 70% ethanol for 20 seconds and then washed with sterile water. Fish were then dissected in sterile conditions and cooled with ice. They were skinned by a dorsal incisionl and then using tweezers to pull of the skin carefully from the underlying muscle fascia. The pieces of skin were rinsed immediately in media (DMEM high glucose with HEPES) containing 0,6% Penicillin / Streptomycin and 0,11% Fungizone. Afterwards samples were minced to pieces of about 1mm² size with a scissor in a tip of a FALCON tube. The suspension of isolated pieces was transferred to PBS containing 0.25% EDTA and 1mg/l trypsin (5000 U/mg, Sigma). The proteinase trypsin separates single cells especially fibroblasts from the tissue blocks. Incubation took 25 minutes at 37°C or was performed at 4°C over night. The reaction was stopped by adding 4ml FBS (SIGMA) in order to block the proteinase activity..

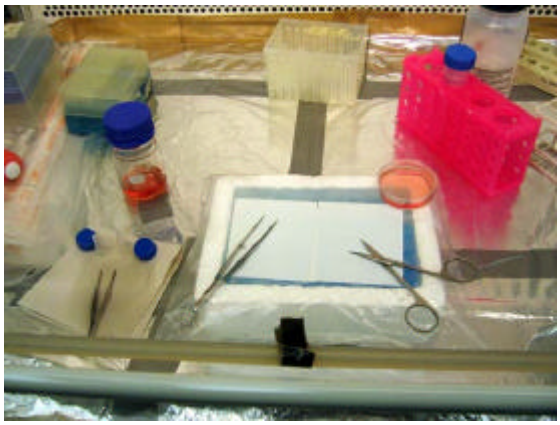

Cell and skin fragment suspension was then filtered through a cell strainer (BD Biosciences) with a pore size of 70µm in order to seperate the cells from the remainig pieces of tissue. To further isolate the cells from smaller fragments, 3ml of medium was added to the sollution and the suspension centrifuged at 500g (approximately 1800 rcf, r=15). The supernatant was rejected and the cell pellets were resuspended and rinsed in cold medium with additional 15% FBS. This procedure was performed twice. During the second run cells were resuspended in 0°C Freeze Medium containing 15% FBS and 15% DMSO as cryoprotectants. Depending on the size of the pellet 6 to 10 ml of freeze medium was used. The cell suspension was transferred to 2ml ice cooled cryotubes and immediatly stored at -40°C. During the transfer to Tübingen thel samples will be kept on dry ice.

Conservation of genetic material in RNA later was performed by immersing a sample of approximately 5mm³ of the specific tissue in to the RNA-later solution. Samples were then stored under cool and dark conditions.

Skin samples of 17 fishes were taken, among them 10 from *Gonostoma gracile,* and stored in 69 cryotubes and 10 samples of muscle tissue were taken and stored in RNA later. In Tübingen, primary cell culture will be established and growth conditions optimised depending on a number of varaibales such as the surface coating, medium additives like

growth factors, FBS and gluccose, as well as the temperature and osmolarity of the medium.

After these initial steps stable culture conditions need to be established in order to start the molecular biological experimetns.
The first step consists in the detection of the clock genes (belonging to *clock*, *per-, bmal,* and *cry* families) using a primer construct derived from known gene sequences in zebrafish, and amplified via PCR. In the next step it will be tested whether different amounts of the detected clock genes can be shown on the level of transcriptional products (mRNA) and protein level, and whether these changes reflect cyclic ahnges indicative of the presence of an oscillator. These experiments will be performed using quantitative analysis of the mRNA content (cDNA realtime PCR of reverse transcripted mRNA) during constant dark, constant light and light / dark conditions assuming that each cell contains an oscillator resposive to external light stimuli. This protocol will also enable to determine the phase lenght and the stability of the core oscilator. Furthermore, the influence of temperature on the phase length and certain clock resetting stimuli that are known from zebrafish culture will be investigated.
Once this paradigm is established for mesopelagic fish, it can be aplied to the study of deep demersal fish which live beyond the penetration depth of sunlight, and which nay therefore show a different activity pattern of clock genes.

6.2.3. Circadian Rhythms in Photosensitivity in shrimp

Systellaspis debilis is a bioluminescent shrimp that vertically migrates from 600 – 700 m during the day to between 150 and 300 m at night. As the general consensus is that light serves as the trigger to cue these migrations, one might anticipate that a circadian rhythm in sensitivity exist as well, with sensitivity increasing in the late afternoon as the sun sets and the animal begins it migration into shallower. A circadian rhythm in the amplitude of the ERG has been clearly shown in species of nocturnally active shallow water crustaceans. However, data obtained from this individual indicate that there is no circadian rhythm in this deep-sea dweller. Although it is clear that sensitivity generally increased over time (very likely the result of utilizing an animal too soon after it was collected in the trawl filled containing bioluminescing organisms), there is no regular increase in sensitivity at sunset, nor a discernible decrease at sunrise.

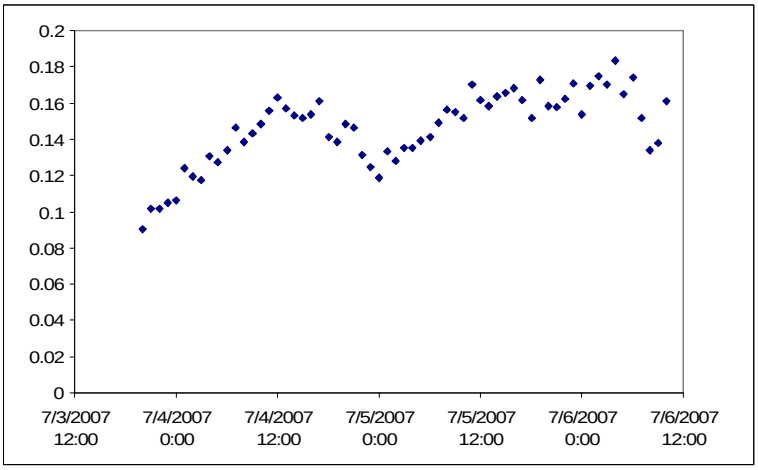

6.3. Hadal Faunal Communities

6.3.1. Deployment Summary

HADAL-LANDER A (video)

	Depth (m)	Latitude	Longitude	Date	Time (utc)
DEP 1a	6133	26° 43.935 S	175° 11.326 W	070707	01:50:30
DEP 2a	7049	26° 48.728 S	175° 18.101 W	080707	07:56:59
DEP 3a	8170	26° 54.962 S	175° 30.734 W	100707	19:56:47
DEP 4a	10,015	24° 16.352 S	175° 90.256 W	120707	22:40:27
DEP 5a	9036	24° 08.074 S	175° 10.951 W	140707	05:10:50

HADAL-LANDER B (stills)

	Depth (m)	Latitude	Longitude	Date	Time (utc)
DEP 1b	6715	26° 43.085 S	175° 15.540 W	070707	02:40:38
DEP 2b	7662	26° 48.559 S	175° 25.605 W	080707	06:45:15
DEP 3b	8776	26° 54.995 S	175° 34.591 W	090707	19:12:03

NOTE: deployment depths are taken from *in situ* pressure sensor (SBE-39) post deployment.

6.3..2. Preliminary results;

Hadal-Lander A (Video)

DEP 1a: Nom 6000m/ Act; 6133m
26° 43.935 S /175° 11.326 W -Kermadec Trench
Hadal-lander A was deployed in the Northern sector of the Kermadec trench at 6133m. The deployment went well, but an alternative to conventional starboard side operations was considered for the next deployments. On the bottom, the lander recorded a succession of scavenging hadal-amphipods consuming the bait. Activity at the bait was punctuated by two species of larger crustaceans (probably a Penaid and Acanthephyra). No fish were observed throughout. 1772 specimens of 4 species of amphipods were recovered in the traps. The species, as yet unidentified, were categorised as A, B C and D and counted with abundances of 94.02%, 4.80%, 0.96% and 0.23% respectively. One individual euphausid was also recovered. Pressure (613 bar) and bottom temperature (1.16ºC) were recorded and accurate descent and ascent rates were ascertained (50 m/min and 35 m/min respectively). An even number of amphipods were preserved in ethanol and DMSO pending genetic population analysis

DEP 2a: Nom 7000m/ Act; 7049m
26° 48.728 S /175° 18.101 W -Kermadec Trench
The lander was deployed again in the Northern sector of the Kermadec trench at 7049m. The new method of deployment (lander first over starboard side) proved much more efficient. On the bottom, the lander recorded more scavenging hadal-amphipods, the same Penaid and Acanthephyra as deployment 1a but most notable was the presence of a fish. Our initial identification is the *Notoliparis kermadecensis*, a fish only ever found once in a trawl in 1952 during the Danish Galathea expedition. If this identification is correct, we have the first images of this species alive, increase its current depth of occurrence by 400m and its geographical location to 7 degrees further north. The fish remained in view of the camera for over two hours, and in one sequence two individuals were visible. The

individual that remained was seen to feed on the amphipods by both sucking them off the sediment surface and swallowing free swimming individuals. 163 specimens of one species of amphipod were recovered in the traps. The species, suspected to be *Hirondella spp*, a known amphipod endemic to depths over 7000m, were labelled species E. Pressure (704 bar) and a slightly higher bottom temperature of 1.31ºC. An even number of individuals from each species were preserved as in Dep 1a.

DEP 3a: Nom 8000m/ Act; 8170m
26^{o} 54.962 S /175^{o} 30.734 W -Kermadec Trench
The lander was deployed again in the Kermadec trench at 8170m. On the bottom, the lander recorded only scavenging hadal-amphipods. 580 specimens of three species of amphipod were recovered in the traps. *Hirondella spp*. were present again and comprised 98.97% of the individuals caught. Two new species to the cruise were found and labelled species F and G and accounted for 0.17% and 0.86% respectively. Pressure (817 bar) and again a slightly higher bottom temperature of 1.46ºC were recorded. An even number of individuals from each species were preserved as in Dep 1a.

DEP 4a: Nom 10000m/ Act; 10015m
24^{o} 16.352 S /175^{o} 90.256 W -Tonga Trench
The lander was deployed in the southern Tonga Trench to just over 10,000m. On the bottom, the lander recorded only scavenging hadal-amphipods. 1850 specimens of *Hirondella spp*. were retrieved. The video footage showed the highly mobile *Hirondella* amphipod occurring at the bait in incredibly high numbers. Pressure (1000 bar) and again a slightly higher bottom temperature of 1.78ºC were recorded. An even number of both species of amphipod were preserved as in Dep 1a.

DEP 5a: Nom 9000m/ Act; 9036m
24^{o} 08.074 S /175^{o} 10.951 W -Tonga Trench
The lander was deployed in the southern Tonga Trench to just over 9000m. On the bottom, the lander recorded only scavenging hadal-amphipods, however this time it was not purely dominated by *Hirondellas*, another species found at the 8000m mark we still present. Over 2000 specimens of *Hirondella spp*. were retrieved. The video footage showed the amphipods arriving at the bait in extremely high numbers (higher than at 10,000m) and extremely quickly after touchdown. Several very large individual amphipods were seen and three were recovered in the traps. Also seen attending the bait was a relatively large unknown shrimp-like crustacean, possibly the same species but larger than one seen at 8000m. Pressure (904 bar) and a bottom temperature of 1.61ºC were recorded.

Hadal-Lander B (Stills)
The second lander was deployed three times at nominal depths of 6500, 7500 and 8500m. During the first deployment, an intermittent connection problem occurred between the battery and the camera resulting in no near bottom images. Attempts to rectify the problem were unsuccessful also resulting in no near bottom images taken on Dep 2. After more tests and a possible solution were tried, the camera failed completely on Dep 3. Attempts by the operators and the ship electronics officer led to the finding of a faulty wet-pluggable bulkhead connector. The fault lay on the wet side that is encapsulated with potting compound and was therefore unfixable at sea. The decision was made to pull the lander from the cruise to save ship time and concentrate efforts on the Video Lander. The stills lander did however record accurate temperature profiles and bottom temperature that will contribute to our transect of the trenches.

Remarks

This was the first hadal cruise of the newly funded HADEEP project and we are extremely pleased with the results. Although it was disappointing that the second lander failed, getting the full 6000-10,000m transect with the video camera was beyond expectation. The sighting of the fish at 7100m is possibly the first real scientific observations of a hadal fish species in regards to behaviour and in an in situ context. Together with the appearances of the penaids we have filmed for the first time predation in the hadal zone. The collection of amphipods will allow us to perform population genetic studies, taxonomy and define the zonation of scavenging amphipods through the trench depths. The temperature data proved that indeed there is a rise in temperature from 5000 to 10,000m. Furthermore, the 10,000m deployment has proven the technological capabilities. This cruise has been an overwhelming success and will hopefully lead to further investigations and general interest/awareness of the hadal and trench environments.

Fig. 6.3.1.DEP 1A - 6133m, Kermadec Trench; A Penaid preying on small amphipods at the bait (left) and the deep-sea shrimp *Acanthephyra* spp. (right).

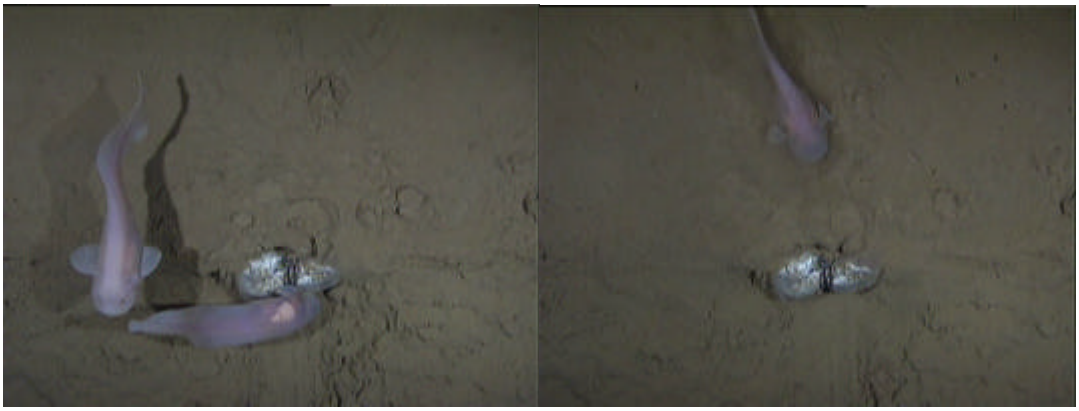

Fig. 6.3.2. DEP 2A – 7049m, Kermadec Trench; *Notoliparis kermadecensis* feeding on scavenging amphipods from around the bait (left) and from the trench-floor (right)

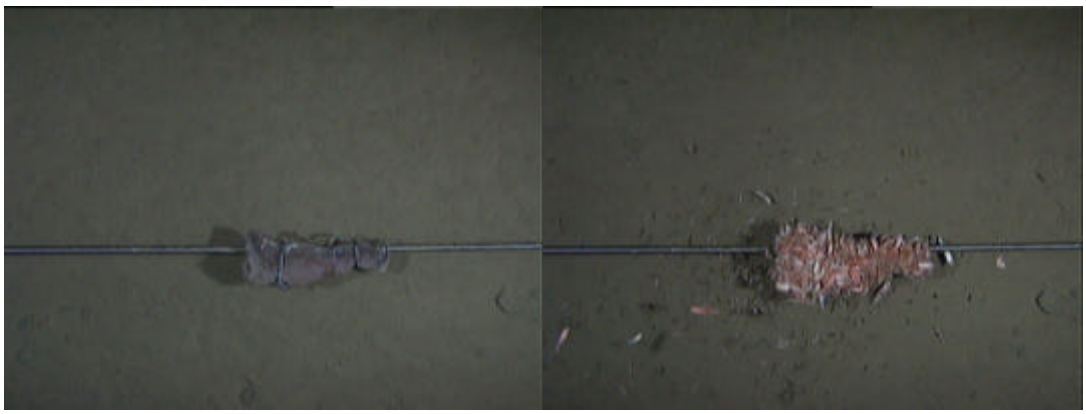

Fig. 6.3.3. DEP 3A – 8130m, Kermadec Trench; Succession of scavenging amphipods, mostly *Hirondellas spp* after 30 minutes (left) and 6 hours (right)

Fig.6.3.4. DEP 4A – 10,015m, Tonga Trench; Succession of scavenging amphipods on the floor of the trench, nearly all *Hirondellas spp* after 10 minutes and 6 hours.

Fig. 6.3.5. DEP 5A – 9036m, Tonga Trench; Amphipods feeding at bait including very large individual left of bait (left) and unknown white crustacean in the top-right (right).

Fig. 6.3.6. Example of the scavenging amphipod *Hirondellas spp,* known to be endemic to depths beyond 7000m

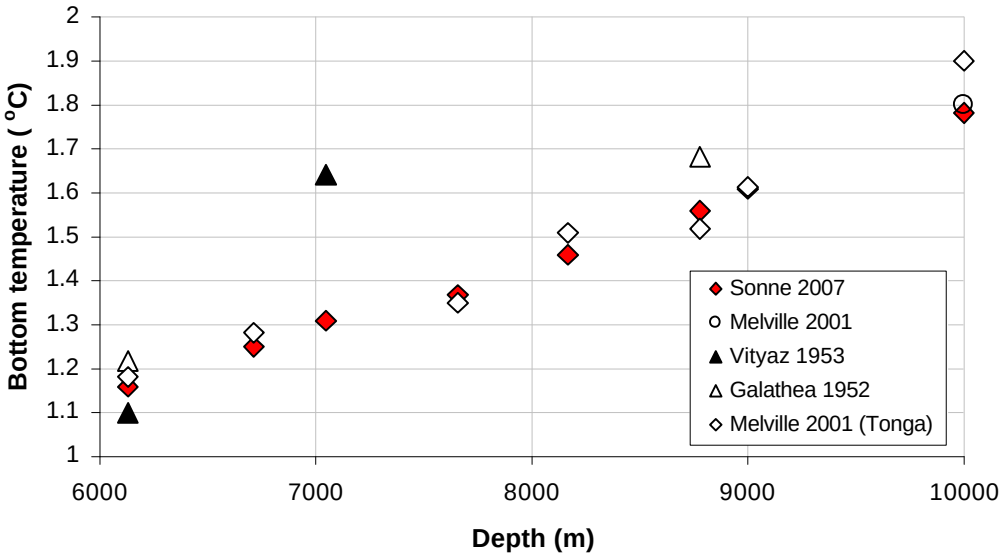

Fig. 6.3.7. Graph showing steady rise in bottom temperature with increasing depths within the trench, data shown against existing trench temperature data.

6.4. Anthropogenic pollutants in the Deep Sea

During this cruise, we performed PCLS of a broad range of mesopelagic fishes and cultivate those slices during 24 hours in the presence of known inducers of CYP1A1 activity, namely 3-methylcholanthrene (25 µM) and co-planar PCB 126 (2 µM/200 nM/ 20 nM). The concentrations were those responsible for EROD induction in *S. salar*.

Fishes were kept in a cold HBSS solution prior to any manipulation. To begin, liver and muscle samples were excised and immediately frozen.. Then, the gills were isolated and cut into little pieces, incubated in 500 µl of L15 medium (comprising 140 ml/l sterile seawater) supplemented with 10% FCS and PenStrep 1X. For this purpose, a 24 multiwell plate was dedicated to each fish. Duplicates of ATP and of EROD measurements were operated for each of 6 conditions, when enough gill pieces were available (L15 only/ 3-MC 25 µM in L15 / 3-MC 25 µM + alpha naphtoflavone 100 µM in L15/ PCB126 2 µM in L15/PCB126 200 nM in L15/ PCB126 20 nM in L15). Alpha naphtoflavone was a negative control for the reaction (CYP1A1 inhibitor), and added in large excess one hour prior to EROD and ATP measurements and was always present as well as 3-MC 25 µM condition. EROD activity and ATP content were also quantified on duplicates prior to the incubations (T0 value). Incubations were performed at 4° C for 21 hours at 200 rpm.

To quantify EROD activities, we used a luminometric measurement with the kit P450 Glo-Assay from Promega. At first, a specific CYP1A1 modified luciferin (CEE-) substrate is added to a gill homogenate, comprising the cytochromes P450. By adding the NADPH regeneration system, luciferin is produced and can therefore be detected by the appropriate Detection Buffer. Alpha naphtoflavone values serve as a negative control and are substracted from the values of experimental conditions to obtain net luminescence. A standard curve of luciferin (not provided by the kit) is also realised to obtain the concentration of luciferin in the samples.

ATP content was measured by luminometry, using the kit ATPlite 1 Step from Perkin-Elmer. Briefly, after homogeneising the gill tissues in 1 ml $HClO_4$ 2%, a brief centrifugation (30 seconds at 13200 rpm) was realised to precipitate the proteins. The supernatant is transferred to a new centrifuge tube containing 120 µl KOH/$KHCO_3$ 3 M/3M which neutralises the ATP. 50 µl of ATPlite 1 Step Reaction Buffer is added to 100 µl of neutralised ATP solution. A standard curve of ATP (provided by the kit) is also realised to obtain the concentration of ATP in the samples.

Unfortunately, due to the consistency and the poor volumes of the livers obtained, we were not able to perform our methodology. Therefore, we focused on gill tissues (prone to CYP1A1 induction) and performed the experimental contaminations mentioned above. Also, we collected samples of liver and muscle to quantify in the future the basal activities of EROD (S9 fractions) and EAOX (GPX, CAT, SOD) in the liver. In the muscle, we will determine the levels of PCBs and DDTs contamination (GC/ECD, ^{63}Ni detector). We also collected muscles and hepatopancreas of shrimps, to compare the levels of contamination, the EAOX and EROD activities with those of mesopelagic fishes.

Concerning the experimental contaminations of gills, nothing can be said at the moment, because of the need to normalise the results obtained to the protein content. However it seems that, if any inductions occured, these were rather small at the concentrations tested. The fishes used for analysis on board were: *Idiacanthus sp.* (1), *Echiostoma sp.* (1), *Argyropelecus aculeatus* (1), *Chauliodus sloani* (1), *Gonostoma gracile* (2).

Samples of muscle/liver were taken from : *Argyropelecus affinis* (2), *Argyropelecus hemigymnus* (2), *Argyropelecus aculeatus* (1), *Gonostoma gracile* (5), *Gonostoma sp.* (5), *Idiacanthus sp.* (3), *Chauliodus sloani* (4), *Lampadena urophaos* (2), *Melanostomias tentaculatus* (1), *Cyclothone sp.* (1), *Echiostoma sp.* (2), *Diaphus longleyi* (1), *Diaphus sp.* (3), *Photostomia sp.* (1), *Scopelarchus analis* (1). Samples of muscle/hepatopancreas were taken from: *Acanthephyra sp.* (4), *Systellaspis debilis* (11), *Sergia splendens* (2), *Sergia sp.* (4), *Oplophorus novaezeelandiae* (2).

6.5. Muscle Physiology (O. Friedrich)

Aims:
We aimed to isolate single intact, living, muscle cells from deep sea fish on board a fully operational research vessel during the SO194 cruise. The objective was to intracellularly stimulate single muscle fibres and concomittantly record Ca^{2+} fluorescence transients to obtain Ca^{2+} release kinetics in relation to the dwelling depths of those fish. The samples were collected from trawls that were performed twice daily in depths between 200 m and 1.000 m.

Specimen and preparation:
During the cruise, 20 trawls were performed from which epiaxial white muscle could be obtained from *Argyropellecius affinis* (3.7.07), *gonostoma gracile* (4.7., 5.7., 8.7., 15.7.07), *stomias boa sp.* (5.7.07), *ichthyostoma* (10.7.07), *diaphus sp.* (11.7.07), *myctophilus* (14.7.07), *Argyropelecus aculeatus* (14.7.07), *chauliodus sp.* (15.7.07) and two unidentified samples for further processing.
The sampling outcome was restricted by the fact that in 25 % of trawls, no appropriate samples were captured in the net (except for some shrimps not used in this project).

Muscle flaps were quickly excised in Ringer solution of 320 mosm and pH 7.3-7.5 and the skin was removed. Small flaps were incubated with collagenase and/or proteinase. The enzymatical digestion protocol was hampered by the fact that enzyme stocks had to be prepared by eye as no mg-scale was available on board. The enzymatical treatment was empirically varied between 5 min and 20 min at room temperature to improve the outcome of single fibre availability. Unfortunately, in many instances, muscles from different species seemed to respond to the enzymatical treatment to completely different degrees. In some cases, short treatments already resulted in complete deterioration of cells whereas 20 min of digestion did not seem to isolate fibres at all from muscle flaps of other species. This hampered the batch sizes we obtained for single fibre experiments.

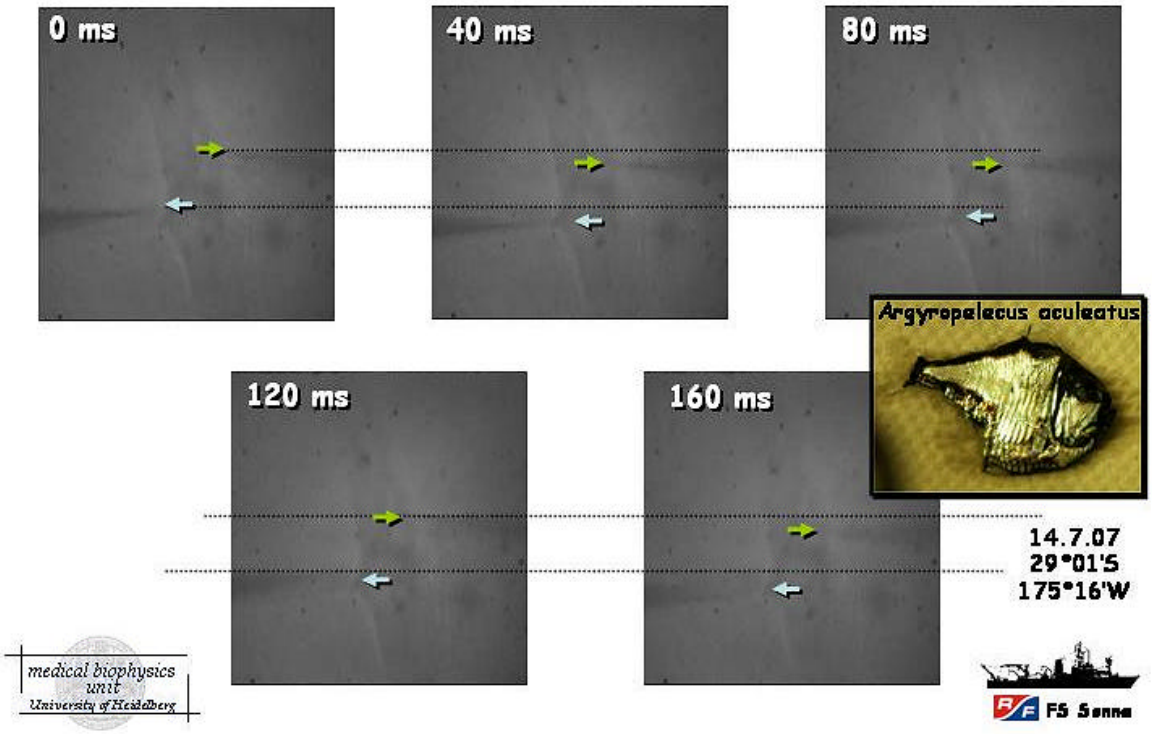

Fig.2: High frequency mechanical vibrations from the running ship engine coupled to the preparation upon single fibre impalement. Although of quite substantial amplitude, microelectrodes remained intracellular for most of the time

After enzymatical isolation, about five to seven single fibres were transferred to an electrophysiology recording chamber and incubated with 10 µM of the Ca^{2+} indicator Fluo-4 AM, first, at room temperature for 30 min for dye loading and then for another 30 min at 37 °C for de-esterification of the dye. The chamber was then transferred to the microscope stage and microeletrodes with a resistance between 4 MΩ and 7 MΩ selected for impalement. The pipettes had tip diameters of ~3 µm.

Microelectrode responses to mechanical vibrations:
One of the main problems that arised were heavy mechanical vibrations of the electrodes that seriously impaired fibre impalement and caused membrane damage. After several unsuccesful experiments, the setup was re-assembled on a layer of air cushions that were used for transport stuffing to reduce mechanical coupling from the hull vibrations. Additionally, the laboratory table (non-pneumatic) was also stuffed with dampening material.

There were two distinct patterns of mechanical vibrations: a **high frequency electrode tip oscillation** originating from the running engine (Fig.2) and a **low frequency drift of the electrode corpus** originating from the sea wave movements (Fig.3).

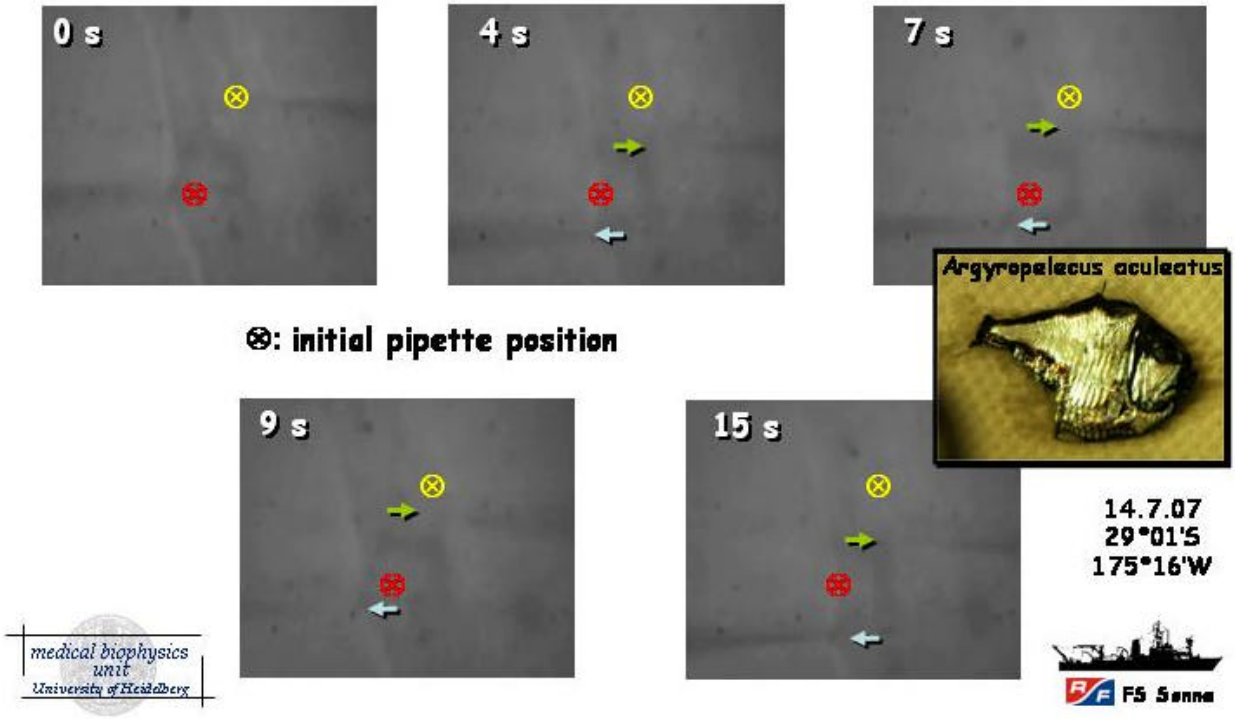

Fig.3: Low frequency mechanical movements (due to waves) that are meachnically coupled via the hull to the pipettes. Due to mass inertia, pipettes follow the wave movements. Arrows depict actual pipette tip positions.

The low frequency drift from wave activity increased during the course of the experiment. This was mostly due to the fact that shortly after retrieving the nets the ship took up speed again. By the time of single fibre isolation and fluochrome staining, the ship usually was already going 13 knots, thus preventing calm recording conditions. During the second week, recording was even abandoned due to bad weather conditions with heavy waves and wind strengths of 5-7.

Epifluorescence Ca^{2+} recordings in resting fibres:
In all experiments, resting Ca^{2+} fluorescence was recorded. Fig.4 shows the transillumination and Fluo-4 image of a single fibre from *chauliodus sp.* (trawl #19, 15.7.07). The fluorescence profile from three line ROIs is also shown. Interestingly, in the XY-image, an inhomogenous distribution of Flu-4 fluorescence with accumulation areas can be seen. This is also apparent from the surface profile plot of Fluo-4 intensity. The origin of these '*hot spots*' could not be further determined with the available measures on board. However, they may be either due to dye compartmentalization or reflect signals from local Ca^{2+} stores that take up residual fluo-4 AM. This behaviour was not seen in all samples, mostly due to a low signal-to-noise ratio from low staining.

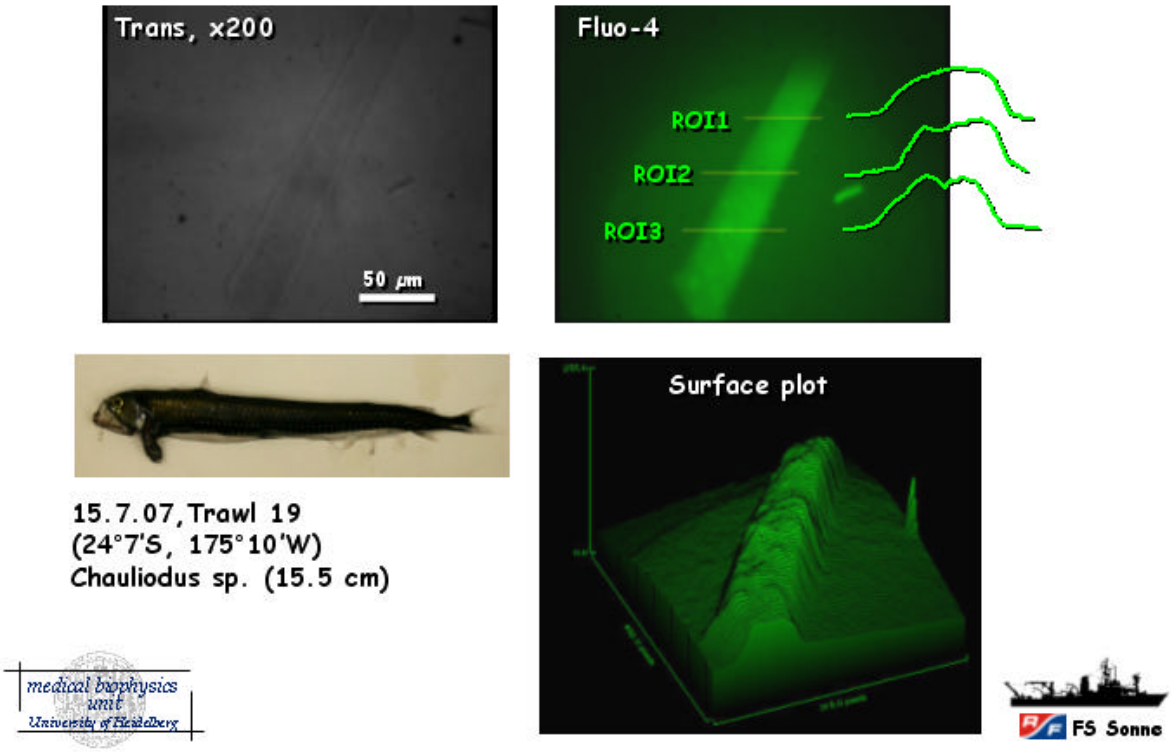

Fig.4: Resting Fluo-4 Ca^{2+} fluorescence in a single muscle fibre from chauliodus sp. The fluorescence image shows some spherical regions of increased fluorescence. This pattern is also refelcted in the intensity surface plot from this fibre.

Intracellular recordings of membrane potentials:
In some successful experiments, pipettes were stable to record intracellular resting potentials. In a first approach, pipettes were driven forth into whole muscle flaps that were freshly dissected without further enzymatic treatment. In Ringer solution containing low 2.5 mM K^+, this gives an indication about the relative K^+ selectivity of the resting membrane. As can be seen from Fig.5A in muscle from gonostoma gracilis (Trawl #7, 5.7.07, 22°50'S, 174°33'W), resting membrane potentials E_m became more negative upon going deeper into the tissue. This behaviour reflects the fact that superficial fibres that have been traumatized or been in contact with air during the processing are more depolarized.

Albeit the strong vibrations that hampered single fibre impalement, our attempts to stimulate single enzymatically isolated fibres were in principle successful. We managed to impale a series of single fibres (~30) after the enzymatic treatment and fluochrome staining. However, most of these fibres already had depolarised resting potentials between -5 mV and -10 mV. Additionally, this finding might also reflect membrane leaks or small

ruptures that induce a breakdown of the membrane potential. In the fibre shown in Fig.5B from *Argyropelecus aculeatus* (Trawl #18, 14.7.07, 24°01'S, 175°16'W), even after injecting a maximum constant negative current, E_m could only be repolarised to about -35 mV. The protocol shown to elicit action potentials then first injects another negative booster current of -1000 nA that further repolarises E_m close to -65 mV before a positive +1000 nA current pulse is applied. During this step pulse, E_m is electrotonically depolarised to -5 mV. The very fast charge dislocation is in the range of 100 ms to 200 ms (see exponential fit in Fig.5B) and reflects passive membrane parameters such as the input resistance R_0 and the input capacitance C_0. However, no action potential could be elicited as Na^+ channels were still inactivated at -65 mV. Concomittantly, there was no activity seen in the fluorescence image as the ryanodine receptors would not have been activated without an action potential.

From the recording, we calculated R_0 to be 2 kΩ, about an order of magnitude smaller than values found by us in our home lab in mammalian muscle fibres treated the same way (~2 MΩ). This fully explains the low resting potentials in the fish muscle fibres that we onserved. The low membrane potential is causing an increased influx of depolarising ions. The C_0 values, however, were about ten times larger compared to mammalian muscle fibres, i.e. 50 pF vs. 5 pF.

As untreated muscle showed much better E_m values but isolated fibres are necessary for intracellular voltage or current clamp, future projects need to improve the fibre isolation technique. At the current stage, we cannot unambigously say which one of the parameters to modify as also different fish muscles seemed to behave differently.

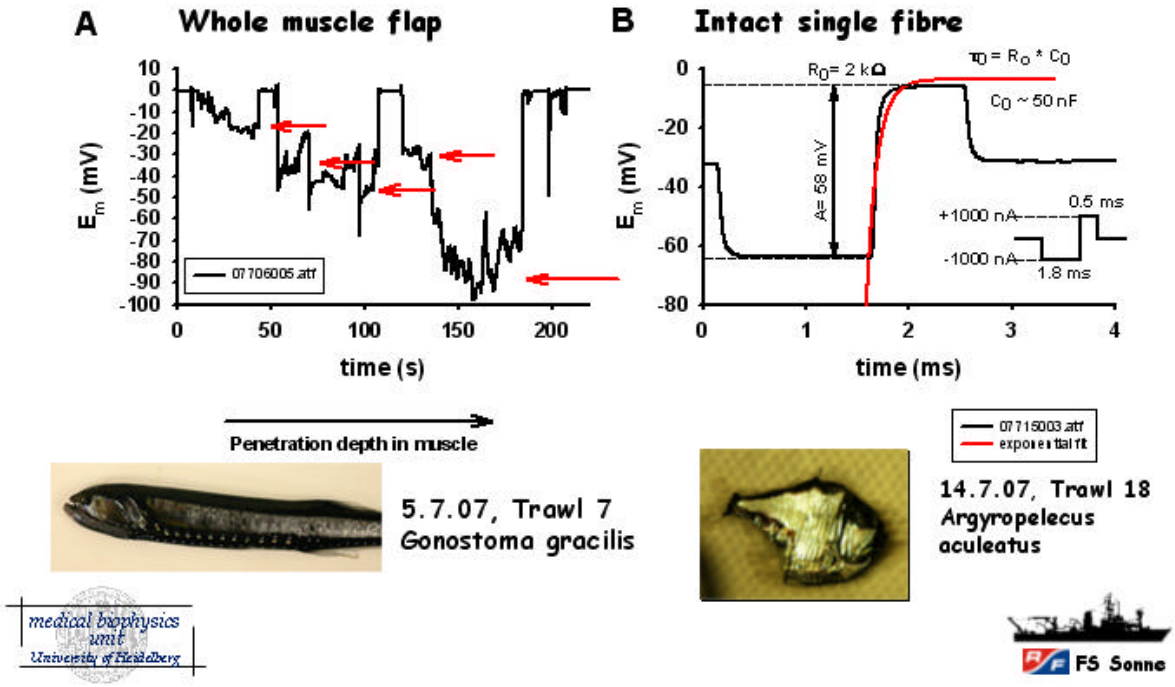

Fig.5: Intracellular recordings of membrane potentials in white skeletal muscle of deep sea fish. **A,** Penetration of electrodes forth and back into an unprocessed freshly dissected muscle flap from *gonostoma gracilis*. Note that E_m values become more polarised upon penetration depth. **B,** Current clamp in a single muscle fibre from Argyropelecus aculeatus. From the electrotonic response, membrane input resistance R_0 and capacitance C_0 were recorded.

Conclusions:

Due to some coincidences (low number of fish in trawls, strong wave activity, heavy coupling of mechanical hull vibrations, low number of single cells after enzymatic processing), recording of action potentials were impossible in this cruise. However, we

strongly believe that this is possible in principle with some of the constraints given further consideration in future trials.

The approach of elucidating ion channel activity and Ca^{2+} homeostasis on board a running ship using intracellular microelectrode applications and fluorescence microscopy is all but a trivial task and still very unique. Once, the techniques will be stably established, ‘on-site’ recording of membrane and Ca^{2+} dynamics will help to shed further light into cellular high ambient pressure adaptations in deep sea fish.

6.6. Bathymetry (E. Flueh)

Simrad EM120 swathmapping system

The EM120 system is a multibeam echosounder (with 191 beams) providing accurate bathymetric mapping up to depths exceeding 11000 m. This system is composed of two transducer arrays fixed on the hull of the ship, which send successive frequency coded acoustic signals (11.25 to 12.6 kHz). Data acquisition is based on successive emission-reception cycles of this signal. The emission beam is 150° wide across track, and 2° along track direction
(Fig. 6.6.1). The reception is obtained from 191 overlapping beams, with widths of 2° across track and 20° along it (Fig. 6.6.1). The beam spacing can be defined as equidistant or equiangular, and the maximum seafloor coverage fixed or not. The echoes from the intersection area (2°*2°) between transmission and reception patterns (Fig. 6.6.1) produce a signal from which depth and reflectivity are extracted. For depth measurements, 191 isolated depth values are obtained perpendicular to the track for each signal. Using the 2-way-travel-time and the beam angle known for each beam, and taking into account the ray bending due to refraction in the water column by sound speed variations, depth is estimated for each beam. A combination of phase (for the central beams) and amplitude (lateral beams) is used to provide a measurement accuracy practically independent of the beam pointing angle. The raw depth data need then to be processed to obtain depth-contour maps. In the first step, the data are merged with navigation files to compute their geographic position, and the depth values are plotted on a regular grid to obtain a digital terrain model (*DTM)*. In the last stage, the grid is interpolated, and finally smoothed to obtain a better graphic representation. Together with depth measurements, the acoustic signal is sampled each 3.2ms and processed to obtain a cartographic representation, commonly named mosaic, where grey levels are representative of backscatter amplitudes. These data provide thus information on the sea-floor nature and texture; it can be simply said that a smooth and soft seabed will backscatter little energy, whereas a rough and hard relief will return a stronger echo. The EM120 was used continuously during cruise SO 194. Bathymetric data were processed routinely onboard during the survey, using the NEPTUNE software from Simrad, available on board and the academic software MB-System from Lamont-Doherty Earth Observatory. Subsequently, the data collected during SO194 will be merged with data collected during previous cruises. A map of the main working area is shown in Figure 6.6.2.

CTD data

The CTD rosette onboard RV SONNE was deployed during cruise SO194 to measure physical oceanographic parameters (Fig. 6.6.3.). The CTD station was run to a water depth of 5000 m at a velocity of 1 m/s continuously measuring the sound speed in-situ. The sound velocity profile obtained is shown in Figure 6.6.4. Accurate sound velocity profiles are needed for calibration of the water sound velocity to transfer the echo times of the bathymetric swath mapping into water depth. The velocity profile exhibits the typical curvature with similar characteristics of measurements conducted elsewhere.

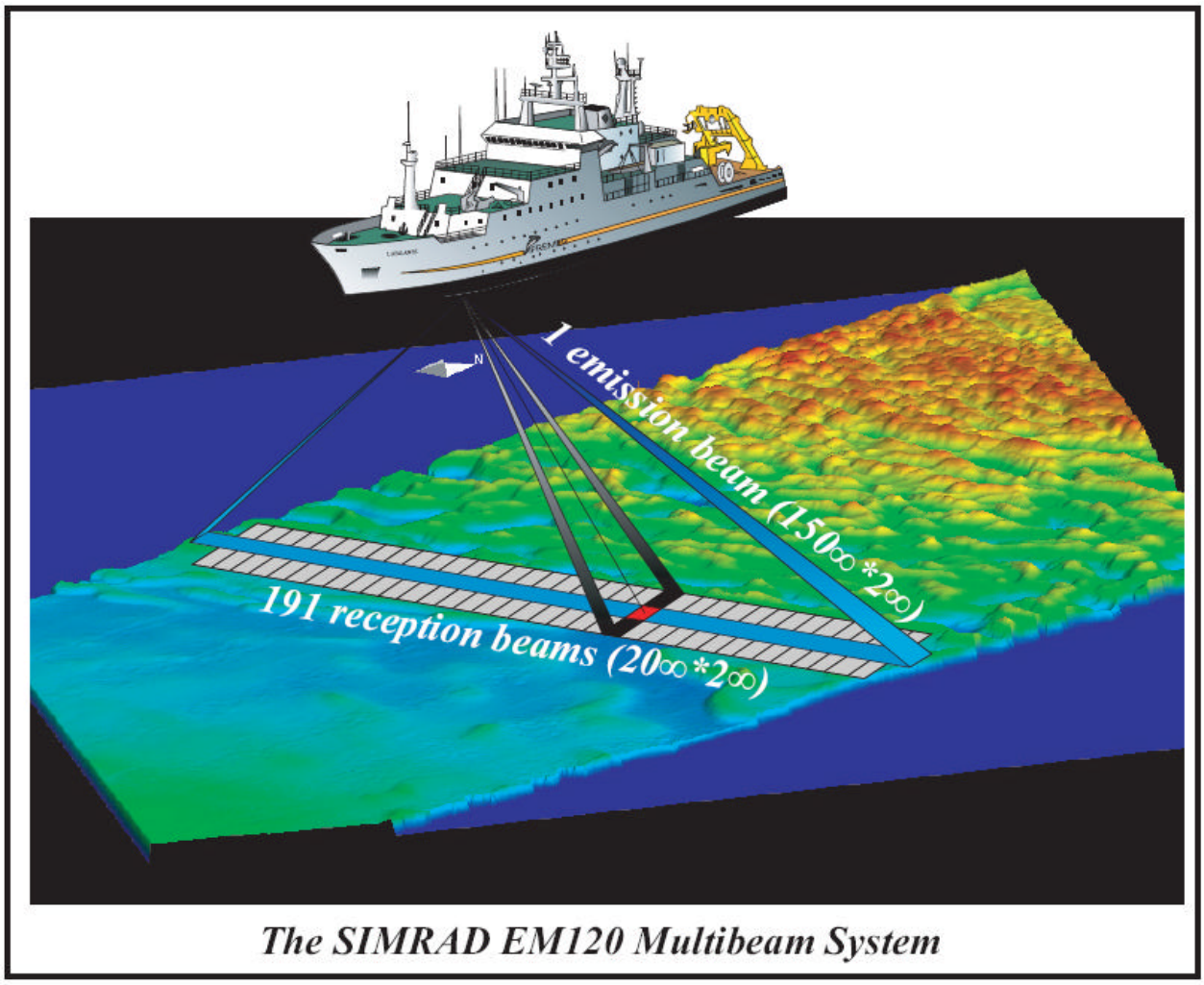

Figure 6.6.1: *Acquisition method for bathymetric and backscatter data from the Simrad EM120 system (crossed beams technique).*

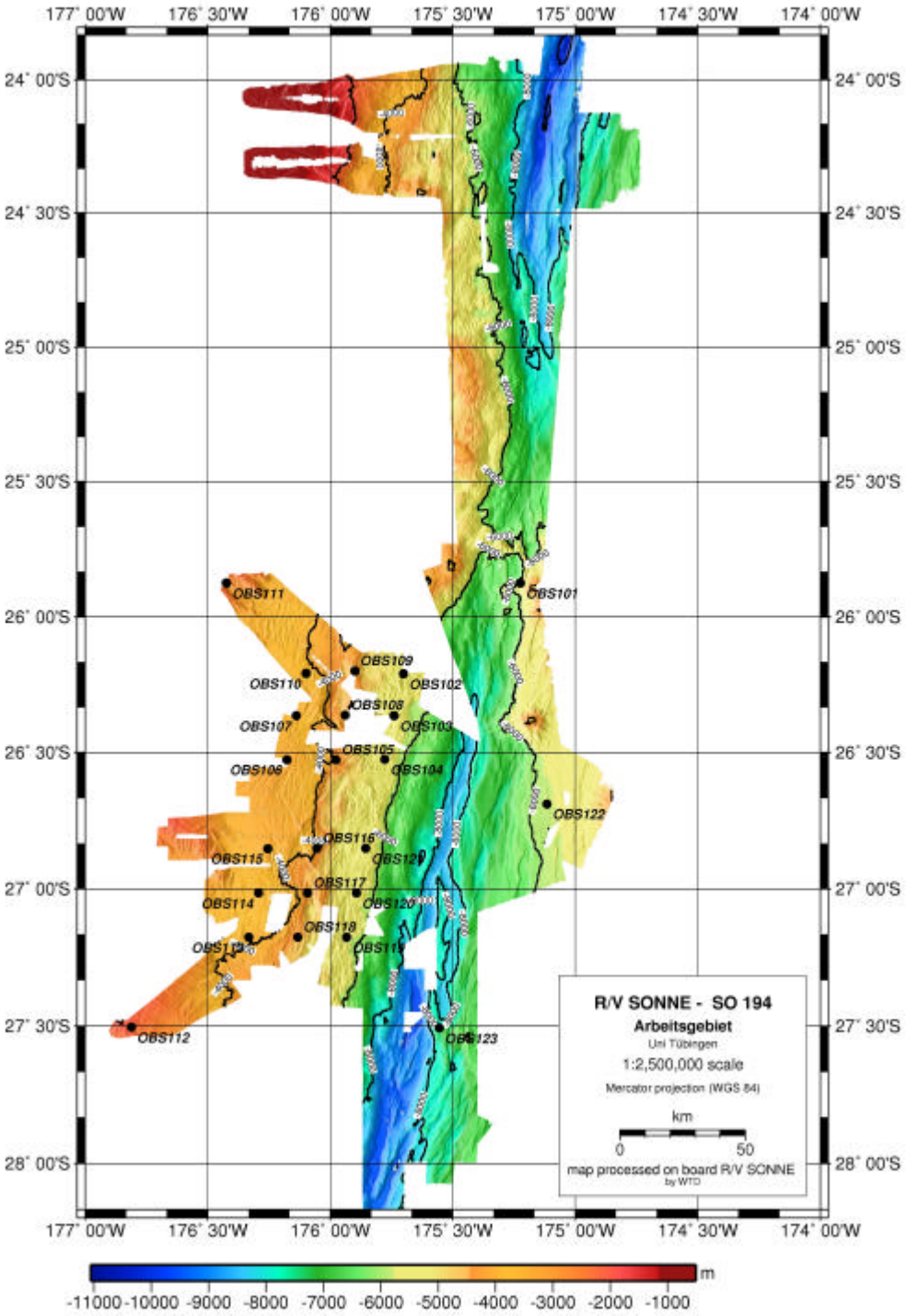

Figure 6.6.2: *Recorded bathymetry in the main working area of the SO 194-cruise.*

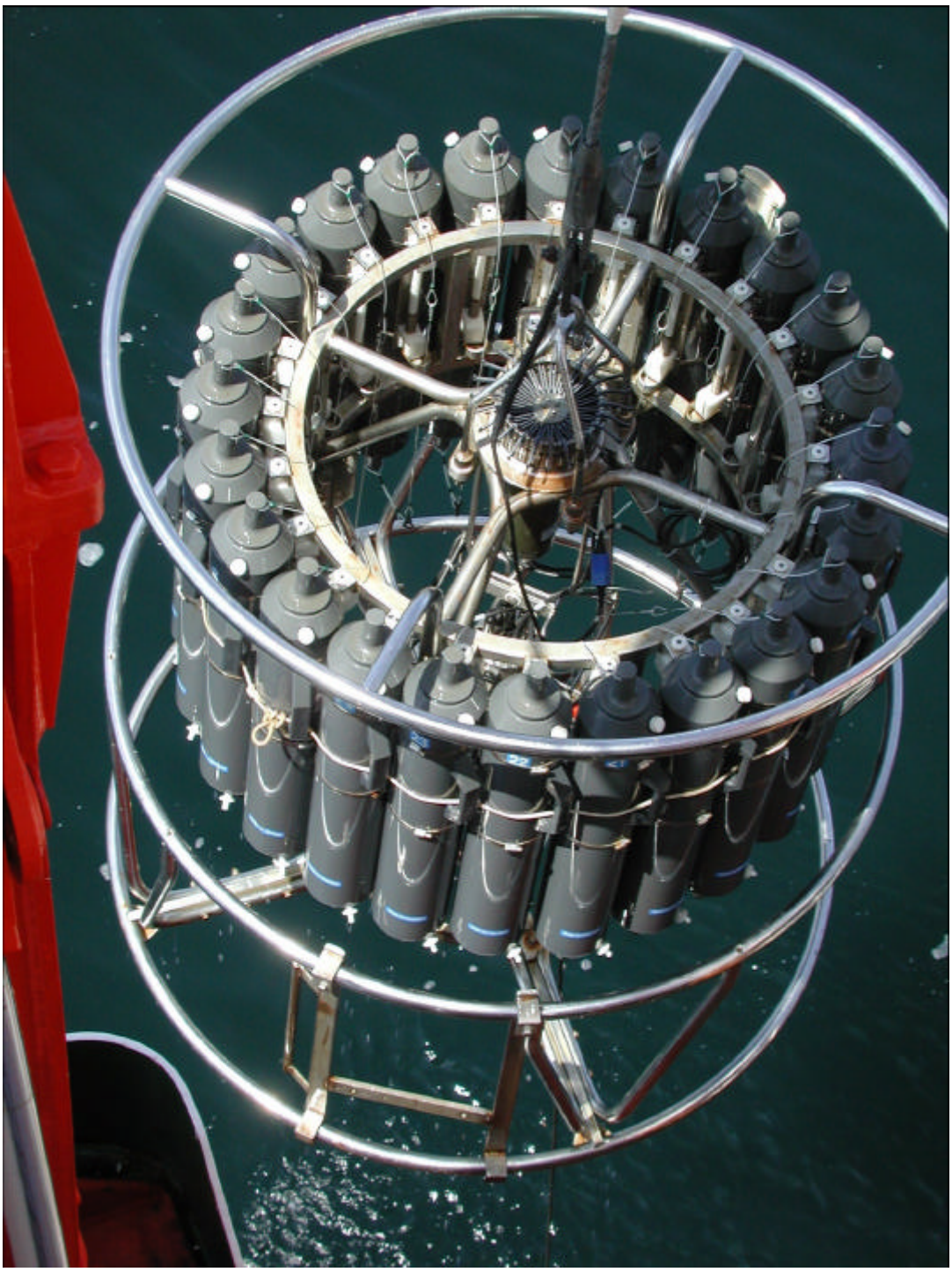

Figure 6.6.3: *RV SONNE's onboard CTD rosette upon deployment.*

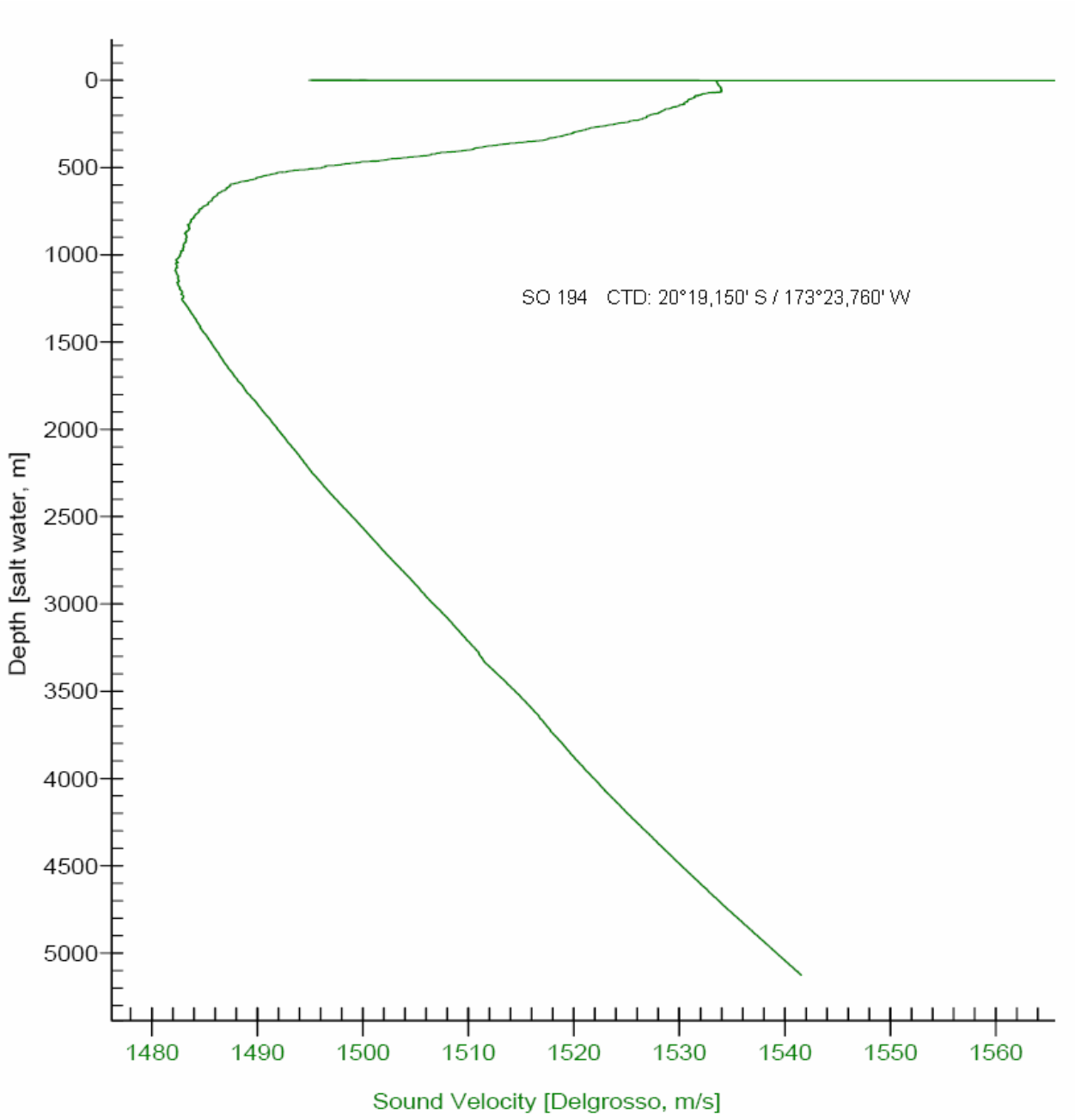

Figure 6.6.4: *Sound velocity profile obtained from CTD measurement during SO194 on 04.07.2007 at 10:00 UTC.*

Acknowledgements:

H.-J. Wagner: DFG Wa 348/24

Lander Project: Part of the HADEEP project funded by the National Environmental Research Council, UK (NERC) and the Nippon Foundation , Japan

Nine of the Ocean Bottom Seismometers deployed were borrowed from the DEPAS instrument pool operated by AWI, Bremerhaven.

References

Behrens, U. D., Douglas, R. H., Sugden, D., Wagner, H. - J., 2000. The effect of melatonin agonists and antagonists on horizontal cell spinule formation and dopamine release in a fish retina. Cell and Tissue Research 299, 299-306.

Collin, S.P., Hoskins, R.V. and Partridge, J.C., 1997: Tubular eyes of deep-sea fishes: a comparative study of retinal ganglion cell topography. Brain Behav.Evol. 50, 335-357

Douglas, R.H., Partridge, J.C. and Hope, A.J, 1995: Visual and lenticular pigments in the eyes of demersal deep-sea fishes. *J. Comp. Physiol. A* 177, 111-122.

Douglas, R.H and Partridge, J.C., 1997: On the visual pigments of deep-sea fish. *J. Fish Biol*. **50**,68-85.

Douglas, R.H., Partridge, J.C. & Marshall, N.J., 1998a: The Eyes of deep-sea fish I: Lens pigmentation, tapeta and visual pigments. *Prog. Ret. Eye Res*. 17(4), 597-636.

Douglas, R.H., Partridge, J.C., Dulai, K., Hunt, D., Mullineaux, C.W., Tauber, A. & Hynninen, P.H.,1998b: Dragon fish see using chlorophyll. *Nature* 393, 423-424.

Ekström, P. and Meissl, H., 1997. The pineal organ of teleost fishes. Reviews in Fish Biology and Fisheries 7, 199-284.

Engdahl, E.R., Villasenor, A. (2002) Global seismicity: 1900-1999, *International Handbook of Earthquake and Engineering seismology*, 81A, 665-690.

Falcón, J., Gothilf, Y., Coon, S. L., Boeuf, G., Klein, D. C., 2003. Genetic, temporal and developmental differences between rhythm generating systems in the teleost fish pineal organ and retina. Journal of Neuroendocrinology 15, 378-382.

Garg, S. K., Sundararay, B. I., 1986. Role of pineal in the regulation of some aspects of circadian rhythmicity in the catfish, *Heteropneustes fossilis* (Bloch). Chronobiologia 13, 1-11.

Gould, W. J., McKee, W. D., 1973. Vertical structure of semi-diurnal tidal currents in the Bay of Biscay. Nature 244, 88-91.

Herring, P.J., 1987: Systematic distribution of bioluminescence in living organisms. Biolum. Chemilum. 1, 147-163

Herring, P.J., 1996: Light, colour and vision in the ocean. In: Oceonography. An illustrated guide(eds. C.P. Summerhayes and S.A. Thorpe) pp. 212-227. Mason Publ., London

Herring, P.J. , 2002. The biology of the deep ocean. Oxford University Press, Oxford, New York

Hirt, B. and Wagner, H.-J., 2005. The organization of the inner retina in a pure-rod deep-sea fish. Brain Behav. Evol. 65, 157-167

Huether, G., 1993. The contribution of extrapineal sites of melatonin synthesis to circulating melatonin levels in higher vertebrates. Experientia 49, 665-670.

James, I. D., 1982. Tidal currents at two deep-sea moorings near the shelf edge. Deep-Sea Research 29, 1099-1111

Kusmic, C., Marchiafava, P. L., Strettoi, E., 1992. Photoresponses and light adaptation of pineal photoreceptors in the trout. Proceedings of the Royal Society London B 248, 149-157.

Lampitt, R.S., Merrett, N.R., Thurston, M.H., 1983. Inter-relations of necrophagous amphipods, a fish presator, and tidal currents in the deep sea. Marine Biology 74, 73-78.

Partridge, J.C. and Douglas, R.H., 1995: Far-red sensitivity of dragon fish. Nature 375, 21-22

Reiter, R. J., 1991. Pineal melatonin: cell biology of its synthesis and of its physiological interactions. Endocrine Reviews 12, 151-180.

Vangrieshaim, A., Khripounoff, A., 1990. Near-bottom particle concentration and flux: temporal variations observed with sediment traps and nephelometer on the Meriadzek Terrace, Bay of Biscay. Progress in Oceanography 24, 103-116.

Wagner, H.-J., Fröhlich, E., Negishi, K. and Collin, S.P., 1998 The eyes of deep-sea fish: II. Functional morphology of the retina. Progress in Retinal and Eye Research, Vol. 17, pp 637-685

Wagner, H.-J., Kemp, K. Priede, I.G. 2007 Rhythms at the bottom of the deep sea: Cyclic current flow changes, and melatonin patterns in two species of demersal fish; Deep Sea Res. I under revision

Wisner R.L. (1974) *The taxonomy and distribution of lanternfishes (Family Myctophidae) of the Eastern Pacific Ocean.* Navy Ocean Research and Development Activity (NORDA) Report-3. pp. 1 -230

Whitehead PJP, Bauchot M-L, Hureau J-C, Nielsen J, Tontonese E (1984) Fishes of the North-eastern Atlantic and the Mediterranean. Paris, Unesco

Appendix

I Sonnetrack

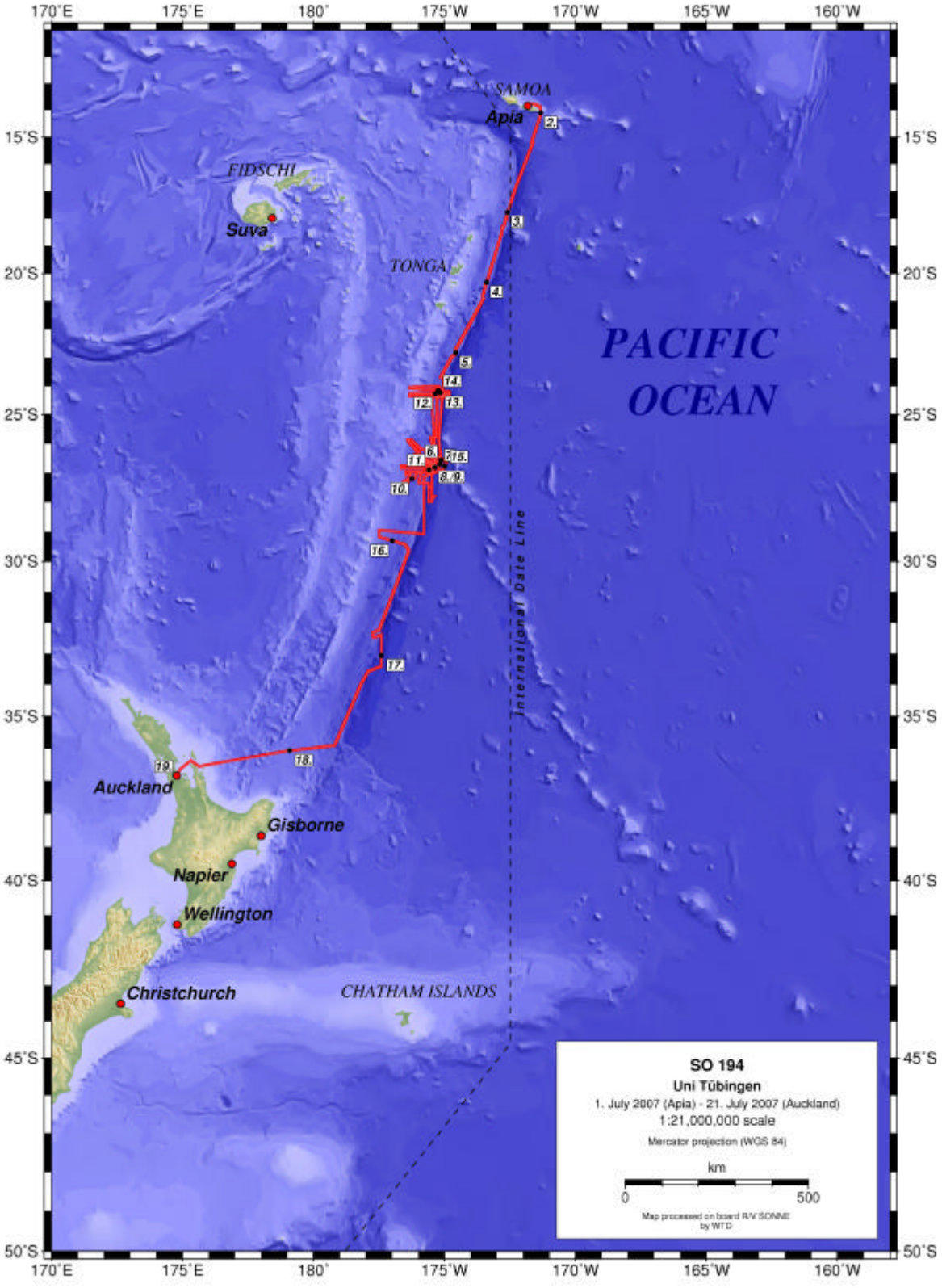

II Ocean Bottom Instrumentation

SO 194 - OBS-Deployment

IV Ocean Bottom Instrumentation

STATION NO.	TYPE	LAT D:M	LON D:M	DEPTH (m)	DEPLOY. DATE	RELEASECODE TIME RELEASE	SENSORS	REC. NO.
OBS 101	AWI Lobster	25° 52,485' S	175° 13,470' W	5850	06.07.2007	446362 (01.02.08 09:00)	HTI 312134 + GÜ-071	MCS 060751
OBS 102	AWI Lobster	26° 12,596' S	175° 42,057' W	5202	07.07.2007	446426 (01.02.08 01:00)	HTI 312125 + GÜ-079	MCS 060720
OBS 103	GEOMAR Lobster	26° 21,811' S	175° 44,310' W	5618	07.07.2007	533622 (01.02.08 02:00)	HTI 84 + Owen 86 (4,5Hz)	MLS 000712
OBS 104	AWI Lobster	26° 31,487' S	175° 46,595' W	5666	07.07.2007	446532 (01.02.08 10:00)	HTI 312124 + GÜ-077	MCS 060711
OBS 105	Dreibein	26° 31,599' S	175° 58,614' W	4096	07.07.2007	0387+0355 (01.02.08 15:00)	HTI 37 + Owen 73 (4,5Hz)	MLS ???
OBS 106	Dreibein	26° 31,551' S	176° 10,575' W	3382	07.07.2007	3624 (01.02.08 20:00)	HTI 82 + Owen 78 (4,5Hz)	MLS 991235
OBS 107	Dreibein	26° 21,831' S	176° 08,323' W	3515	07.07.2007	3614 (01.02.08 21:00)	HTI 90 + Owen 57 (4,5Hz)	MLS 991249
OBH 108	gr. Kugel	26° 21,747' S	175° 56,349' W	4230	07.07.2007	3619 (01.02.08 19:00)	HTI 83	MLS 991250
OBS 109	Dreibein	26° 11,981' S	175° 53,998' W	4251	07.07.2007	03B6+0355 (01.02.08 13:00)	HTI 32 + Owen 82 (4,5Hz)	MLS 061201
OBS 110	Dreibein	26° 12,491' S	176° 05,965' W	3733	07.07.2007	03B7+0355 (01.02.08 16:00)	HTI 27 + Owen 58 (4,5Hz)	MLS 991248
OBS 111	AWI Lobster	25° 52,494' S	176° 25,444' W	2763	07.07.2007	446635 (01.02.08 11:00)	HTI 312129 + GÜ-078	MCS 060706
OBS 112	AWI Lobster	27^° 30,220' S	176° 48,663' W	2096	11.07.2007	446276 (01.02.08 07:00)	HTI 312123 + GÜ-073	MCS 060723
OBS 113	Dreibein	27° 10,610' S	176° 19,988' W	3958	11.07.2007	03B3+0355 (14.01.08 15:00)	HTI 65 + Owen 19 (4,5Hz) + PARO 98613	MTS 050814
OBS 114	Dreibein	27° 00,903' S	176° 17,583' W	3648	11.07.2007	03B2+0355 (14.01.08 16:00)	HTI 76 + Owen 64 (4,5Hz)	MLS 040304
OBS 115	AWI Lobster	26° 51,119' S	176° 15,306' W	3348	09.07.2007	446324 (01.02.08 00:00)	HTI 312130 + GÜ-072	MCS 060713
OBS 116	Dreibein	26° 51,087' S	176° 03,306' W	3741	09.07.2007	0398+0355 (01.02.08 18:00)	HTI 86 + Owen 80 (4,5Hz)	MTS 041104
OBH 117	gr. Kugel	27° 00,889' S	176° 05,553' W	4369	11.07.2007	0397+0355 (01.02.08 14:00)	HTI 87	MLS 061202
OBS 118	GEOMAR Lobster	27° 10,569' S	176° 07,943' W	4445	10.07.2007	533736 (01.02.08 03:00)	Owen 83 (4,5Hz)	MLS 010407
OBS 119	AWI Lobster	27° 10,627' S	175° 56,021' W	5659	10.07.2007	446673 (01.02.08 08:00)	HTI 312112 + GÜ-070	MCS 060724
OBS 120	GEOMAR Lobster	27° 00,886' S	175° 53,588' W	5295	10.07.2007	534123 (01.02.08 04:00)	Owen 84 (4,5Hz)	MLS 991247
OBS 121	GEOMAR Lobster	26° 51,105' S	175° 51,294' W	5293	09.07.2007	534071 (01.02.08 06:00)	HTI 39 + Owen 85 (4,5Hz) + PARO 98616	MTS 050810
OBS 122	AWI Lobster	26° 41,296' S	175° 06,972' W	5789	07.07.2007	446460 (01.02.08 12:00)	HTI 312135 + GÜ-080	MCS 060707
OBS 123	AWI Lobster	27° 30,435' S	175° 33,318' W	7669	10.07.2007	446574 (01.02.08 05:00)	HTI 312118 + GÜ-069	MCS 060712

III Species List (Wagner)

Station # 1 TUT (Tucker Trawl) 2.7.07

Coordinates:
net out: 19.20
depth: ~ 200 m
net in: 21.45

Scopelarchus analis	45 mm	total PA (f. Immuno)	21:57
Argyropelecus aculeatus	80 mm	pineal: freeze	22:04
Idiacanthus fasciola	490 mm	brain PA (f. Immuno)	22:15
Idiacanthus fasciola	205 mm	brain PA (f. Immuno)	22:20
Argyropelecus aculeatus	30 mm	pineal: freeze	22:25
		brain (f. Immuno)	22:26

Station # 2 TUT 3.7.07

Coordinates: 17^0 45' S 172^0 35' W
net out: 10.30
depth: ~ 500 m, open for 2 hrs (not sure)
net in: 14.45

Argyropelecus aculeatus	40 mm	pineal: freeze	15:05
		brain + rets PA (f. Immuno)	15:06
Argyropelecus aculeatus	30 mm	pineal: freeze	15:09
		brain + rets PA (f. Immuno)	15:11
1 unbekannte Spezies	70 mm	4% PA (total), Sammelbehälter	15:15

Station # 3 TUT 3.7.07

Coordinates: 18^0 22' S 172^0 46' W
net out: 18.55
depth: ~ 200 m ?, open for 2 hrs
net in: 21.30

Gonostoma gracile	130 mm	pineal: freeze	21:59
Foto 117-1767ff		brain + rets PA (f. Immuno)	22:02
Chaliodus (sloani)	160 mm	pineal: freeze	22:10
Foto 117-1771ff		brain + rets PA (f. Immuno)	22:11
Idiacanthus fasciola	240 mm	brain + rets PA (f. Immuno)	22:30
Foto 117-1775			
1 unbekannte Spezies		4% PA (total), Sammelbehälter	22:32
Foto 117-1776			
Argyropelecus aculeatus	23 mm	brain + rets PA (f. Immuno)	22:35
Argyropelecus aculeatus	20 mm	brain + rets PA (f. Immuno)	22:38
Melamphaenoid (Poromitra?)	70 mm	brain+ rets PA (f. Immuno)	22:45
Lampanyctus	93 mm	pineal: freeze	22:58
		brain + rets PA (f. Immuno)	23:03

Station # 4 „Releasertest“ (?) **4.7.07**

Coordinates: 20^0 24' S 173^0 27' W
net out: 13.30
depth: ~ 500 m, open for 2,5 hrs
net in: 16.30

Argyropelecus aculeatus	50 mm	pineal: freeze	17:15
Argyro. hemigymnus	30 mm	fragl. pineal: freeze	16:51
		brain + rets PA (f. Immuno)	16:52
Argyro. hemigymnus	25 mm	pineal: freeze	17:00
		brain + rets PA (f. Immuno)	17:01
Argyro. hemigymnus	25 mm	pineal *) sicher!: freeze	17:04
		brain + rets PA (f. Immuno)	17:05
Argyro. hemigymnus	25 mm	pineal: freeze	17:07
		brain + rets PA (f. Immuno)	17:09

Station # 6 TUT **4.7.07**

Coordinates: 20^0 48' S 173^0 32' W
net out: 18.30
depth: ~ 200 m ?, open for 2,5 hrs
net in: 21.40

Gonostoma gracile	125 mm	pineal: deep freeze	22:03
		brain + rets PA (f. Immuno)	22:05
Idiacanthus fasciola	148 mm	pineal (?): deep freeze	22:20
		brain + rets PA (f. Immuno)	22:22
2 x Squid		4% PA (total), Sammelbehälter	22:25
Aal (Leptocephalus Larvenstadium)		4% PA (total), Sammelbehälter	22:26
unbekannter Aal		4% PA (total), Sammelbehälter	22:30
Scopelarchus analis	55 mm	total PA (f. Immuno)	22:40
Scopelarchus analis	30 mm	total PA (f. Immuno)	22:43
Argyro. hemigymnus	20 mm	brain + rets PA (f. Immuno)	22:57

Station # 7 TUT **5.7.07**

Coordinates: 22^0 50' S 174^0 33' W
net out: 8.30
depth: ~ 500 m, open for 2,5 hrs
net in: 13.10

Stomias boa	124 mm	brain + rets PA (f. Immuno)	13:32
Gonostoma gracile	128 mm	DEXTRITC (opticus) 2d	13:57
Foto 117-1855f		f. rets + brain	
		(zu Hause nachpräparieren!)	
Argyropelecus aculeatus	35 mm	pineal: deep freeze (sehr schön!)	14:01
		brain + rets PA (f. Immuno)	14:03
Argyropelecus aculeatus	24 mm	pineal: deep freeze (sehr schön!)	14:07
		brain + rets PA (f. Immuno)	14:08

Station # 8 TUT **5.7.07**

Coordinates: 23^0 42' S 175^0 08' W
net out: 18.30
depth: ~ 175 - 200 m, open for 2,5 hrs
net in: 21.40

Scopelarchus analis	34 mm	DEXTRITC (opticus) 2d f. rets + brain (zu Hause nachpräparieren)	22:09
Gonostoma gracile	170 mm	pineal: deep freeze	22:11
		brain + rets PA (f. Immuno)	22:13
Gonostoma gracile	130 mm	pineal: deep freeze	22:19
		brain + rets PA (f. Immuno)	22:22
Gonostoma gracile	110 mm	pineal: deep freeze	22:20
		brain + rets PA (f. Immuno)	22:24
Gonostoma gracile	120 mm	pineal: deep freeze	22:26
		brain + rets PA (f. Immuno)	22:28
Photostomias guernei	65 mm	head total PA (f. Immuno)	22:33
Rons ID: So7/30		nicht präpariert !	
Gonostoma gracile	120 mm	pineal: deep freeze	22:35
		brain + rets PA (f. Immuno)	22:37
Gonostoma gracile	75 mm	pineal: deep freeze	22:38
		brain + rets PA (f. Immuno)	22:40
Gonostoma gracile	75 mm	pineal: deep freeze	22:41

Station # 14 TUT **7.7.07**

Coordinates: 24^0 45' S 175^0 16' W
net out: 14.40
depth: ~ 200 m, open for 2,5 hrs
net in: 18.25

kein für uns verwertbarer Inhalt

Station # 17 TUT **7.7.07**

Coordinates: 26^0 50' S 175^0 22' W
net out: 20.00
depth: ~ 150 m, open for 1 hr
net in: 21.50
kein für uns verwertbarer Inhalt

Station # 19 TUT **8.7.07**

Coordinates: 26^0 46' S 175^0 15' W
net out: 9.00
depth: > 500 m, open for 3 hrs
net in: 13.10
kein für uns verwertbarer Inhalt

Station # 21 TUT **8.7.07**

Coordinates: 26^0 45' S 175^0 45' W
net out: 18.30
depth: 1 hr at 250 m, 1 h at 200 m
net in: 21.15

Gonostoma gracile	150 mm	pineal: deep freeze	21:35
		brain + rets PA (f. Immuno)	21:36
Photostomias	150 mm	4% PA für Plastination	
Rons ID: So7/43		nicht präpariert !	
Gonostoma gracile	130 mm	pineal: deep freeze	21:47
		brain + rets PA (f. Immuno)	21:49
Argyropelecus aculeatus	30 mm	pineal: deep freeze	21:50
		brain + rets PA (f- Immuino)	21.52
Argyropelecus aculeatus	5 cm	pineal: deep freeze	21:57
(Rhomb. + Telenc. lädiert)		brain + rest PA (f. Immuno)	21:59
3 x fragl. Poromitra (total) für Justin in 2% GA, 2% PA (EM-Fix.)			22:00

Station # 24 TUT **10.7.07**

Coordinates: 26^0 54' S 175^0 30' W
net out: 8.20
depth: ~ 500 m, open for 3 hrs
net in: 11.30 (Netzkabel beim einholen gerissen!)

Ophistoproctus grimaldii	70 mm	brain + rets PA (f. Immuno)	13:00
(kam spät aus dem Netz; ohne Haut)			

Station # 26 TUT **10.7.07**

Coordinates: 27^0 53' S 175^0 28' W
net out: 18.30
depth: 1 hr at 250 m, 1 hr at 175 m
net in: 21.15

Argyropelecus aculeatus	38 mm	pineal: deep freeze	21:31
Argyropelecus aculeatus	38 mm	pineal: deep freeze	21:34
(nur zwei pins; Gehirne sahen nicht mehr gut aus)			
Gonostoma gracile	135 mm	pineal: deep freeze	21:36
		Kopf: PA für Ag-Block-Imprägnation	

Station # 31 TUT **11.7.07**

Coordinates: 27^0 13' S 176^0 13' W
net out: 11.30
depth: ~ 500 m, open for 3 hrs
net in: 15.30

Argyro. hemigymnus 30 mm pineal: deep freeze 15:52
Kopf: PA für Ag-Block-Imprägnation

Station # 34 TUT **11.7.07**

Coordinates: 27^0 30' S 176^0 48' W
net out: 19.30
depth: ~ 175 - 200 m, open for 1 hr(200) and 1 hr (175)
net in: 21.30

kein für uns verwertbarer Inhalt

Station # 37 TUT **12.7.07**

Coordinates: 26^0 56' S 175^0 30' W
net out: 8.40
depth: verified 700 – 800 m, open for 2 hrs
net in: 12.45

Alepocephalus (sehr klein) total PA (f. Immuno) 13:05

Station # 44 TUT **14.7.07**

Coordinates: 24^0 14' S 175^0 09' W
net out: 11.00
depth: verified 600 – 800 m, open for 3 hrs
net in: 15.30

Dolichopterus sp. 115 mm DEXTRITC (opticus) 2d 16:35
f. rets + brain
(zu Hause nachpräparieren)

Station # 48 TUT **14.7.07**

Coordinates: 24^0 01' S 175^0 16' W
net out: 18.30
depth: 200 – 300 m, open for 1 hr (500 m rope), and 1 hr (400 m rope)
net in: 21.10

Argyropelecus aculeatus 57 mm pineal: deep freeze 21:16
Kopf: PA für Ag-Block-Imprägnation 21:18

Argyropelecus aculeatus 25 mm pineal: deep freeze 21:29
Kopf: PA für Ag-Block-Imprägnation 21:31

Station # 50 TUT **15.7.07**

Coordinates: 24^0 07' S 175^0 10' W
net out: 8.15
depth: 600 – 700 m, open for 4 hrs (1000 m rope)
net in: 13.30

Gonostoma gracile (jung)	40 mm	total PA	13:36
Gonostoma gracile (jung)	38 mm	total PA	13:37
Chauliodus sloani	150 mm	pineal: deep freeze	13:42
		Kopf: PA für Ag-Block-Imprägnation	13:45
Sternoptyx diaphana	15 mm	Kopf: PA für Ag-Block-Imprägnation	13:49
Gonostoma gracile (jung)	28 mm	total PA	13:50
Photostomias	31 mm	total PA	13:57

Station # 53 TUT **15.7.07**

Coordinates: 24^0 38' S 175^0 17' W
net out: 18.30
depth: 200 – 300 m, open for 2,5 hrs (500 m rope)
net in: 21.10

Scopelarchus analis	50 mm	total PA	22:05
Scopelarchus analis	45 mm	total PA	22:07
Gonostoma gracile	125 mm	pineal: deep freeze	22:12
		Kopf: PA für Ag-Block-Imprägnation	22:13
2 Poromitra (total) für Justin in 2% GA, 2% PA (EM-Fix.)			22:17
Scopelarchus analis	50 mm	DEXTRITC (opticus) 2d	22:22
		f. rets + brain	
		(zu Hause nachpräparieren)	
Gonostoma gracile	132 mm	pineal: deep freeze	22:34
		Kopf: für Ag-Block-Imprägnation	22:36
Echiostoma	210 mm	4% PA (total), Sammelbehälter	08:15 !